

First-principles theory of magnetic multipoles in condensed matter systems

Michi-To Suzuki^{1*}, Hiroaki Ikeda², and Peter M. Oppeneer³

¹*RIKEN Center for Emergent Matter Science, 2-1 Hirosawa, Wako, Saitama 351-0198, Japan*

²*Department of Physics, Ritsumeikan University, Kusatsu, Shiga 525-8577, Japan*

³*Department of Physics and Astronomy, Uppsala University, P. O. Box 516, SE-751 20 Uppsala, Sweden*

The multipole concept, which characterizes the spacial distribution of scalar and vector objects by their angular dependence, has already become widely used in various areas of physics. In recent years it has become employed to systematically classify the anisotropic distribution of electrons and magnetization around atoms in solid state materials. This has been fuelled by the discovery of several physical phenomena that exhibit unusual higher rank multipole moments, beyond that of the conventional degrees of freedom as charge and magnetic dipole moment. Moreover, the higher rank electric/magnetic multipole moments have been suggested as promising order parameters in exotic hidden order phases. While the experimental investigations of such anomalous phases have provided encouraging observations of multipolar order, theoretical approaches have developed at a slower pace. In particular, a materials' specific theory has been missing. The multipole concept has furthermore been recognized as the key quantity which characterizes the resultant configuration of magnetic moments in a cluster of atomic moments. This cluster multipole moment has then been introduced as macroscopic order parameter for a noncollinear antiferromagnetic structure in crystals that can explain unusual physical phenomena whose appearance is determined by the magnetic point group symmetry. It is the purpose of this review to discuss the recent developments in the first-principles theory investigating multipolar degrees of freedom in condensed matter systems. These recent developments exemplify that *ab initio* electronic structure calculations can unveil detailed insight in the mechanism of physical phenomena caused by the unconventional, multipole degree of freedom.

1. Introduction

The multipole formulation has proven to be a very fruitful as well as foundational concept in physics.¹⁾ More than a century ago the single electron was discovered to have a unique monopole charge. Diatomic molecules became classified after their electric dipole moment. The possible existence of the Dirac magnetic monopole would have fundamental consequences²⁾ and has been much discussed. On the basis of the Maxwell equations the dynamics of electrically charged bodies became generalized, leading to the multipole description of their charge distributions.³⁾ The multipole description has subsequently become used in many branches of physics, including nuclear physics^{4,5)} and solid state physics (see, e.g., Refs.^{6–9)}). In this review we focus on the appearance of electric or magnetic multipole moments in condensed matter systems.

Condensed matter systems display a richness of physical phenomena, such as e.g. strongly correlated electron behavior, complex magnetic orders, orbital order, unusual forms of superconductivity and quantum critical behavior. This diversity of phenomena can be attributed to the multiple degrees of freedom available to the electronic system that, in itself or in conjunction to lattice degrees of freedom, can have access to entangled spin and orbital states. In particular, the electron clouds around nuclei in crystalline materials can be systematically characterized by using the multipole expansion. Since electrons on filled atomic shells lead only to spherical charge distributions, the electrons in open shells are responsible for the anisotropic charge and spin distributions and thus for the eventual appearance of multipolar order. It turns out, however, that the appearance of true multipolar order, that is, of rank higher than dipolar order, is actually rare in solid state compounds. Thus far, true multipolar order has been discovered, or predicted, for about a dozen crystalline materials, such as, CeB₆,^{10–21)} R₃Pd₂₀X₆ (R: Ce, Pr, X: Si, Ge),^{22–32)} PrPb₃,^{33–42)} PrMg₃,^{43–46)} PrFe₄P₁₂,^{47–61)} PrRu₄P₁₂,^{62–70)} PrOs₄Sb₁₂,^{49,71–76)} SmRu₄P₁₂,^{77–82)} PrT₂X₂₀ (T: Ir, Rh, X: Zn; T: V, Ti, X: Al),^{83–97)} DyB₂C₂,^{98–108)} HoB₂C₂,^{109–112)} DyPd₃S₄,^{113–116)} CePd₃S₄,^{117–119)} UO₂,^{9,120–125)} NpO₂,^{9,126–137)} AmO₂,^{61,138–140)} UPd₃,^{141–151)} and URu₂Si₂.^{152–168)}

These compounds have in common that the exotic multipolar electric or magnetic distribution occurs on the lanthanide or actinide ion and are thus generated by the *f* electrons. More general, typical features of *f* electron systems are localized character, that tends to enforce the strong electron-electron repulsion, a significant orbital degree of freedom, allowing for anisotropic orbital states, and strong spin-orbit (S-O) coupling which leads to entangled spin and orbital moments.

*michito.suzuki@riken.jp

A major question is which theoretical description is suitable to unveil insight in the origin of the multipolar order in crystal systems. Single ion crystal-electric field (CEF) theories could previously provide understanding of aspects of multipolar ordered ionic states, often in relation to the local point group symmetry and assumptions made regarding the CEF level scheme.^{6–9, 11, 152, 169)} However, this approach has limitations as it considers basically only the atomic *f*-orbitals yet without materials' specific aspects, such as e.g. hybridization, which can significantly modify the materials' properties. Conversely, the density-functional theory (DFT) (see, e.g. Ref.¹⁷⁰⁾) offers a first-principles framework for the efficient and accurate calculation of materials' specific properties. However, this framework employing the common approximations used in electronic structure calculations, such as the local spin density approximation (LSDA) and generalized gradient approximation (GGA), often fails to capture important aspect of the *f* electronic states due to the incompletely captured strong electron correlation effect in the LSDA or GGA exchange-correlation interaction. The weakness to describe sufficiently the strong *f*-electron correlation immediately leads to a difficulty to obtain the correct ground state of a strongly correlated electron system, since the strong electron correlation is usually inseparable from the complex orbital degree of freedom. To treat multipolar degrees of freedom from first principles, it is thus needed to treat strong local electron correlations, spin-orbit interaction, and the multi-orbital *f* electron character on an equal footing.

Recently, first-principles electronic structure calculations have been shown to be suitable for investigation of the multipole ordered states in correlated solid state materials.^{63, 122, 128, 155, 156, 160, 171, 172)} Hence, the way to consider multipole systems in condensed matter physics is now shifting more to the materials' specific aspect as compared to the single-ion treatment in CEF theory. Such first-principles calculations could recently provide insight in the multipole order phases appearing in the actinide dioxides^{122, 128)} and, more generally, demonstrated the possibility of performing fully first-principles study of complex ordered phase in *f* electron compounds. Combining the first-principles calculations with a group theoretical analysis led to a powerful tool to investigate hidden order parameters with the multipole degree of freedom.¹⁷²⁾ While these *ab initio* calculations describe the anomalously ordered zero temperature ground state, extensions to the description of e.g. phase diagrams have been recently undertaken. Reliable estimations of physical quantities related to the multipolar degree of freedom is a difficult task, but the situation has significantly improved by recent developments of a first-principles approach to construct tight-binding models.¹⁷³⁾ In addition, calculations of multipole fluctuations have provided important information about

instability for the phase transition to a hidden order phase and unconventional superconductivity of heavy Fermion compounds.^{160, 174)} Lastly, the development of multipole theory has recently led to new areas of condensed matter physics where the concept is becoming employed. As the multipole classification scheme can be generalized to systems characterized by a specific point group symmetry, multipole theory is becoming used for the classification of off-diagonal response phenomena, such as the electric-magnetic effect and the anomalous Hall effect in antiferromagnets.^{175–181)}

In the following, we discuss first in Sec. 2 the basic concept of the multipole degree of freedom. In Sec. 3, the first-principles approach to investigate the multipolar ordered phases is discussed first, after which we review the first-principles calculation of multipole ordered phases, mainly focusing on the actinide dioxides. The relation between the electronic structures obtained from the first-principles calculations and the CEF analysis is provided. In Sec. 4, we discuss the first-principles calculations of multipole fluctuations and review the study of superconducting pairing mediated by multipole fluctuations in CeCu₂Si₂. In Sec. 5, we focus on the long-standing problem of the hidden-order phase of URu₂Si₂ and discuss the first-principles approach to identify the possible order parameters of this phase, using first-principles calculations and group theoretical analysis. Lastly, in Sec. 6 we provide an outlook on the emerging multipolar theory to describe transport phenomena with the introduction of the study of the anomalous Hall effect in the antiferromagnetic phases of Mn₃Z (Z=Sn, Ge), and conclude this survey in Sec. 7.

2. Multipole moments in condensed matter system

2.1 General concept of the multipole moment

The multipole moments are mathematically defined as expansion coefficients of the multipole expansion of $f(\theta, \phi)$ defined on the surface space ($0 \leq \theta \leq \pi, 0 \leq \phi < 2\pi$) satisfying the condition $\int_0^{2\pi} d\phi \int_0^\pi d\theta \sin \theta |f(\theta, \phi)|^2 < \infty$.¹⁸²⁾ When the function $f(\theta, \phi)$ is expanded as:

$$f(\theta, \phi) = \sum_{\ell=0}^{\infty} \sum_{m=-\ell}^{\ell} a_{\ell m} Y_{\ell m}(\theta, \phi), \quad (1)$$

the expansion coefficient $a_{\ell m}$ is the multipole moment. The multipole moments are thus obtained from

$$a_{\ell m} = \int_0^{2\pi} d\phi \int_0^\pi d\theta \sin \theta Y_{\ell m}^*(\theta, \phi) f(\theta, \phi), \quad (2)$$

where ℓ is called the rank of multipole moments, using the orthogonality relation of spherical harmonics. Since the spherical harmonics form a complete orthonormal basis set on the

sphere space, the function $f(\theta, \phi)$ is fully identified with the multipole moments from Eq. (1).

In condensed matter physics, the angular distribution of a spin-polarized electron cloud around a nucleus can be characterized by spherical harmonics. The electric multipole moments, which measure the anisotropy of charge distribution, are defined as the projection of the charge density $\rho_e(\mathbf{r})$ onto the spherical harmonics:

$$Q_{\ell m} \equiv \sqrt{\frac{4\pi}{2\ell+1}} \int d\mathbf{r} (r^\ell Y_{\ell m}^*(\theta, \phi)) \rho_e(\mathbf{r}), \quad (3)$$

where the integration is over a suitably chosen atomic volume. The magnetic multipole moment is defined by introducing the magnetic monopole charge, which is related to the magnetization distribution defined by $\rho_m(\mathbf{r}) = -\nabla \cdot \mathbf{m}(\mathbf{r})$, and accordingly gives

$$\mathcal{M}_{\ell m} \equiv \sqrt{\frac{4\pi}{2\ell+1}} \int d\mathbf{r} (r^\ell Y_{\ell m}^*(\theta, \phi)) \rho_m(\mathbf{r}). \quad (4)$$

The partial integration of Eq. (4) leads to

$$\mathcal{M}_{\ell m} = \sqrt{\frac{4\pi}{2\ell+1}} \int d\mathbf{r} \nabla (r^\ell Y_{\ell m}^*(\theta, \phi)) \cdot \mathbf{m}(\mathbf{r}). \quad (5)$$

This equation implies that the magnetic multipole moments are the quantities characterizing the angular distribution of the magnetization $\mathbf{m}(\mathbf{r})$. Further details of this formulation can be found in Refs.^{5,6)}

The multipole moment is thus a quantity which classifies the spacial and angular shape of a charge or magnetization distribution. Multipole moments are denoted according to their rank ℓ , such as $\ell = 0$: monopole, $\ell = 1$: dipole, $\ell = 2$: quadrupole, $\ell = 3$: octupole, $\ell = 4$: hexadecapole, $\ell = 5$: triakontadipole or dotriacontapole, and $\ell = 6$: tetrahexacontapole. This nomenclature stems from the Greek notation for the 2^ℓ -numbers. The prefactors in Eqs. (3) and (4) are chosen such that Q_{00} corresponds to the total enclosed charge and \mathcal{M}_{1m} corresponds to the magnetic dipole moment, respectively, though the choice has arbitrariness. Electric multipole moments have the unit of $e \times (\text{length})^\ell$ and magnetic multipoles have $\mu_B \times (\text{length})^{\ell-1}$, where e is the elementary charge and μ_B is the Bohr magneton. It is straightforward to see that the rank zero electric multipole moment corresponds to the enclosed total electric charge. The ordinary magnetic moment is obviously given by the rank-1 magnetic dipole moment. The rank zero magnetic multipole moments, corresponding to magnetic monopole charge, do not appear in the multipole expansion, reflecting the relation $\nabla \cdot \mathbf{B} = 0$, but it can be a useful concept for composite objects (see e.g.^{176, 177, 183, 184)}).

A useful connection between multipole expressions using spherical harmonics and those

based on Cartesian coordinates is obtained from

$$r^\ell Y_{\ell m}(\hat{\mathbf{r}}) = \sqrt{\frac{2\ell+1}{4\pi}(\ell+m)!(\ell-m)!} \times \sum_{pqs} \left(-\frac{x+iy}{2}\right)^p \left(\frac{x-iy}{2}\right)^q z^s, \quad (6)$$

where p , q , and s are zero or positive integers that satisfy $p+q+s=\ell$ and $p-q=m$.¹⁸²⁾

2.2 Symmetry properties of multipole moments

In condensed matter physics, multipole moments are often introduced as mathematical tool to characterize the point group symmetry breaking. The $\rho_e(\mathbf{r})$ and $\rho_m(\mathbf{r})$ are even and odd, respectively, for the time reversal operation, leading to $Q_{\ell m} \rightarrow Q_{\ell m}$ and $M_{\ell m} \rightarrow -M_{\ell m}$ for the time reversal operation. The space inversion operation transforms the electric charge density, magnetic charge density and magnetic moment density as: $\rho_e(\mathbf{r}) \rightarrow \rho_e(-\mathbf{r})$, $\rho_m(\mathbf{r}) \rightarrow -\rho_m(-\mathbf{r})$, $\mathbf{m}(\mathbf{r}) \rightarrow \mathbf{m}(-\mathbf{r})$, respectively. As a result, the relation $Y_{\ell m}(-\hat{\mathbf{r}}) = (-1)^\ell Y_{\ell m}(\hat{\mathbf{r}})$ leads to the parity of the rank ℓ multipole moments for the spacial inversion as $(-1)^\ell$ for the electric multipoles and $(-1)^{\ell-1}$ for the magnetic multipoles. From these relations, the electric (magnetic) multipole moments are finite only for even (odd) rank when the system has the spacial inversion symmetry.

The multipole moments are classified according to the irreducible representations (IREP) of the point group, taking a linear combination of Eqs. (3) and (4) that is reflecting the transformation property under the corresponding point group operations.^{6, 11, 69, 152, 169)} To use this, it is convenient to start with considering the multipole moments classified according to the highest point group symmetry, i.e. cubic group O_h or hexagonal group D_{6h} . The multipole expression can then be applied to multipole degree of freedom on an atomic site whose symmetry is lower than O_h or D_{6h} , and the multipole moments are re-classified according to the IREPs of the point group. In the following we adopt the Bethe notation, such as Γ_7 and Γ_8 , for the IREPs of orbitals including the effect of spin-orbit coupling and Mulliken notation, such as A_1 and E , for the IREPs to which multipole moments belong, with the notation of g and u for even and odd parity for space inversion symmetry, respectively, and $+$ and $-$ for time reversal symmetry.

3. Multipolar order

3.1 First-principles approach to multipolar ordered phase

Multipolar order has been observed particularly in materials containing elements with open $4f$ or $5f$ electron shells.^{10, 12, 22, 24, 33–35, 47–49, 71, 77, 78, 83–85, 98–100, 113, 120, 121, 126, 127, 141)} These

f electron materials are characterized by relatively localized and correlated *f* states, having a significant orbital disproportionation and/or anisotropic hybridization, and a strong spin-orbit interaction. More than a decade of research devoted to determining the optimal *ab initio* computational approach showed that good descriptions could be achieved with the DFT+*U* (Ref.¹⁸⁵⁾) and DFT+DMFT methods.¹⁸⁶⁾ The +*U* approach is particularly suitable for capturing the strong local *f*-electron correlations whereas the DMFT approach is able to include effects of low-energy dynamic fluctuations in the electronic structure, beyond the Kohn-Sham DFT formulation.

Both the LDA+*U* and GGA+*U* methods with S-O interaction included have been successful in capturing the ground state properties of *f*-electron compounds.^{128, 187–197)} In spite of some limitations this method is especially suited to describe the local character of *f* electrons on the same footing with the electronic band description. The LDA+*U* method^{185, 198–200)} provides the one-electron Hamiltonian as

$$h_{\text{LDA}+U} = h_{\text{LDA}} + \sum_{\tau} \sum_{\gamma\gamma'} |\tau\ell\gamma\rangle v_{\gamma\gamma'}^{\tau\ell} \langle\tau\ell\gamma'|, \quad (7)$$

where h_{LDA} is the conventional Kohn-Sham single-electron Hamiltonian that contains the kinetic energy, Coulomb-Hartree interactions, exchange-correlation energies, and relativistic correction terms, $|\tau\ell\gamma\rangle$ denote the local basis set, γ (γ') is an index related to an orbital m (m') and a spin s (s') quantum number, or, alternatively, double-valued irreducible representations of the site symmetry of the correlated *f* electron site obtained through a unitary transformation. The on-site Coulomb potential is given by

$$\begin{aligned} v_{\{ms\}\{m's'\}}^{\tau\ell} &= \sum_{m''m'''} \left[\delta_{ss'} \sum_{s''} n_{\{m'''s''\}\{m''s''\}}^{\tau\ell} \times \right. \\ &\quad \langle mm''|W|m'm''\rangle \\ &\quad - n_{\{m'''s\}\{m''s'\}}^{\tau\ell} \langle mm''|W|m'''m'\rangle \Big] \\ &\quad - \delta_{mm'} \delta_{ss'} \left[U(n^{\tau\ell} - \frac{\eta^{\tau\ell}}{2}) - J(n_s^{\tau\ell} - \frac{\eta_s^{\tau\ell}}{2}) \right], \end{aligned} \quad (8)$$

where τ and ℓ are the atom's index and angular momentum of the orbitals, respectively, for which the +*U* potentials are introduced. $n_{\{ms\}\{m's'\}}^{\tau\ell}$ is the local spin-orbital electron occupation matrix, $n_s^{\tau\ell} = \sum_{m=-\ell}^{\ell} n_{\{ms\}\{ms\}}^{\tau\ell}$, $n^{\tau\ell} = \sum_s n_s^{\tau\ell}$. $\eta^{\tau\ell} = \frac{1}{2} \sum_s \eta_s^{\tau\ell}$ depends on the type of double counting term, specifically, $\eta_s^{\tau\ell} = 1$ for the fully localized limit and $\eta_s^{\tau\ell} = \frac{1}{2\ell+1} \sum_{m=-\ell}^{\ell} n_{\{ms\}\{ms\}}^{\tau\ell}$ for the around mean field formulation.^{199, 201)} The electron occupation matrix $n_{\gamma\gamma'}^{\tau\ell}$ pertaining to a certain ion can be calculated for the local space spanned by the local bases inside the

atomic or muffin-tin (MT) spheres around the selected atom as:

$$n_{\gamma\gamma'}^{\tau\ell} = \int_{\text{MT}} dr_{\tau} r_{\tau}^2 \rho_{\gamma\gamma'}^{\tau\ell}(r_{\tau}), \quad (9)$$

with

$$\rho_{\gamma\gamma'}^{\tau\ell}(r_{\tau}) = \frac{1}{N} \sum_{kb} \langle \tau\ell\gamma | kb \rangle \langle kb | \tau\ell\gamma' \rangle, \quad (10)$$

where $|kb\rangle$ are the Bloch band states (eigenstates of Eq. (7)) that are projected on to the local basis, N is the number of \mathbf{k} points in reciprocal space and r_{τ} is the radial component of the position vector \mathbf{r}_{τ} measured from the center of the atom τ . The occupation matrix as well as the charge density is determined selfconsistently in the framework of the LDA+ U method. The matrix elements of the Coulomb interaction of f electrons is expressed as

$$\begin{aligned} \langle m_1 m_2 | W | m_3 m_4 \rangle &= \delta_{m_1+m_2, m_3+m_4} \\ &\times \sum_{k=0}^6 c^k(\ell m_1; \ell m_3) c^k(\ell m_4; \ell m_2) F^k, \end{aligned} \quad (11)$$

where the F^k are the Slater-Condon parameters,^{202,203)} and c^k is the Gaunt coefficient.^{204,205)} In practical calculations F_0 is taken as $F_0 = U$, the Hubbard U parameter. The Hund's coupling parameter J is related with the higher order Slater integrals as $J = (286F_2 + 195F_4 + 250F_6)/6435$ for f electrons.¹⁸⁵⁾ The ratio between the higher order Slater integrals is obtained from hydrogenic radial wave functions, such as $F_4/F_2 = 0.138$ and $F_6/F_2 = 0.0151$,²⁰⁶⁾ and it is convenient to choose only U and J as parameters in the LDA+ U calculations.

The multipolar ordered states are calculated by introducing the specific symmetry breaking by considering the local symmetry of the multipole moment, which is characterized by the IREP, and the configuration of the multipole moments in the crystal structure. General symmetry properties of multipolar ordered states are discussed in the Appendix. In the LDA+ U method, one can introduce the symmetry breaking through the initial electron occupation matrix, since appearing multipole order parameters involve the multiple spin and orbital degrees of freedom as well as the local occupation matrix, that make it suitable to calculate complex multipolar ordered phases. For instance, nonmagnetic calculations are performed with the relation $n_{\{-m-s\}\{-m'-s'\}}^{\tau\ell} = (-1)^{m+m'+s-s'} n_{\{ms\}\{m's'\}}^{\tau\ell*}$ for the electron occupation matrix, Eq. (9), to preserve the time reversal symmetry,¹⁹⁶⁾ and this relation should be removed to calculate the magnetic multipolar ordered states. Other relations between the matrix elements are identified by investigating the transformation property of the density matrix for the point group operations, depending on the local atomic site symmetry on which the density matrix is de-

fined. Furthermore, the relation between the local principal axes of the multipole moments on different atoms are determined when the magnetic space group of the ordered state is identified (See the Appendix). Since a large Coulomb U tends to increase the anisotropic character of the f states, the full-potential treatment²⁰⁷⁾ is an important ingredient, too, to adequately reproduce the behavior of anisotropic f states in correlated materials. In recent explicit calculations the full-potential linearized augmented plane wave (FLAPW) band-structure method with the $+U$ implementation has therefore been used.^{122, 128, 196, 208)}

It is known that the large U introduced in the LDA+ U method can induce some metastable states especially in calculations of ordered states and may lead to convergence to an electronic state that is inconsistent with the realistic ground state.^{188, 209–212)} To avoid this problem, experimental information concerning the CEF ground states and the order parameters can be used to control the occupations for the initial density matrix and guide convergence to the proper ground state.

The local multipole moments can be obtained from the local spin-orbital occupation matrix. This quantity is computed selfconsistently, starting from an initial density matrix and allowing for suitable symmetry breaking. The expectation values of the local operators $O^{\tau\ell}$ defined for the local basis on a specific atom τ and orbital ℓ are calculated with the local basis set $\{|\tau\ell\gamma\rangle\}$ inside the MT spheres, following the expressions

$$\begin{aligned} O^{\tau\ell}(\mathbf{r}_\tau) &\equiv \frac{1}{N^2} \sum_{\mathbf{k}b} \sum_{\mathbf{k}'b'} \sum_{\gamma\gamma'} \langle \mathbf{r}_\tau | \mathbf{k}b \rangle \langle \mathbf{k}b | \tau\ell\gamma \rangle O_{\gamma\gamma'}^{\tau\ell} \\ &\quad \times \langle \tau\ell\gamma' | \mathbf{k}'b' \rangle \langle \mathbf{k}'b' | \mathbf{r}_\tau \rangle, \end{aligned} \quad (12)$$

and the integration inside the muffin-tin sphere is

$$\begin{aligned} \langle O^{\tau\ell} \rangle &= \int_{\text{MT}} d\mathbf{r}_\tau O^{\tau\ell}(\mathbf{r}_\tau) \\ &= \sum_\gamma \sum_{\gamma_1\gamma_2} \int d\mathbf{r}_\tau r_\tau^2 \rho_{\gamma\gamma_1}^{\tau\ell}(r_\tau) O_{\gamma_1\gamma_2}^{\tau\ell} \rho_{\gamma_2\gamma}^{\tau\ell}(r_\tau). \end{aligned} \quad (13)$$

A matrix element of the multipole operators is systematically calculated with Steven's operators technique, and the explicit expressions for the local multipole operators $O^{\tau\ell}$ for sites with specific local crystal symmetries have been listed.^{6, 11)} When the multipole moments align antiferromagnetically, the antiferromagnetic alignment of the local principal axis at each atomic site is assured by posing the proper magnetic space group symmetry for the antiferroic multipolar order.

3.2 Introduction to the AnO_2 compounds

Recently, f electron materials containing actinide elements have drawn considerable interest, stimulated by observations of intriguingly ordered ground states emerging at low temperatures. These conditions are in particular met in the rare-earth and actinide compounds, which have provided a treasure trove of a rich variety of multi-orbital physics over many years. A striking example is the low-temperature ordered ground state of NpO_2 , which, after many years of investigations could experimentally be established to be due to a high-rank magnetic multipolar order, in the absence of any dipolar moment formation.^{7–9)}

The quest for the hidden order parameter in NpO_2 started sixty years ago when an unusual phase transition to an unknown ordered phase was discovered below $T_0 \sim 25$ K in specific heat measurements.²¹³⁾ Subsequent magnetic susceptibility measurements revealed also a clear phase-transition anomaly,^{129, 214)} but no ordered dipole magnetic moment could be detected in neutron scattering experiments^{130, 215)} and Mössbauer spectroscopy.^{216, 217)} However, muon spin rotation (μ SR) measurements revealed the breaking of time-reversal symmetry in the mysteriously ordered phase.¹³¹⁾ Tremendous experimental and theoretical efforts have been invested to reach an explanation of the peculiar low-temperature phase (see e.g. Ref.⁹⁾). A higher order magnetic octupole moment was first suggested.^{132, 218)} Important insight was obtained from resonant x-ray scattering²¹⁹⁾ that identified the electric symmetry as triple- \mathbf{q} antiferro quadrupolar (AFQ) long range order of (111) oriented multipole moments below T_0 and suggested the (time-reversal symmetry broken) antiferro order of T_{2g} -magnetic multipole moments as primary order parameter.^{126, 133)} X-ray Bragg scattering experiments were initially interpreted as evidence for the absence of rank-5 multipole moments,²²⁰⁾ but this possibility was re-examined later.²²¹⁾ Nuclear magnetic resonance (NMR) experiments further supported the $3\mathbf{q}$ ordering of magnetic multipole moments, detecting the splitting of the ^{17}O spectra due to the symmetry lowering around the oxygen sites accompanied by the $3\mathbf{q}$ ordering below T_0 .^{127, 134, 222)} Then, it has been realized that the order parameter has T_{2g} symmetry with type-I AF ordering of magnetic multipoles.^{135, 223)} Inelastic neutron scattering measurements and theoretical analysis could finally identify triple- \mathbf{q} antiferro ordered multipoles of rank-5 (triakontadipoles) of the T_{2g} symmetry as the leading order parameter.^{128, 136, 224)}

While the physical features of NpO_2 are outstanding, the other actinide dioxides are of scientific interest as well.²²⁵⁾ All known AnO_2 compounds with $5f$ electrons ($An = \text{U}, \text{Np}, \text{Pu}, \text{Am}, \text{and Cm}$) crystallize in the FCC structure, shown in Fig. 1, characterized by the space group $Fm\bar{3}m$ (O_h^5 , No. 225), and all compounds are insulators with sizeable band gaps of

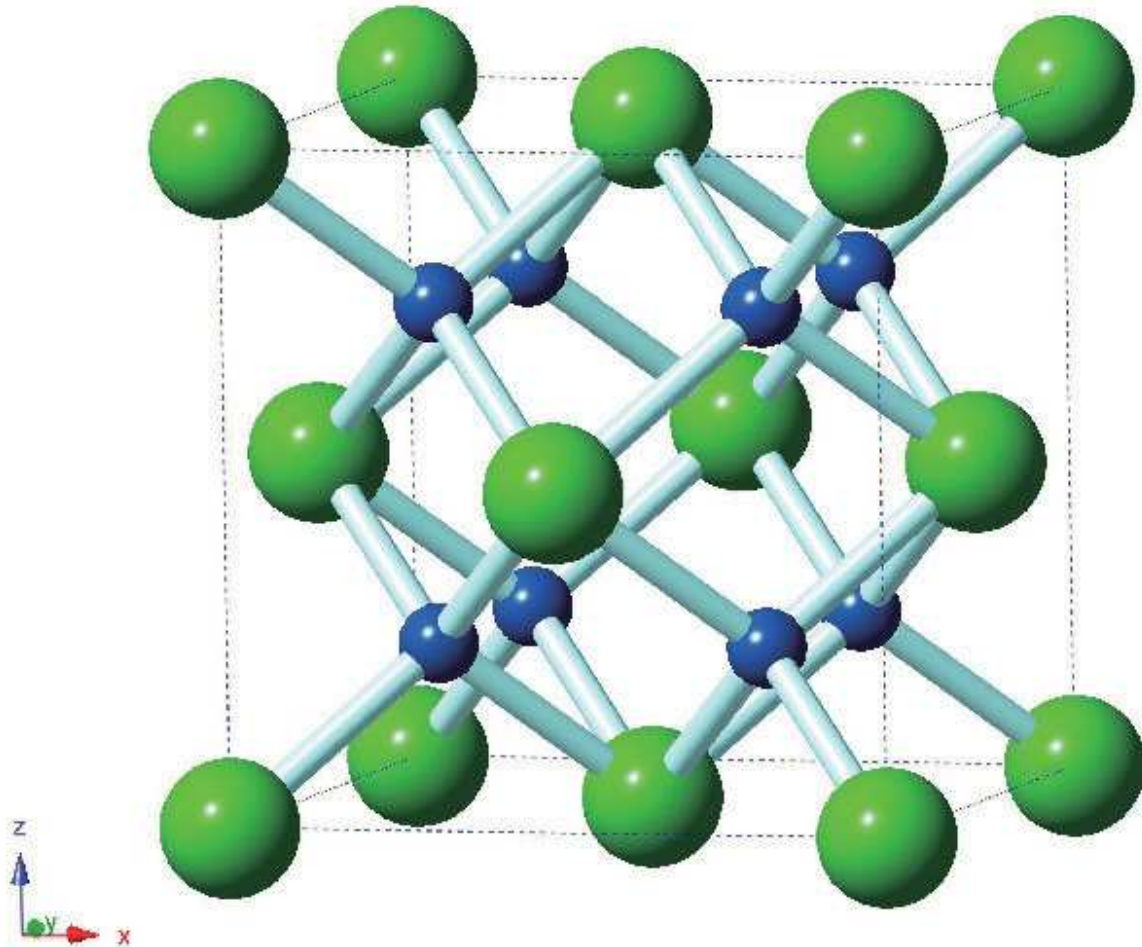


Fig. 1. (Color online) The cubic fluorite crystal structure of the AnO_2 compounds. Green spheres depict the actinide An ion, blue spheres the oxygen atoms.

about 2 eV.^{226–228)} The 14 one-electron f orbitals are split by the spin-orbit interaction in the $j = 5/2$ and $j = 7/2$ orbitals, which are further split by the cubic CEF, see Fig. 2. On the basis of the point charge model, the energy level of the Γ_8 one-electron orbital is expected to be lower than that of the Γ_7 orbital in the $j = 5/2$ orbitals since the oxygen anions are located along the [111] direction, to which the Γ_7 orbital extends.^{137,229)} The filling of the Γ_8 orbital by two, three, and four f electrons leads to the Γ_5 triplet, $\Gamma_8^{(2)}$ quartet, and Γ_1 singlet CEF ground state in the L - S coupling scheme, which are consistent with the experimental observations for UO_2 ,^{230,231)} for NpO_2 ,^{232,233)} and for PuO_2 ,^{234,235)} respectively.

In spite of the alike insulating and structural properties, the AnO_2 compounds show a wide variety of magnetic ground states. UO_2 exhibits an antiferromagnetically ordered ground state below $T = 30$ K^{213,236–239)} that later on was shown to be a $3q$ magnetic dipole or-

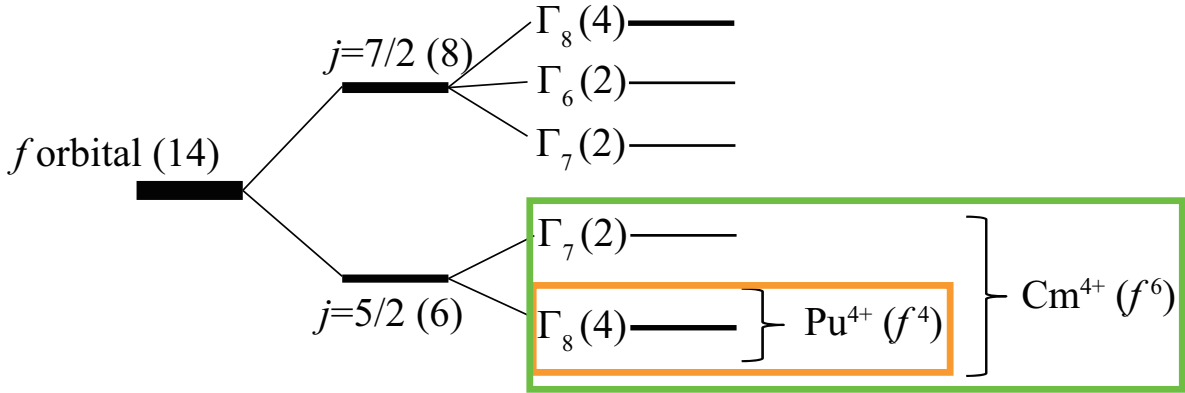


Fig. 2. (Color online) Schematics of the splitting of the 14 one-electron f orbitals. Spin-orbit interactions splits the orbitals in $j = 5/2$ and $j = 7/2$ orbitals, which are further split by the cubic crystal field. The number in the brackets denotes the degeneracy of the orbitals (from Ref.¹²²). ©2013 American Physical Society

dered state.^{123, 240, 241} The dipolar $3q$ magnetic order is accompanied by a $3q$ ordering of quadrupoles, which in turn are related to a distortion of the $5f$ charge density in the direction of dipole moments.^{120, 123}

PuO_2 does not show any magnetic phase transition, rather, the magnetic susceptibility is temperature-independent up to 1000 K.²⁴² The nonmagnetic ground state of PuO_2 has been confirmed by a recent Pu-NMR study²⁴³ and it can be understood from a CEF analysis for the Pu^{4+} ion that gives a nonmagnetic singlet state as the CEF ground state.^{225, 234, 235}

AmO_2 undergoes a conspicuous phase transition at around 8.5 K.²⁴⁴ While a peak structure in the magnetic susceptibility was found,²⁴⁴ neutron-diffraction measurements could not detect any antiferromagnetic dipolar order in agreement with the Mössbauer measurement.^{245, 246} Hence, the features of AmO_2 are similar to those of NpO_2 , and therefore an antiferro multipolar ordered ground state is expected in AmO_2 . The CEF ground state of the Am^{4+} ion in AmO_2 was thought to be a Γ_7 doublet.^{244, 247, 248} However, the Γ_7 state has no degree of freedom for the higher rank multipoles and therefore seems to contradict the experiments. A recent CEF analysis based on the $j-j$ coupling model discussed an instability of the Γ_7 ground state and possibility of stabilization of the Γ_8 ground state, which could induce higher order multipoles without inducing a dipole moment.¹³⁸ Notably, there exist many experimental challenges to distinguish the essential bulk contribution, because of the strong self-radiation damage caused by alpha decay in this material.^{249–252}

For the rare human-made compound CmO_2 only a few experiments have thus far been reported.^{253, 254} The Cm^{4+} ion ($5f^6$ occupancy) is expected to have a nonmagnetic ground state (Fig. 2), however a paramagnetic moment has been detected;²⁵³ This observation has

been explained within the $j - j$ coupling model assuming the energy proximity of a magnetic excited state.²⁵⁵⁾

The anomalous low-temperature properties of the AnO_2 compounds have been theoretically addressed with various approaches. CEF analyses have been carried out for UO_2 (Refs.^{230,231,256,257)}, for NpO_2 (Refs.^{232,233)}, and the whole series.²⁵⁸⁾ Theory of the $3q$ magnetic order of UO_2 has also been developed,^{124,259–262)} as well as $j - j$ coupling theory^{229,263)} and multipole symmetry analysis¹²⁵⁾ for NpO_2 . First-principles theory has also been employed to unravel physical and chemical properties of the AnO_2 compounds^{264–272)}. The vibrational lattice dynamics measured by inelastic neutron or inelastic x-ray scattering could recently be explained by GGA+ U calculations for UO_2 and NpO_2 .^{273,274)} However, first-principles calculations of the ordered multipolar phases is an entirely different matter, as outlined in the following.

3.3 First-principles calculation of AnO_2 ground states

The electronic structure calculation is necessary to understand the origin of the energy gap formation in materials. However, the basic approximations of the first-principles calculation, such as the local density approximation (LDA) and generalized gradient approximation (GGA), do not reproduce the energy gap observed in the AnO_2 compounds.^{122,209,275–277)} First-principles calculations taking into account the strong Coulomb interaction have been applied to UO_2 ,^{257,264–270)} to NpO_2 ,^{128,268,270)} and to PuO_2 ^{209,267,268,270,271,278–282)} though some of the studies assume ordered states different from the experimentally observed ones. Since the strong Coulomb interaction must be included in the calculations to reproduce the energy gap, the insulating AnO_2 compounds are referred to as Mott insulators.^{266,272,283)}

The detailed electronic structure investigation for the ground states of AnO_2 was performed using the LDA+ U method.^{122,128)} In the LDA+ U calculations, the Coulomb U parameter has been chosen as $U = 4$ eV and the exchange J in the range of 0 – 0.5 eV. These values have previously been shown to provide an accurate description of measured properties of actinide dioxides.^{278,284,285)} The double-counting term has been chosen as in the fully localized limit,²⁸⁶⁾ leaving out the spin dependency of the Hund's coupling part to adapt it for the nonmagnetic LDA part of Eq. (8). To illustrate the effect of strong Coulomb interaction on the energy gap formation we focus first on the electronic structures of PuO_2 and of NpO_2 , and compare their ground state's electronic property, as obtained by LDA and LDA+ U calculations. Figures 3(a) and (b) show the density of states (DOS) of PuO_2 obtained from LDA and LDA+ U calculations, respectively, assuming the nonmagnetic constraint as discussed in

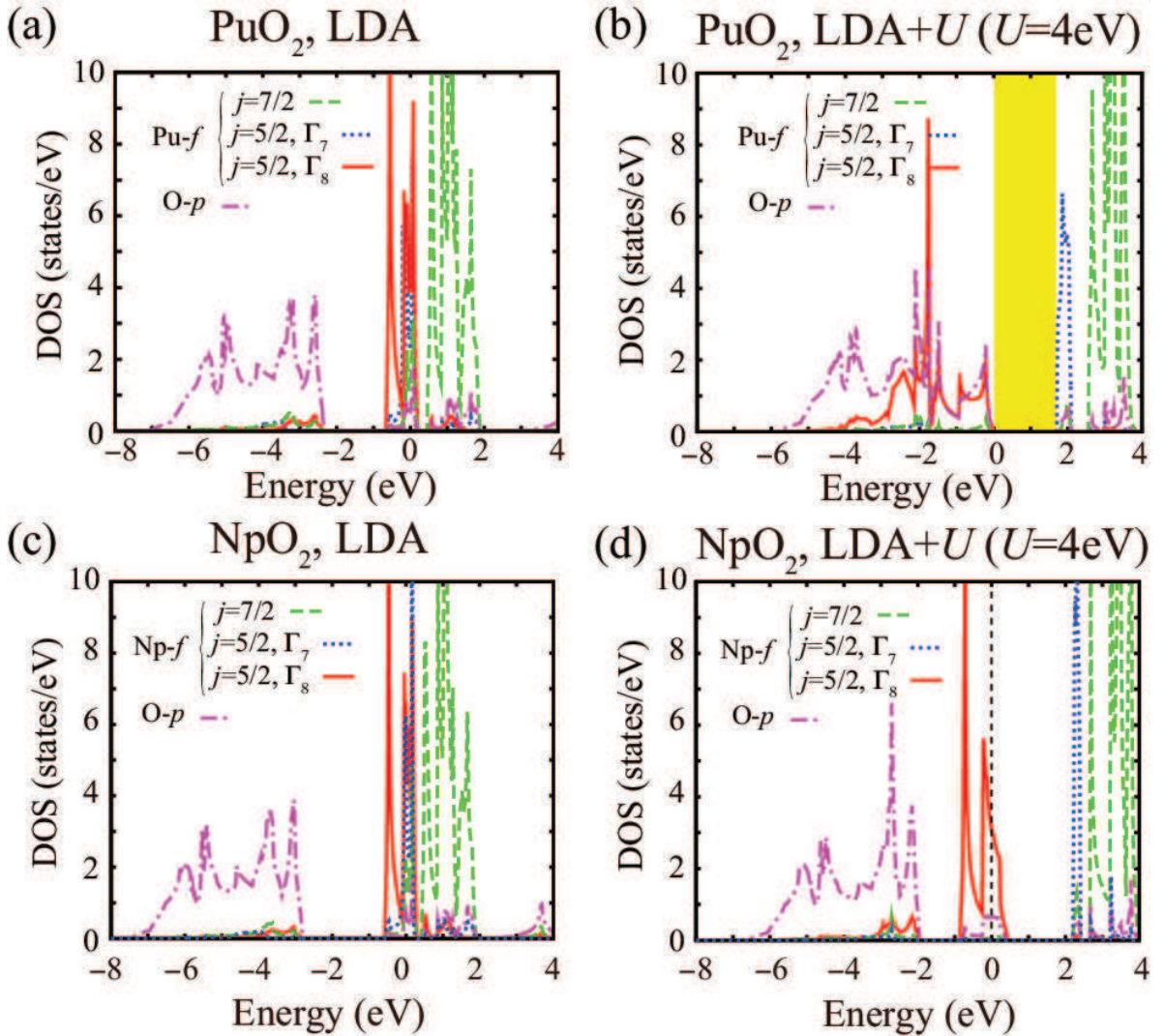


Fig. 3. (Color online) Density of states (DOS) calculated for the nonmagnetic solutions of PuO_2 and of NpO_2 , left panels using the LDA and right panels using the LDA+ U method. The $j = 5/2$ orbitals are projected on the Γ_7 and Γ_8 one-electron orbitals shown in Fig. 2. From Ref.¹²²

Sec. 3.1. In the LDA calculation, the Γ_7 and Γ_8 $j = 5/2$ orbitals of f electrons are present in the narrow energy region around the Fermi energy resembling energetically degenerate sextet orbitals, due to the absence of orbital dependence of the Coulomb interaction. Since the four f electrons of the Pu^{4+} ion occupy the sextet-like orbitals, the resulting electronic structure has the Fermi level located around the middle of the $j = 5/2$ orbitals and hence results in a metallic state. Conversely, the LDA+ U calculations reproduce the energy gap by inducing the orbital splitting between the Γ_7 and Γ_8 orbitals with the full occupation of the Γ_8 quartet orbitals, corresponding to the Γ_1 singlet CEF ground state observed experimentally.^{234,235)} The nonmagnetic LDA+ U calculations induce a similar splitting for the f -orbitals of NpO_2 as

Splitting of one electron orbital (schematic)

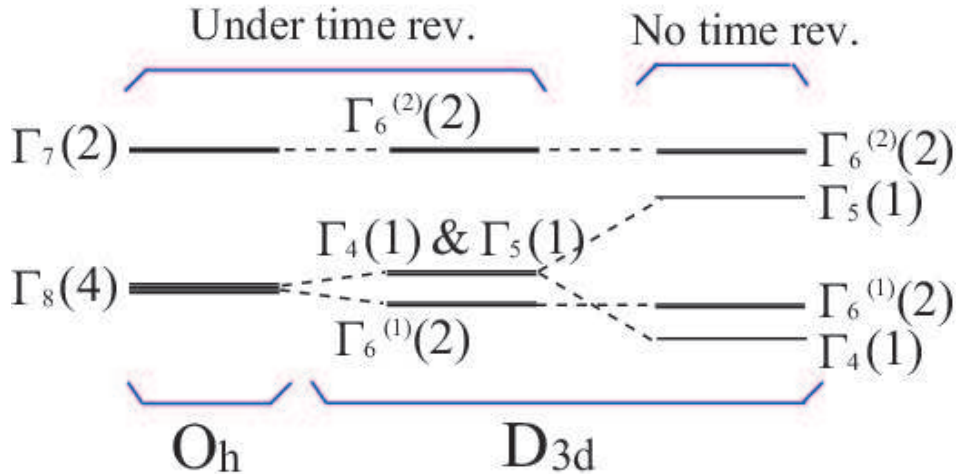


Fig. 4. (Color online) One electron energy level scheme of the $Np\ j = 5/2\ f$ orbitals at the local Np site in NpO_2 . The Γ_8 quartet in the cubic O_h symmetry with time-reversal symmetry splits in the reduced D_{3d} symmetry ($Pn\bar{3}m$ space group) in one doublet $\Gamma_6^{(1)}$, and two singlets, Γ_4 and Γ_5 that are degenerate under time-reversal symmetry. This degeneracy is lifted by time-reversal symmetry breaking. From Ref.¹²²⁾ ©2013 American Physical Society

shown in Figs. 3(c) and (d). However, since the Np^{4+} ion has three f electrons, the LDA+ U calculations lead to a metallic ground state within the nonmagnetic calculations due to the incomplete occupation of the Γ_8 quartet orbitals as shown in Fig. 3(d). The large Coulomb repulsion in NpO_2 however renders the metallic states with the dense f -states around the Fermi level unstable and a certain magnetic order is expected to appear to obtain a total energy gain through the concomitant one-electron orbital splitting.

To obtain the $3q$ antiferroic multipolar ordered state in selfconsistent electronic structures calculations the proper symmetry of the magnetic space group needs to be considered. Here, these require specifically a unit cell consisting of four elementary unit cells and the magnetic space group $Pa\bar{3}$ for UO_2 and $Pn\bar{3}m$ for NpO_2 .^{122, 128, 287)} The influence of the reduced symmetry of the latter space group on the one-electron level scheme is shown in Fig. 4. The reduced D_{3d} symmetry leads to a splitting of the quartet Γ_8 one-electron orbital into two energy-degenerate singlet orbitals, Γ_4 and Γ_5 , and a doublet $\Gamma_6^{(1)}$ orbital, in the absence of time-reversal symmetry breaking. Allowing for time-reversal symmetry breaking leads to a further splitting of the two degenerate singlet orbitals. Hence, the magnetic T_{2g}^- multipolar order of NpO_2 could split the $j = 5/2\ f$ orbitals as shown in Fig. 4. Adopting the D_{3d} point group symmetry and time-reversal symmetry breaking, the LDA+ U calculation indeed pre-

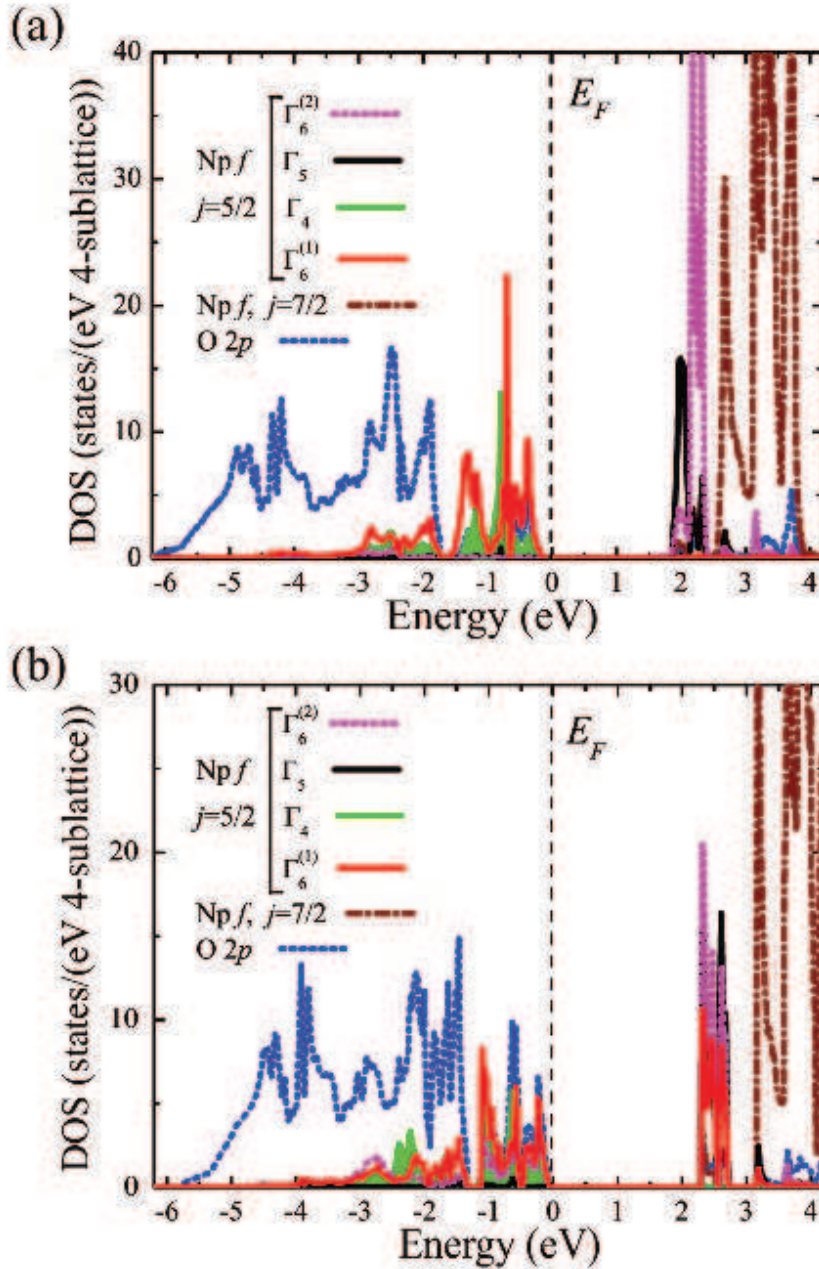


Fig. 5. (Color online) Density of states calculated for the magnetic $3q\ T_{2g}$ multipolar ordered state of NpO_2 for $U = 4$ eV, (a) with $J = 0$ and (b) with $J = 0.5$ eV. The Np $j = 5/2$ states are projected on the one-electron orbitals given schematically in Fig. 4.^{122, 128)} ©2010 The American Physical Society

dicts the insulating ground state with the characteristic energy gap of around 2 eV as shown in Fig. 5.¹²²⁾ The energy gap is formed, for $J = 0$, due to the symmetry-induced splitting between the Γ_4 , $\Gamma_6^{(1)}$ and Γ_5 , $\Gamma_6^{(2)}$ states, see Fig. 4. In the one-electron energy level scheme, the splitting between the Γ_4 and Γ_5 singlet orbitals, which are degenerate under time-reversal

O_h CEF

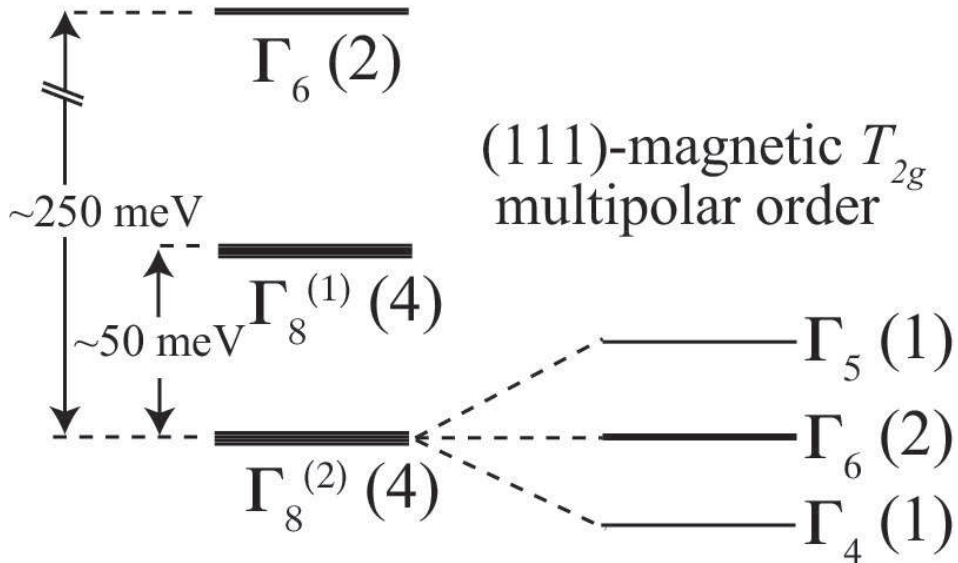


Fig. 6. Paramagnetic O_h CEF levels^{136,233)} and splitting of the ground-state Γ_8 quartet in the magnetic multipolar ordered state of NpO_2 within the $L\text{-}S$ coupling scheme.

symmetry, leads to the formation of the magnetic $(111)\text{-}T_{2g}^-$ octupole moment without inducing any magnetic dipole moment when the electrons occupy one of the singlet orbitals. This magnetic multipolar ordered state is expected to correspond to a singlet ground state in the $L\text{-}S$ coupling scheme under the $(111)\text{-}T_{2g}^-$ multipolar order, split from the paramagnetic Γ_8 quartet CEF ground state, see Fig. 6. The explicit calculations showed that, in the absence of any magnetic dipole moment, a magnetic T_{2g} multipolar ordered state is obtained for NpO_2 , which is sensitive to the Hund coupling parameter J in the LDA+ U method. The Hund coupling induces the hybridization between the $\Gamma_6^{(1)}$ and $\Gamma_6^{(2)}$ $j = 5/2$ one-electron f orbitals, whose origins are the Γ_7 and Γ_8 paramagnetic $j = 5/2$ f -orbitals as can be observed from the DOS for the one-electron orbitals calculated with $J = 0.5$ eV in Fig. 5 (b). The Hund's coupling related hybridization of the $\Gamma_6^{(1)}$ and $\Gamma_6^{(2)}$ f orbitals leads to a dependence of the multipolar moment on J , which is illustrated in Fig. 7. This coupling enhances the magnetic triakontadipole (rank-5 multipole) moment and suppresses the magnetic octupole (rank-3 multipole) moment (see Fig. 7(b)) in correspondence to the computed change in the occupations of the $\Gamma_6^{(1)}$ and $\Gamma_6^{(2)}$ orbitals, and the off-diagonal ($\Gamma_6^{(1)}, \Gamma_6^{(2)}$) matrix elements (Fig. 7(a)). These findings show that, when the Hund's rule coupling J is turned on, the magnetic distribution is dominated by

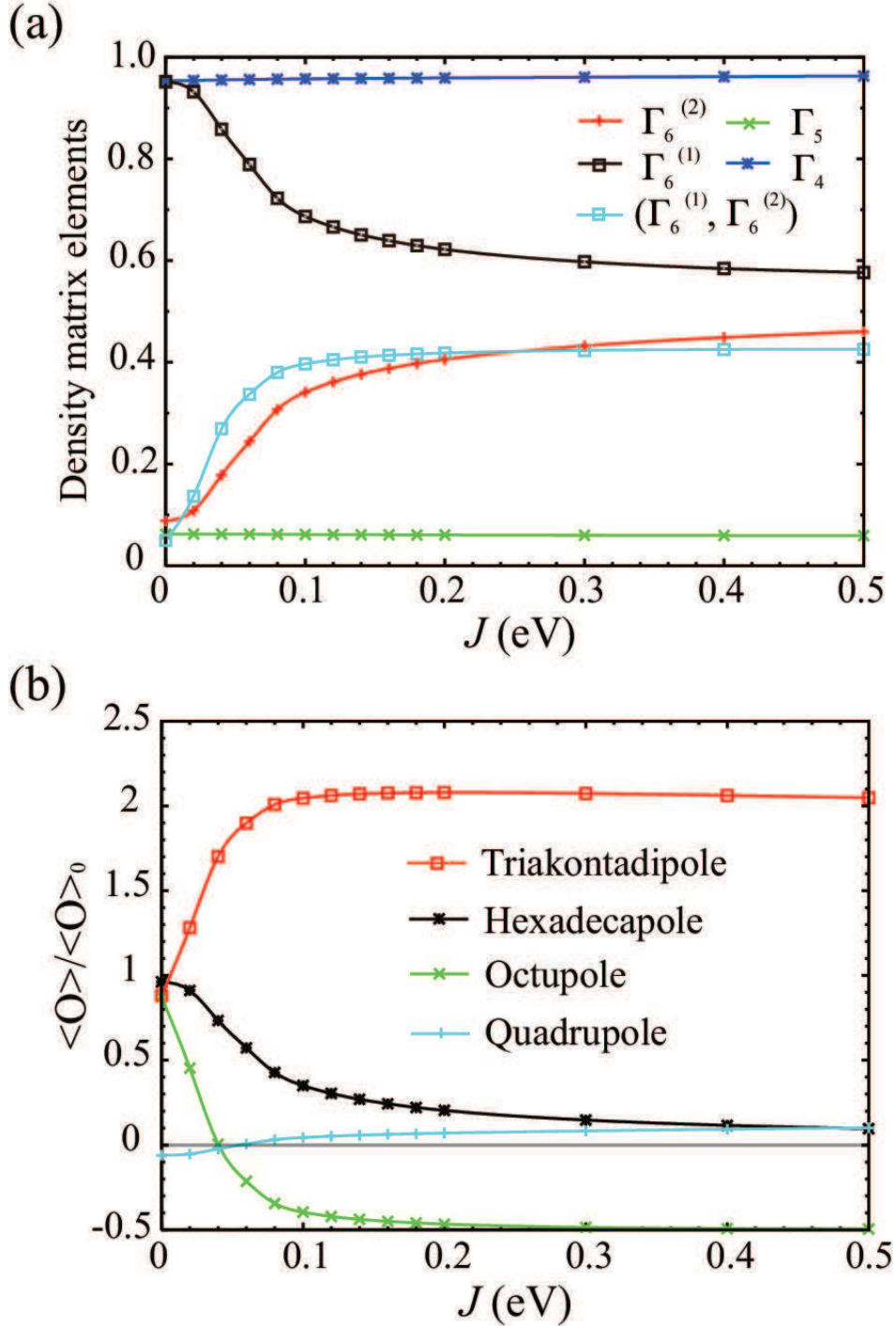


Fig. 7. (Color online) Calculated dependence on the Hund coupling parameter J of (a) the electron occupation matrix elements, and (b) the multipole moments of NpO_2 .^{122, 128)} ©2010 The American Physical Society

the rank-5 triakontadipole, which becomes enhanced, whereas the rank-3 octupole moment is suppressed. Hence, the T_{2g}^- triakontadipole moment can be regarded as the leading magnetic order parameter, a finding that is consistent with the analysis of inelastic neutron scattering

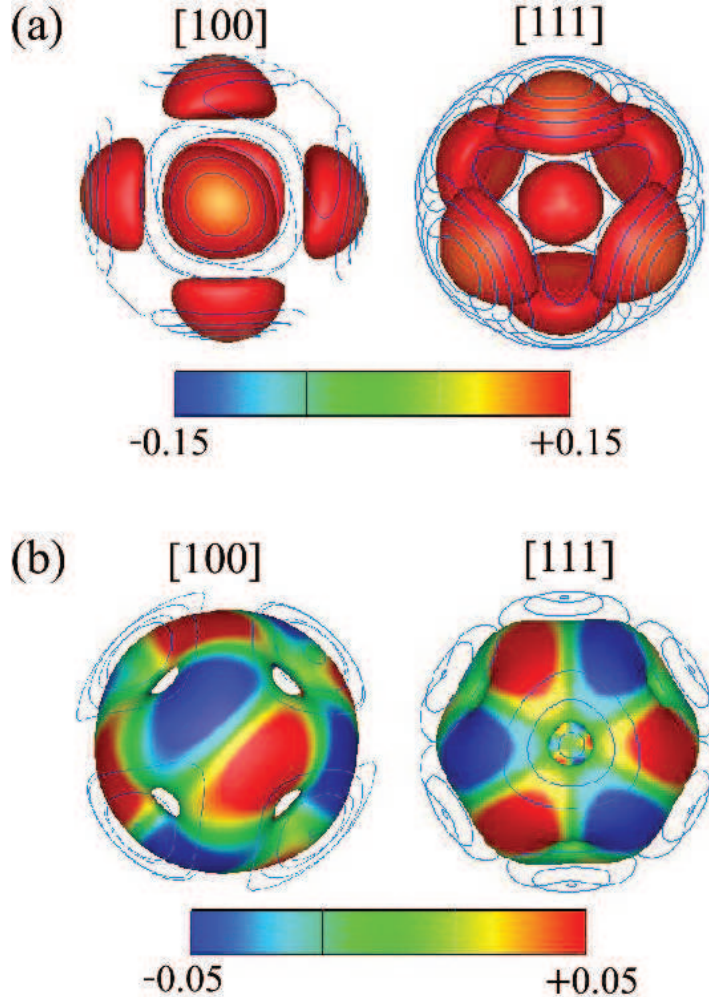


Fig. 8. (Color online) Spacial distributions of the magnetic moment densities of (a) UO_2 and (b) NpO_2 , for two different viewing directions, [100] and [111], computed with $U = 4 \text{ eV}$ and $J = 0.5 \text{ eV}$. The magnetic moment distributions are depicted on the isosurfaces of the charge densities for the [111] component, with magnitudes as given by the color bars with μ_B unit. The thin lines show the contour map of the charge density on a spherical surface. From Ref.¹²²⁾ ©2013 American Physical Society

measurements.^{136, 224)} The computed nonzero electric quadrupole moment, that appeared as the secondary order parameter for the magnetic multipolar order (See the Appendix), is in accordance with resonant x-ray scattering experiments.^{126, 133, 219)}

The spacial distributions of the charge and magnetic moment on the actinide ion, calculated with the LDA+ U method ($U = 4 \text{ eV}$ and $J = 0.5 \text{ eV}$), are shown in Fig. 8 for UO_2 and NpO_2 . The dominating dipolar magnetic nature of the $3q$ antiferromagnetic ground state of UO_2 can be clearly recognized. The magnetic distribution on Np, conversely, is very different. This spacial distribution, seen along the [111] axis, reveals several closely spaced areas

with opposite directions of the local magnetization that alternate strongly around the Np ion. This plot illustrates that the main contribution to the unique hidden order parameter of NpO_2 stems from high-rank magnetic multipoles, and moreover, provides a first-principles confirmation^{122, 128)} of their important role in the emergence of this anomalously ordered phase.

4. Multipole fluctuations

It is already well-understood that the coupling of atomic dipole moments via the Heisenberg-Dirac exchange or Anderson super-exchange interactions leads to the occurrence of long-range magnetic order in condensed matter systems. Similarly, the exchange coupling of higher-order atomic multipole moments must be responsible for the formation of long-range multipolar order, even in the absence of any dipole moments,^{9, 128)} and fluctuations of the multipole order lead to phase transitions. In general, the divergence of a susceptibility characterizes a second-order phase transition. Possible phase transitions can be found by investigating the propagation vector dependence of the susceptibilities in the nonmagnetic state. Recently, first-principles calculations of susceptibilities within the random-phase approximation (RPA) have been applied to f -electron compounds.^{160, 288)} In following sections, we explain the procedure and outline the study of the superconducting pairing mechanism for CeCu_2Si_2 as an application of the first-principles calculation of the multipole susceptibility.

4.1 First-principles tight-binding model

An effective tight-binding model of electronic states is helpful to analyze the orbital degree of freedom in strongly correlated systems and investigate the electronic structures in the context of topological phenomena. Downfolding by the Wannier function^{173, 289)} is a useful technique to obtain the effective hopping matrix in a real-space representation. Generally, the Fourier transformation of the thus-obtained hopping matrix provides the following hopping Hamiltonian in reciprocal space,

$$\begin{aligned} H_0 &= \sum_{\mathbf{k}} \sum_{\tau\tau'\ell\ell'\gamma\gamma'} h_{\mathbf{k}\tau\ell\gamma, \tau'\ell'\gamma'} a_{\mathbf{k}\tau\ell\gamma}^\dagger a_{\mathbf{k}\tau'\ell'\gamma'} \\ &= \sum_{\mathbf{k}} \sum_b \varepsilon_{kb} a_{kb}^\dagger a_{kb}, \end{aligned} \quad (14)$$

where a , a^\dagger are annihilation and creation operators, respectively, ε_{kb} the band energies, and $h_{\mathbf{k}\tau\ell\gamma, \tau'\ell'\gamma'}$ are the hopping Hamiltonian matrix elements. The hopping Hamiltonian can be

decomposed into three parts that read as follows:

$$\begin{aligned}
 H_0 = & \sum_k \left\{ \sum_{\gamma\gamma'}^{(f)} h_{k\gamma\gamma'}^{(f)} f_{k\gamma}^\dagger f_{k\gamma'} \right. \\
 & + \sum_{\tau\ell\gamma, \tau'\ell'\gamma'}^{(c)} h_{k\tau\ell\gamma, \tau'\ell'\gamma'}^{(c)} c_{k\tau\ell\gamma}^\dagger c_{k\tau'\ell'\gamma'} \\
 & \left. + \left(\sum_{\tau\ell\gamma}^{(c)} \sum_{\gamma'}^{(f)} V_{k\tau\ell\gamma\gamma'} c_{k\tau\ell\gamma}^\dagger f_{k\gamma'} + h.c. \right) \right\}, \tag{15}
 \end{aligned}$$

where the first term denotes the correlated f electrons, whose atom and orbital are represented with the index (f) , the second term denotes the non-interacting conduction electrons, represented by (c) , and the third represents the hybridization between them. The Hubbard type on-site interaction can be included for the correlated f electron space, as follows,

$$\begin{aligned}
 H'^{(f)} = & \frac{U}{2} \sum_m^{(f)} \sum_\sigma f_{m\sigma}^\dagger f_{m\bar{\sigma}}^\dagger f_{m\bar{\sigma}} f_{m\sigma} \\
 & + \frac{U'}{2} \sum_{m \neq m'}^{(f)} \sum_{\sigma\sigma'} f_{m\sigma}^\dagger f_{m'\sigma'}^\dagger f_{m'\sigma'} f_{m\sigma} \\
 & + \frac{J}{2} \sum_{m \neq m'}^{(f)} \sum_{\sigma\sigma'} f_{m\sigma}^\dagger f_{m'\sigma'}^\dagger f_{m\sigma'} f_{m'\sigma} \\
 & + \frac{J'}{2} \sum_{m \neq m'}^{(f)} \sum_\sigma f_{m\sigma}^\dagger f_{m\bar{\sigma}}^\dagger f_{m'\bar{\sigma}} f_{m'\sigma}. \tag{16}
 \end{aligned}$$

The obtained Hamiltonian is a kind of Anderson lattice model with a material's specific band structure. The electronic state can be analyzed with a variety of numerical techniques in strongly correlated systems, such as the DMFT method. Here we introduce the RPA susceptibilities obtained by the orthodox diagram expansion in terms of the Hubbard interaction defined above. They provide the first step to analyze the electronic state, and possible phase transitions into superconductivity and multipolar orderings.

4.2 Multipolar susceptibility

The generalized multipole-multipole correlation function in the correlated f -orbital space of two multipoles $A^{(f)}$ and $B^{(f)}$ can be evaluated from

$$\langle\langle A^{(f)}, B^{(f)} \rangle\rangle = \sum_{\gamma_1\gamma_2\gamma_3\gamma_4} A_{\gamma_2\gamma_1}^{(f)} \chi_{\gamma_1\gamma_2, \gamma_3\gamma_4}^{\text{RPA}(f)} B_{\gamma_3\gamma_4}^{(f)}, \tag{17}$$

where γ_i denotes one of the spin-orbital components and specific representations of multipoles $A^{(f)}$ and $B^{(f)}$ are given following the local (on-site) symmetry. $\chi^{\text{RPA}(f)}$ is the RPA

susceptibility defined as:

$$\chi_{\gamma_1\gamma_2,\gamma_3\gamma_4}^{\text{RPA}(f)}(\mathbf{q}) = \chi_{\gamma_1\gamma_2,\gamma_3\gamma_4}^{0(f)}(\mathbf{q}) + \sum_{\gamma_5\gamma_6\gamma_7\gamma_8} \chi_{\gamma_1\gamma_2,\gamma_5\gamma_6}^{0(f)}(\mathbf{q}) \Gamma_{\gamma_5\gamma_6,\gamma_7\gamma_8}^{0(f)} \chi_{\gamma_7\gamma_8,\gamma_3\gamma_4}^{\text{RPA}(f)}(\mathbf{q}), \quad (18)$$

$$\chi_{\gamma_1\gamma_2,\gamma_3\gamma_4}^{0(f)} = -T \sum_{\mathbf{k},n} G_{\gamma_1\gamma_3}^{0(f)}(\mathbf{k} + \mathbf{q}, i\omega_n) G_{\gamma_4\gamma_2}^{0(f)}(\mathbf{k}, i\omega_n), \quad (19)$$

where $\Gamma^{0(f)}$ is the four point vertex of Hubbard type interaction and $G^{0(f)}(\mathbf{k}, i\omega_n)$ is the non-interacting Green function with the momentum \mathbf{k} and Matsubara frequency ω_n ,

$$G_{\gamma\gamma'}^{0(f)}(\mathbf{k}, i\omega_n) = \frac{\langle (f)\gamma | \mathbf{k}, b \rangle \langle \mathbf{k}, b | (f)\gamma' \rangle}{i\omega_n - \varepsilon_{\mathbf{k}b} + \mu}. \quad (20)$$

In multi-orbital systems, vertex corrections can be crucial by hybridizing not only different wave vectors \mathbf{Q} and frequencies ω but also multi-channels such as electric and magnetic channels. The RPA susceptibility usually enhances a magnetic channel too much, and this can be improved by including the mode-mode coupling through the vertex corrections.^{160,288)}

4.3 Superconducting gap

Multipole fluctuations have also been applied to investigate theoretically the interaction mediating the Cooper pair formation of superconductivity in heavy electron system.¹⁷⁴⁾ The gap function $\Delta^{(f)}(\mathbf{k})$ is obtained by solving the linearized BCS gap equation,

$$\lambda \Delta_{\gamma\gamma'}^{(f)}(\mathbf{k}) = - \sum_{\mathbf{k}'} \sum_{\gamma_1\gamma_2\gamma_3\gamma_4} V_{\gamma_1\gamma_2,\gamma_3\gamma_4}^{(f)}(\mathbf{k} - \mathbf{k}') \times G_{\gamma_1\gamma_3}^{(f)}(\mathbf{k}') G_{\gamma_2\gamma_4}^{(f)}(\mathbf{k}')^* \Delta_{\gamma_3\gamma_4}^{(f)}, \quad (21)$$

with $V_{\gamma_1\gamma_2,\gamma_3\gamma_4}^{(f)}(\mathbf{k} - \mathbf{k}')$ the pairing potential defined by the multipolar fluctuations, given as

$$V_{\gamma_1\gamma_2,\gamma_3\gamma_4}^{(f)}(\mathbf{q}) = \Gamma_{\gamma_1\gamma_2,\gamma_3\gamma_4}^{0(f)} + \sum_{\gamma_5\gamma_6\gamma_7\gamma_8} \Gamma_{\gamma_1\gamma_2,\gamma_5\gamma_6}^{0(f)} \chi_{\gamma_5\gamma_6,\gamma_7\gamma_8}^{(f)}(\mathbf{q}) \Gamma_{\gamma_7\gamma_8,\gamma_3\gamma_4}^{0(f)}. \quad (22)$$

$\chi^{(f)}(\mathbf{q})$ is $\chi^{0(f)}(\mathbf{q})$ for the second-order perturbation and $\chi^{\text{RPA}(f)}(\mathbf{q})$ for the RPA. The transition temperature T_c is obtained as the temperature when the maximum eigenvalue λ is unity.²⁹⁰⁾

The first-principles calculation of multipole fluctuations was applied to investigate the pairing mechanism of superconductivity in the heavy Fermion compound CeCu₂Si₂¹⁷⁴⁾ and possible order parameters of hidden order phase of URu₂Si₂.¹⁶⁰⁾ In both cases, the first-principles calculations show a crucial contribution of high-rank magnetic multipoles to the multipole susceptibility.

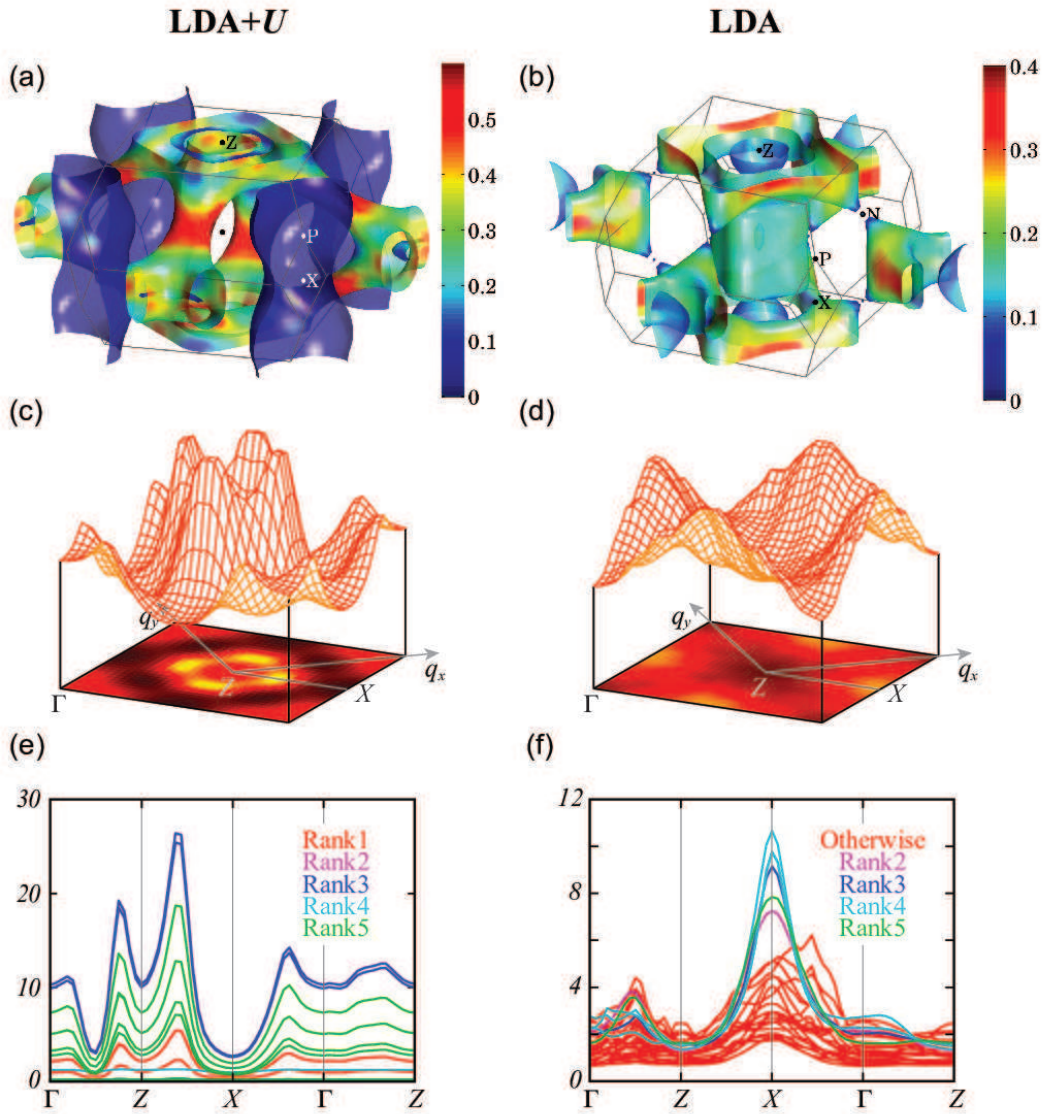


Fig. 9. (Color online) (Top) Calculated Fermi surface of nonmagnetic CeCu_2Si_2 colored by the Fermi velocity. (Middle) The in-plane magnetic dipole susceptibilities computed for $\mathbf{Q} = (q_x, q_y, 0.5)$, and (Bottom) a complete set of multipole susceptibilities along the high-symmetry lines. The left-hand figures correspond to the LDA+ U case, and the right-hand panels to the ordinary LDA case. In (c), incommensurate peaks at around $\mathbf{Q} = (0.21, 0.21, 0.5)$ and the corresponding points are consistent with INS measurement (from Ref.¹⁷⁴) ©2015 American Physical Society

4.4 CeCu_2Si_2

This compound is the first discovered heavy-Fermion superconductor.²⁹¹⁾ This compound crystallizes in the body-centered tetragonal structure (space group No. 139, $I4/mmm$). The

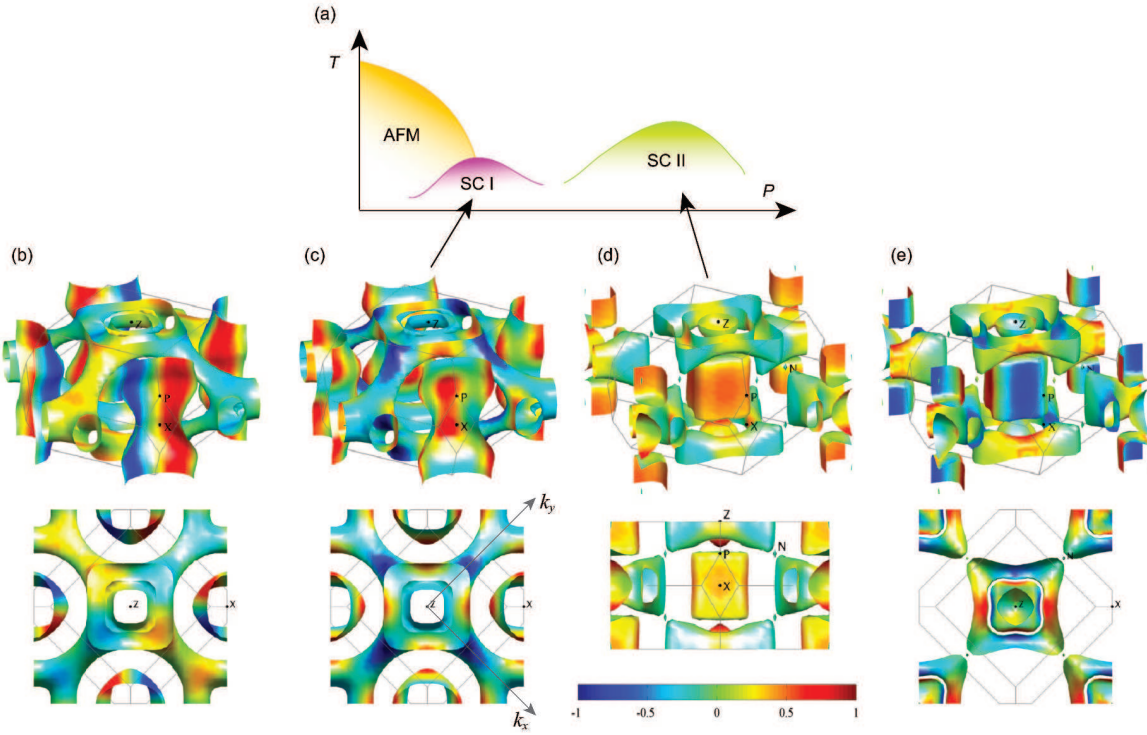


Fig. 10. (Color online) (a) Schematic pressure (P) – temperature (T) phase diagram for CeCu_2Si_2 , showing the AFM phase and two superconducting phases. (b–e) Possible superconducting gap structures corresponding to order parameters of (b) $d_{x^2-y^2}$ [$\sim \cos(2k_x) - \cos(2k_y)$], (c) s_{\pm} [$\sim \cos(2k_x) + \cos(2k_y)$] from the LDA+ U Fermi surface, (d) another type s_{\pm} [$\sim \cos(k_x)\cos(k_y)\cos(k_z)$] in the LDA case, and (e) d_{xy} -wave [$\sim \sin(k_x)\sin(k_y)\cos(k_z)$] pairing states. (From Ref.¹⁷⁴). ©2015 American Physical Society

BCS-like specific heat jump at the transition temperature ($T_c \leq 1$ K) indicates that the correlated heavy electrons form the Cooper pairs. It has long been considered that this is a prototypical example of a nodal d -wave superconductor mediated by magnetic fluctuations, based on several experimental observations, such as the T^2 behavior of low-temperature specific heat,^{292,293} no coherence peak just below T_c and the T^3 behavior in NMR relaxation rate $1/T_1$,^{294–296} and the resonance-like enhancement in inelastic neutron scattering (INS) measurements²⁹⁷ and so on.²⁹⁸ However, in contrast to these observations, the recent specific heat measurement,²⁹⁹ penetration depth, and thermal conductivity measured down to very low temperatures³⁰⁰ have indicated that the superconducting order parameter is fully gapped. Consequently, the gap structure and the pairing mechanism in this material have been hotly debated. Although generally the Fermi surface (FS) topology is crucially important for superconductivity, it is not yet so clear for CeCu_2Si_2 . Theoretically, two or three types of FSs have been proposed based on the ordinary LDA calculations,³⁰¹ LDA+ U method²⁹⁹ and the renormalized band theory³⁰² (See Figs. 9(a) and (b)). Figures 9(c) and (d) depict the correspond-

ing magnetic dipole susceptibilities calculated within RPA.¹⁷⁴⁾ They show the characteristic \mathbf{Q} structure due to Fermi surface nesting; an incommensurate peak at $\mathbf{Q} = (0.21, 0.21, 0.5)$ in Fig. 9(c), and a hump at around the X point in Fig. 9(d). The former is consistent with the peak position observed in the INS measurement,²⁹⁷⁾ while the latter has not been observed. This implies that the FS as obtained from the LDA+ U , that shows similar trends with that of the renormalized band theory, is more appropriate rather than the LDA FS. Figures 9(e) and (f) illustrate multipole susceptibilities along high-symmetry lines, computed with Eq. (17). The dominant fluctuations are of octupole type in Fig. 9(e) and of hexadecapole type in Fig. 9(f). Furthermore, from Eq. (21), these high-rank multipole fluctuations can lead to the $d_{x^2-y^2}$ -wave and s_{\pm} -wave pairing states (See Fig. 10). The latter is compatible with the full-gap nature observed recently.²⁹⁹⁾ It deserves to be mentioned, though, that quite recently, a study of the impurity effect by electron irradiation demonstrated the robustness of superconductivity against disorder,^{300,303)} indicative of conventional s -wave pairing without sign-change. Thus, this issue is still to be clarified along with the FS topology.

5. Hidden order

5.1 The hidden order phase of URu₂Si₂

The mysterious hidden order (HO) phase of the heavy-Fermion URu₂Si₂ has drawn much attention in condensed matter physics during the last three decades. URu₂Si₂, which crystallizes in the body-centered tetragonal structure (space group No. 139, $I4/mmm$), exhibits a clear second-order phase transition at $T_{HO}=17.5$ K, which is signaled by a large entropy loss,^{304–306)} a large reduction of the carrier number,^{304,307,308)} and the emergence of a partial gap.^{309–312)} Neutron and X-ray scattering investigations revealed that there exists a vanishingly small dipole magnetic moment in the HO phase,^{313–315)} which depends on sample purity but is much too small to explain the large entropy change seen at the phase transition.³¹⁶⁾ Unravelling the origin of the HO phase of URu₂Si₂ subsequently became the object of intense investigations, ongoing as much today. The underlying origin of the low-temperature order could not unambiguously be disclosed, even after thirty years (see Refs.^{161,317)} for recent reviews on the status of the HO).

NpO₂ has been the archetypal example of a compound displaying a HO phase, whose mystery has been solved in recent years, as discussed in Sec. 3.2. Applying the lessons learned from the great efforts paid to identify the HO phase of NpO₂ to solve the origin of the enigmatic HO phase of URu₂Si₂ can be helpful, however, it is important to realize that some properties of the electronic and ordered states in URu₂Si₂ are different from those of NpO₂.

which makes the situation for the identification of the order parameter more complex. One of the clear differences between the hidden order phase of URu_2Si_2 and the low-temperature magnetic multipolar phase of NpO_2 is the strong itinerant character of the f -electrons in URu_2Si_2 (see, e.g., Refs.^{318,319}), as compared to the localized $5f$ character of NpO_2 (see, e.g. Refs.^{9,133,135}), which causes an ambiguity for the experimental determination of the applicable CEF level scheme. Thus far, no evidence of localized f states or CEF excitations in URu_2Si_2 could be detected.¹⁶¹⁾ Another crucial difference between the two compounds is the symmetry property of the ordinary antiferromagnetic order in URu_2Si_2 .¹⁷²⁾ The latter property is in the focus of the Appendix.

The understanding of the electronic properties of URu_2Si_2 has nonetheless increased much. Among the interesting characteristics of URu_2Si_2 are the proximity of an antiferromagnetic (AFM) ordered phase that can be induced by a small pressure (of ~ 0.6 GPa).^{320–329)} Interestingly, the Fermi surfaces of URu_2Si_2 hardly change between the HO and AFM phases as obtained from de Haas-van Alphen and Shubnikov-de Haas measurements.^{330–333)} In spite of the nearly identical Fermi surfaces an unconventional superconducting phase only emerges out of the HO phase at temperatures below 1.5 K.^{308,334)} A further similarity of the phases is the appearance of a longitudinal spin wave mode at wavevector $Q_0 = (0, 0, 1)$ in the HO phase which freezes to become the static long-range order of the AFM phase.^{335,336)} One of the crucial questions in the quest for the origin of the HO has been: which symmetry is spontaneously broken at the HO transition? A number of recent measurements have provided evidence for a breaking of the body-centered translation vector in the HO phase, leading to a doubling of the unit cell and a folding of the Brillouin zone.^{337–339)} The breaking of time-reversal symmetry could not unambiguously be established (see, e.g. Refs.^{340–342}); the spuriously small magnetic dipole moment in the HO phase that could be of extrinsic origin prohibits an unambiguous identification. A remarkable set of experiments led to the conclusion that the four-fold symmetry of the tetragonal basal plane is broken and that the HO is hence a “nematic” phase.^{343–347)} Although this symmetry-breaking was reported e.g. in X-ray Bragg scattering³⁴⁶⁾ and NMR³⁴⁷⁾ experiments, the results of other microscopic probes such as the NQR spectra^{348,349)} still remain controversial. Furthermore, recent electronic Raman experiments^{162,163,339)} revealed a sharp low-lying excitation with A_{2g} symmetry. The static A_{2g} Raman signal closely resembles the uniform J_z susceptibility. In the HO phase, A_{1g} mode is also active. These findings may impose a strong constraint on the theoretical models.

So far, many theories have been proposed to explain the enigmatic HO phase of URu_2Si_2 (see Refs.^{161,317}). Among the proposed explanations, the possible formation of multipolar or-

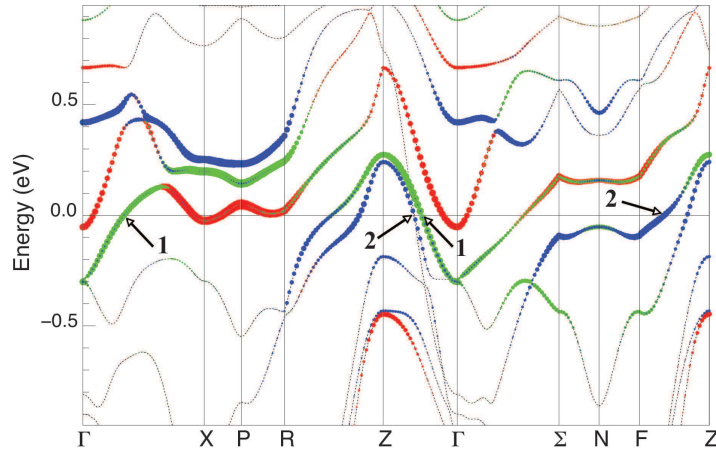


Fig. 11. (Color online) Band structure of nonmagnetic URu_2Si_2 in the BCT structure. Colors of the fat bands denote the uranium $5f_{5/2}$ character; specifically, green depicts the $j_z = \pm 5/2$ character, blue the $j_z = \pm 3/2$ character, and red the $j_z = \pm 1/2$ character. The indices 1 and 2 denote the nested bands at the Fermi energy that are predominately formed from $j_z = \pm 5/2$ and $\pm 3/2$ states (from Ref.³⁷¹⁾). ©2011 American Physical Society

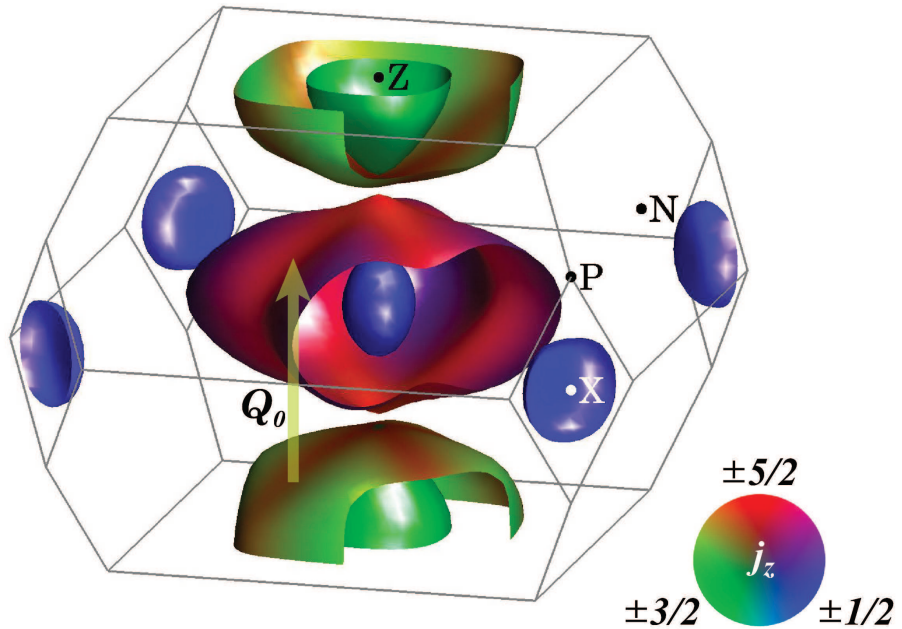


Fig. 12. (Color online) Calculated (LDA) Fermi surface of URu_2Si_2 with the amount $j=5/2$ orbital components indicated by the colors. (From Ref.¹⁶⁰⁾. ©2012 Macmillan Publishers Limited.

der on the uranium ion takes a prominent place.^{152–160, 162, 164, 350–355}) Other competing theories are based on the presence of a Fermi surface instability and a concomitant gap opening due to a rearrangement of itinerant $5f$ electrons near the Fermi energy.^{318, 356–368)} From a theoret-

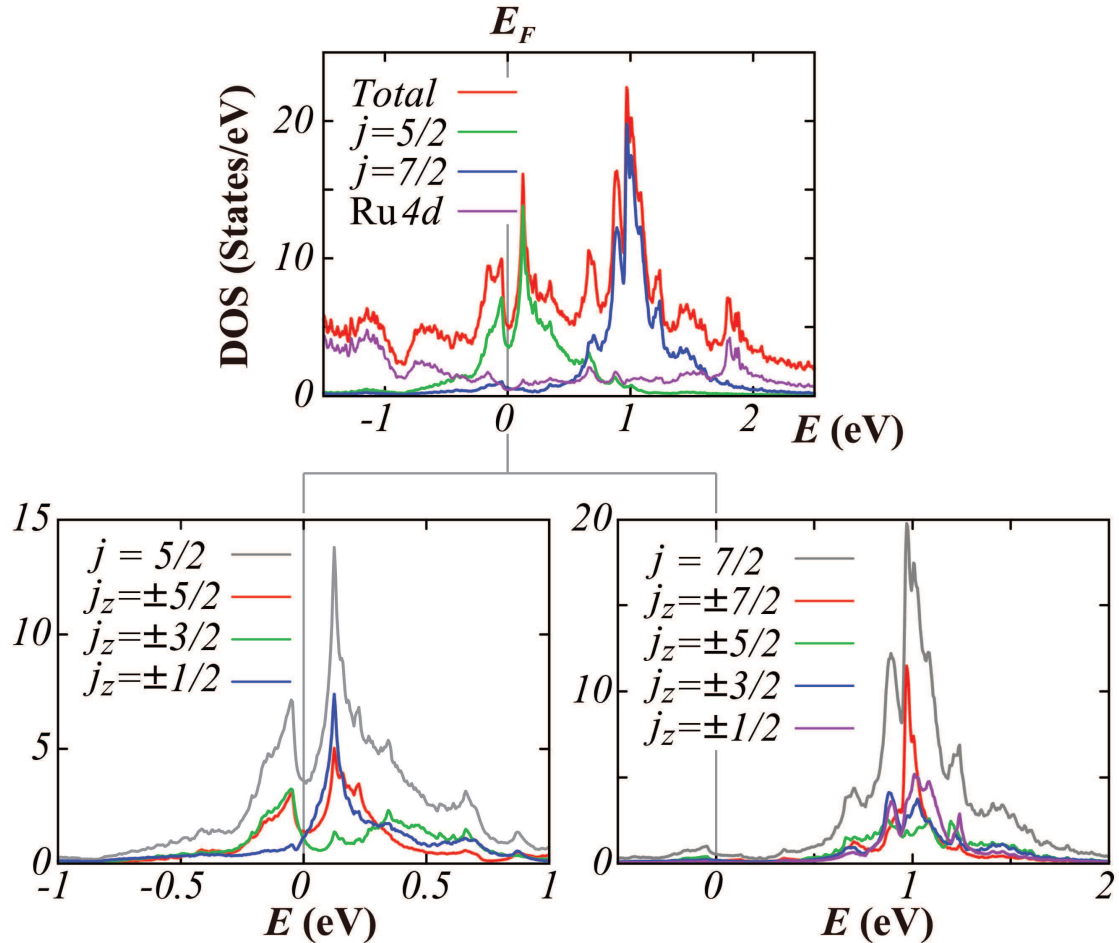


Fig. 13. (Color online) Partial density of states of URu_2Si_2 in the nonmagnetic state. The lower panels show the j_z -projected partial density of states for the $j = 5/2$ and $j = 7/2$ manifolds (from Ref.¹⁶⁰). ©2012 Macmillan Publishers Limited.

ical view point, the dual nature of f electrons, which can be itinerant or localized, makes the situation complicated. In addition, experimental techniques cannot straightforwardly provide evidence for one particular model. At present, as the primary HO parameter, dipolar magnetic order J_z can be excluded due to the presence of a bicritical point, at $p < 0.6 \text{ GPa}$ where the HO temperature and Néel temperature meet the first-order phase boundary of the HO-AFM transition,^{321,326–329} from which follows the different symmetries for the order parameters of the HO and AFM phases due to lacking of a bilinear term of these order parameters in the Landau free energy.^{152,367} Resonant X-ray scattering experiments could not observe any quadrupole.^{165,369} So far, the existence of higher order electric/magnetic multipole could not be unambiguously detected.^{166,370} Under such situation, *ab initio* calculations and the group theoretical approach^{157,172} can provide useful knowledge.

To predict the most likely multipoles, *ab initio* electronic structure calculations of URu_2Si_2 in the nonmagnetic and AFM phases have been performed.^{160,318,361,371–373} These calculations notably correctly reproduce many of the known properties of URu_2Si_2 , as e.g. details of the AFM phase, lattice properties and Fermi surface. First-principles calculation based on the LDA well reproduced the de Haas-van Alphen and Shubnikov-de Haas experiments.^{318,333,361} The calculated LDA band dispersions of URu_2Si_2 in the nonmagnetic phase are shown in Fig. 11. The colors highlight which bands have dominantly uranium $j = 5/2$ character.^{160,371} It can be recognized that the bands at the Fermi surface consist primarily of $j_z = \pm 5/2$, $\pm 3/2$, and $\pm 1/2$ states. The $j_z = \pm 5/2$ and $\pm 3/2$ bands (labeled 1 and 2) form two nested Fermi surface sheets that are connected by the nesting vector $\mathbf{Q}_0 = (0, 0, 1)$ as shown in Fig. 12. It can be recognized that the Γ and X-point pocket consist mainly of $j_z = \pm 1/2$ character, whereas the Z-point centered sheets contain dominantly $j_z = \pm 3/2$ character, and the large Γ -centered sheet $j_z = \pm 5/2$ character.

In Fig. 13 we show the calculated LDA density of states (DOS) in an energy interval around the Fermi energy.¹⁶⁰ It can again be observed that $5f$ states near the Fermi energy stem fully from the $j = 5/2$ sextuplet. The Fermi level is in the hybridization gap. The $j = 7/2$ multiplet is located at around 1 eV higher due to the S-O interaction. The $5f$ occupation number is 2.07 for $j = 5/2$ and 0.64 for $j = 7/2$.¹⁶⁰ The computed $5f$ occupation is consistent with several recent spectroscopic experiments.^{374,375}

In Fig. 14 we show the magnetization distributions of possible AF magnetic multipolar ordered (MPO) states around each uranium atomic site as calculated by the LDA+ U method, assuming a Coulomb $U = 2$ eV, which is relatively larger than theoretically expected values (less than 1.0 eV^{155,318}) to emphasize the characters of the distributions. In this figure, the spacial magnetization distributions reflect the magnetic symmetries for each IREP. The charge distributions show no qualitative change for the A_{1g}^- , A_{2g}^- , B_{1g}^- , B_{2g}^- -MPO states by preserving the same symmetry with that of the nonmagnetic state, but it is deformed in the E_g^- -MPO state reflecting the secondary induced ferroic E_g^+ electric multipolar order as discussed in the Appendix.

As shown in the following section, the multipole RPA susceptibility (Fig. 15) in this material indicated the dominant Ising-type J_z correlation at commensurate $\mathbf{Q}_0 = (0, 0, 1)$ due to the Fermi surface nesting. In addition, some high-rank multipole correlations are enhanced due to the j_z components on the nested Fermi surface, indicative of the E_g^- triakontadipole as the first candidate and A_{1g}^- triakontadipole as the second candidate for the possible multi-

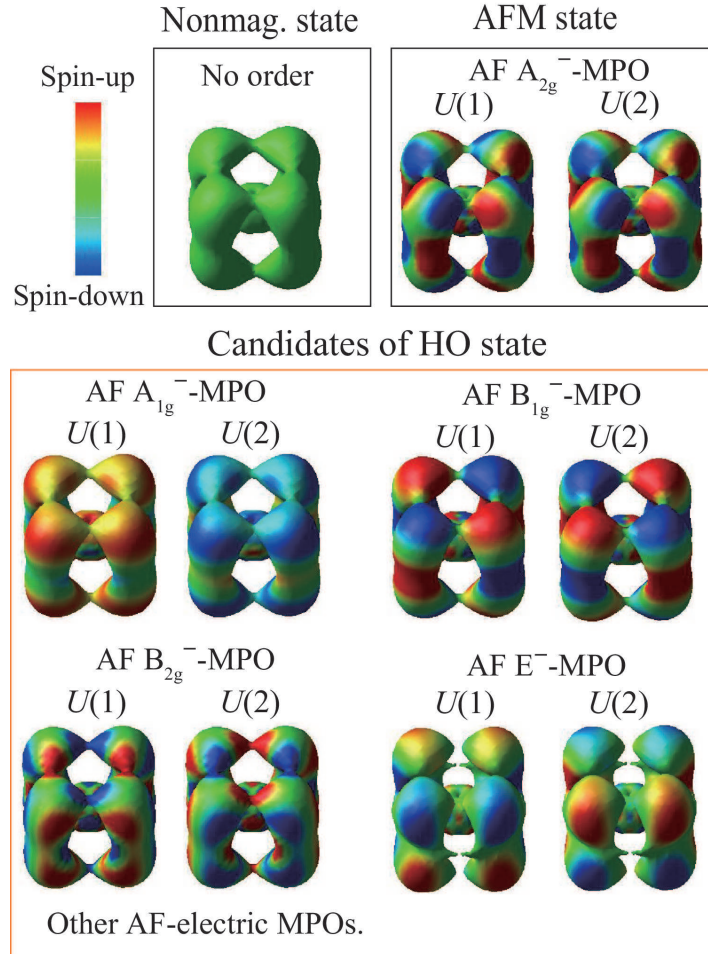


Fig. 14. (Color online) Charge density and magnetization distribution of magnetic multipolar ordered (MPO) states in URu_2Si_2 , computed with $U = 2 \text{ eV}$ and $J = 0$ in the LDA+ U method. The magnetization distributions depict the spin-component along the [001] axis and are shown on the isosurfaces of the charge densities on the two uranium ions related to one another by the body-center translation. The distributions are viewed from the [111] direction.

pole. Interestingly, the antiferroic configuration of the E_g^- and A_{1g}^- multipoles have completely different character from the view point of symmetry, as discussed in detail in the Appendix. First, the E_g^- multipole moments contain both the magnetic dipole and octupole moments, but the lowest rank multipole moment which belongs to the A_{1g}^- IREP contains only the triakontadipole moment. This means that ordering of E_g^- triakontadipole moments can bring with it these lower rank multipoles, though the rank-1 magnetic dipole moments are expected to be very small on the basis of the LDA+ U calculations,¹⁷²⁾ while the A_1^- multipole moments cannot. Second, since the multipoles of E_g^- IREP are transformed as an axial vector orthogonal to the four-fold rotation axis, this ordering breaks the four fold symmetry of the system while

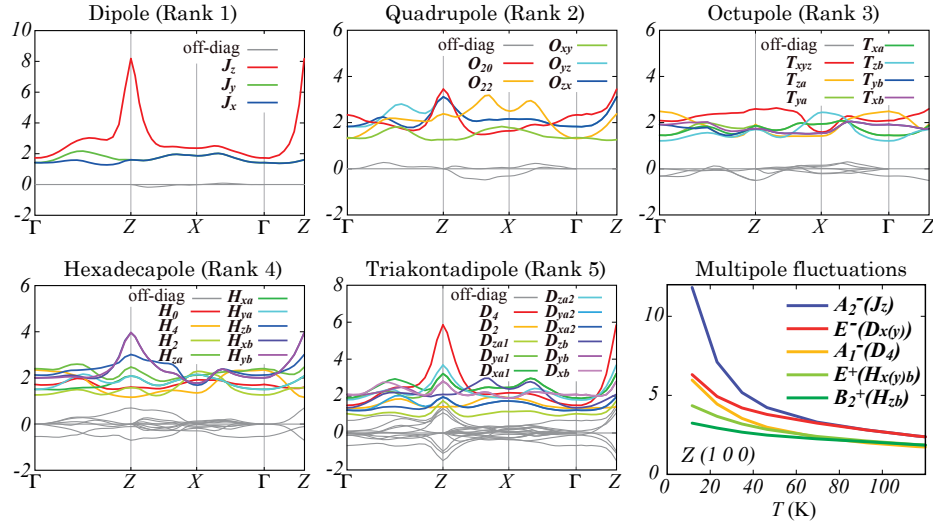


Fig. 15. (Color online) Multipole susceptibilities computed for URu_2Si_2 along high-symmetry lines in the BZ, using Eq. (17), and computed temperature dependence of the most divergent susceptibilities for each IREP at the Z point. The on-site multipoles J , O , T , H , and D denote the magnetic dipole (rank-1), electric quadrupole (rank-2), magnetic octupole (rank-3), electric hexadecapole (rank-4), and magnetic triakontadipole (rank-5), respectively, see Ref.¹⁶⁰⁾ for details of the specific representations. Note that in a generic k point, all rank multipoles with identical IREP in the little group of k can be mixed. It is implied by the presence of off-diagonal correlations.

the multipoles of A_{1g}^- representation invert their sign only through the time-reversal operation, and hence the corresponding order preserves the local point group symmetry.

5.2 Multipole susceptibilities

On the basis of the itinerant band structure and adopting a Coulomb $U \sim 1$ eV, for the nonmagnetic state of URu_2Si_2 , multipole fluctuations have been studied within the RPA and beyond.¹⁶⁰⁾ Figure 15 shows calculated multipole susceptibilities along the high symmetry lines. In the dipole susceptibilities, we can see that the J_z susceptibility shows a peak structure at the Z point and a hump structure at the incommensurate wavevector $\mathbf{Q}_1 = (1.4, 0, 0)$, while the in-plane $J_{x(y)}$ susceptibilities are inactive. These specific \mathbf{Q} vectors and the remarkable Ising-type anisotropy are consistent with the INS measurements.^{336, 376)} In addition, some high-rank multipole susceptibilities, such as that of hexadecapole and triakontadipole, are also enhanced at the Z point. These characteristic features come from the FS nesting and $j = 5/2$ f -orbital characters constructing the FS. Among these enhanced susceptibilities, the most divergent susceptibility provides a candidate for the HO parameter. Generally, since susceptibilities with the same IREP are mixed each other, the most divergent susceptibility

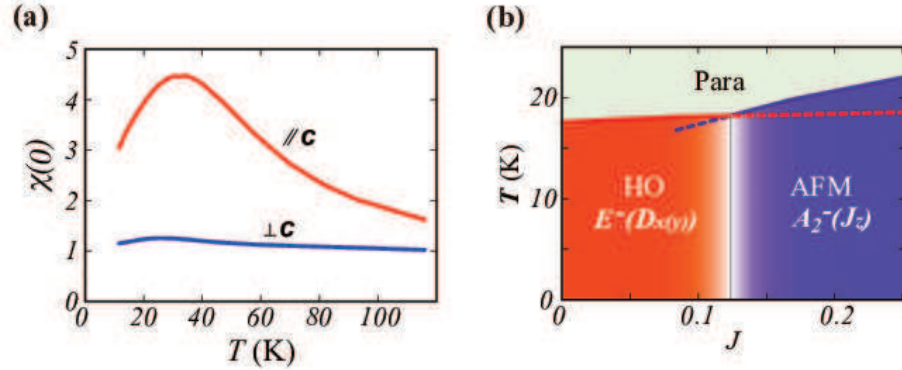


Fig. 16. (Color online) (a) Temperature dependence of uniform susceptibility obtained from beyond RPA calculations. (b) The phase diagram for the E^- order parameter as a function of the Hund's coupling parameter J (from Ref.¹⁶⁰). ©2012 Macmillan Publishers Limited.

is evaluated by diagonalizing $\hat{\chi}(\mathbf{Q}_0)$. As a consequence, antiferro E_g^- and A_{1g}^- multipolar ordered states with mainly triakontadipole components are obtained as candidates for the HO state. These order parameters are consistent with some observations that might imply time-reversal symmetry breaking, such as the internal field in NMR,³⁴²⁾ μ SR,³⁷⁷⁾ and the polar Kerr effect,³⁴⁰⁾ though it is not yet definitely established whether these experimental observations are intrinsic in the HO phase or not. Moreover, the E_g^- state is consistent with the reported nematic feature,^{343–347)} but induces in-plane dipole $J_{x(y)}$ moments, which are of the order of $10^{-4}\mu_B$, experimentally.^{342,378–380)}

Beyond the RPA calculations, including vertex corrections like the Maki-Thompson and the Aslamazov-Larkin terms, we can obtain the Ising-type uniform susceptibility (Fig. 16(a)), and near degeneracy of the E_g^- HO state and A_{2g}^- AFM state (Fig. 16(b)).¹⁶⁰⁾ This is the first example that the large Ising anisotropy in the static temperature-dependent magnetic susceptibility³⁰⁴⁾ was discussed on the basis of the first-principles electronic structure. The phase diagram of near-degenerate E_g^- and A_{2g}^- orderings is very similar to the pressure-temperature phase diagram.^{321,326–329)} This may indicate that the E_g^- multipole is the HO order parameter. On the other hand, in the LDA+DMFT approach,¹⁵⁶⁾ A_{2g}^+ hexadecapole order was discussed as the HO parameter. However, this multipole is not obtained from electronic structure calculations based on the (nearly) itinerant f -electron picture. The discrepancy is an issue to needs to be solved in the future. In this regard, recent analyses of a possible CEF level scheme in nonresonant inelastic X-ray scattering³⁸¹⁾ and in elastic constant measurements^{382,383)} could be helpful to understand the formation of the heavy-fermion state.

6. Cluster multipole theory

6.1 Cluster multipole and physical phenomena of magnetic compounds

Macroscopic physical phenomena are customary discussed with respect their specific order parameters; of recent interest in condensed matter physics are composite magnetic monopole moments and coupled electric and magnetic order parameters (e.g., in multiferroics).^{175–180, 183, 184, 384, 385)}

A new area, in which multipole moments recently gained importance, is that of the Hall conductivity in antiferromagnets. The anomalous Hall effect (AHE) is usually observed in ferromagnetic metals, and therefore it has traditionally been believed to be related to the nonzero ordered dipole magnetization. Meanwhile, the AHE has recently been studied for a certain type of noncollinear antiferromagnetic materials.^{386–398)} In particular, a large anomalous Hall conductivity (AHC) has been observed for noncollinear magnetic phases with only little resulting dipolar magnetization due to their noncollinear antiferromagnetic arrangement. These compounds have a vanishingly small macroscopic in-plane magnetization, of about $M \sim 0.002 \mu_B$ for Mn_3Sn ^{399, 400)} and $M \sim 0.005 \mu_B$ for Mn_3Ge .^{397, 398, 401)} Previously, non-co-planer magnetic alignments characterized by a finite scalar spin chirality was known to induce the AHE,³⁸⁴⁾ but the co-planer magnetic configuration of Mn_3Z has no such scalar spin chirality, which raises the question where the large AHC originates from. The magnetic degree of freedom which induces the AHE in Mn_3Z was recently identified by introducing the concept of the cluster multipole moment, which is an extension of the ordinary magnetic multipole moment that characterizes the magnetization distribution around an atomic site.¹⁸¹⁾

Cluster multipole theory offers an elegant way to obtain the magnetic order parameters that classify the broken magnetic point group symmetry due to the presence of the specific magnetic configuration in the crystal. To calculate these, one first has to determine the proper atomic clusters on which the cluster multipole moments are defined. For the magnetic order characterized by the ordering vector $\mathbf{q} = \mathbf{0}$, an atomic cluster in a crystal is defined as the atoms transformed in each other by the point symmetry operations in the space group \mathcal{G} of the crystal system. In case of $\mathbf{q} \neq \mathbf{0}$ order, whose magnetic unit cell is larger than the crystal unit cell, \mathcal{G} is replaced, in the same context, with the subgroup of the crystal space group reflecting the reduced translation and rotation symmetry operations with the super cell. The operation elements of the space group \mathcal{G} contains the translational operations combined with the point group operations. Symmorphic space groups have only the primitive translation operations which characterize the translation period. In this case, the atomic clusters consist of the atoms

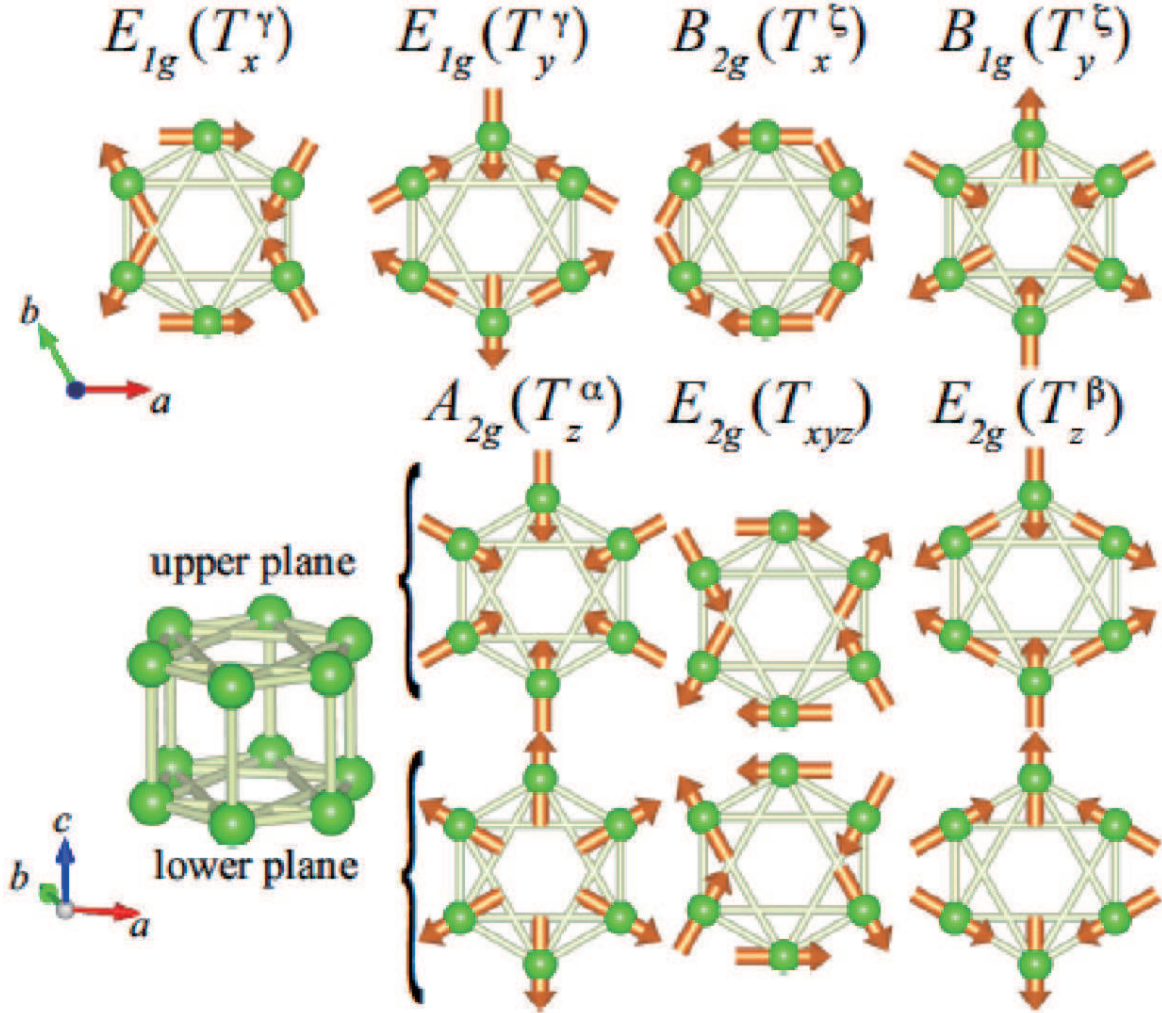


Fig. 17. (Color online) Examples of in-plane magnetic configurations of the hexagonal crystal structure that have zero cluster magnetic dipole moment but nonzero magnetic octupole moments, classified according to the D_{6h} IREPs (from Ref.¹⁸¹⁾). ©2017 American Physical Society

that are related to one another by the point group operation of \mathcal{G} in the magnetic unit cell. The other space groups \mathcal{G} , nonsymmorphic space groups, contain translation operations which differ from the primitive translations by a successive point group operation. These space groups can be decomposed as

$$\mathcal{G} = \sum_{i=1}^{N_{\text{coset}}} \{R_i | \tau_i\} \mathcal{H}, \quad (23)$$

where \mathcal{H} is the maximal symmorphic subgroup of \mathcal{G} . An atomic cluster is defined as the atoms related to one another by the point group operations of \mathcal{H} in the magnetic unit cell. Note that the origin of the cluster is determined, except the degree of freedom to choose the origin satisfying the space group operation, as the spacial point which satisfy all of the point

group symmetry of \mathcal{H} . Other clusters in the crystal are defined as well after shifting the origin by the translation τ_i in Eq. (23) and/or by the primitive translation operations.

Once the clusters have been identified the magnetic configuration in each cluster can be characterized by cluster multipole moments,¹⁸¹⁾ analogous to the local magnetic multipole moments of magnetic distributions on an atom, that are defined as

$$M_{pq}^{(\mu)} \equiv \sqrt{\frac{4\pi}{2p+1}} \sum_{i=1}^{N_{\text{atom}}^{(\mu)}} \nabla_i (|\mathbf{R}_i|^p Y_{pq}(\theta_i, \phi_i)^*) \cdot \mathbf{m}_i , \quad (24)$$

where $N_{\text{atom}}^{(\mu)}$ is the number of atoms of the μ -th cluster, \mathbf{m}_i is a magnetic moment on the i -th atom, $\nabla_i \equiv \frac{\partial}{\partial \mathbf{R}_i}$, $\mathbf{R}_i \equiv (X_i, Y_i, Z_i)$ is the position of the i -th atom, Y_{pq} are the spherical harmonics, and R_i , θ_i and ϕ_i are the distance, polar angle and azimuthal angle, respectively, of the i -th atom. Figure 17 shows examples of in-plane magnetic configurations characterized by cluster octupole moments classified according to the D_{6h} IREPs.¹⁸¹⁾ Summing up the multipole moments in all the clusters, one obtains the order parameters reflecting the broken magnetic point group symmetry caused by the presence of the periodic magnetic configuration in the crystal. The macroscopic magnetization of the cluster multipole moments is thus obtained by summing the cluster multipole moments for all atomic clusters,

$$M_{pq} = \frac{N_{\text{atom}}^{\text{u}}}{N_{\text{atom}}^{\text{c}}} \frac{1}{V} \sum_{\mu=1}^{N_{\text{cluster}}} M_{pq}^{(\mu)} , \quad (25)$$

where $N_{\text{atom}}^{\text{u}}$ is the number of atoms in the magnetic unit cell, N_{cluster} is the number of inequivalent clusters, which is the multiplication of the number of symmetrically inequivalent atoms by N_{coset} , and $N_{\text{atom}}^{\text{c}}$ is the number of atoms contained in these clusters. The macroscopic magnetization of the cluster multipoles is classified according to the point group symmetry of the crystal in the same way as the local multipole moments on atoms.^{6,11)} Since the appearance of macroscopic physical phenomena generated by magnetic states is determined by the magnetic point group symmetry, these physical phenomena could be characterized by the macroscopic magnetization of the cluster multipole moments.

6.2 Anomalous Hall effect and cluster multipole moments

Large anomalous Hall conductivities (AHC) have recently been observed in Mn_3Z ($\text{Z}=\text{Sn}$, Ge) that are noncollinear antiferromagnets with vanishingly small magnetization and, according to conventional understanding, should exhibit negligible anomalous Hall conductivities.^{396–398)} Mn_3Z crystallizes into the hexagonal structure that belongs to the space group $P6_3/mmc$ (No. 194, Fig. 18). The nonsymmorphic space group $P6_3/mmc$ is decomposed in

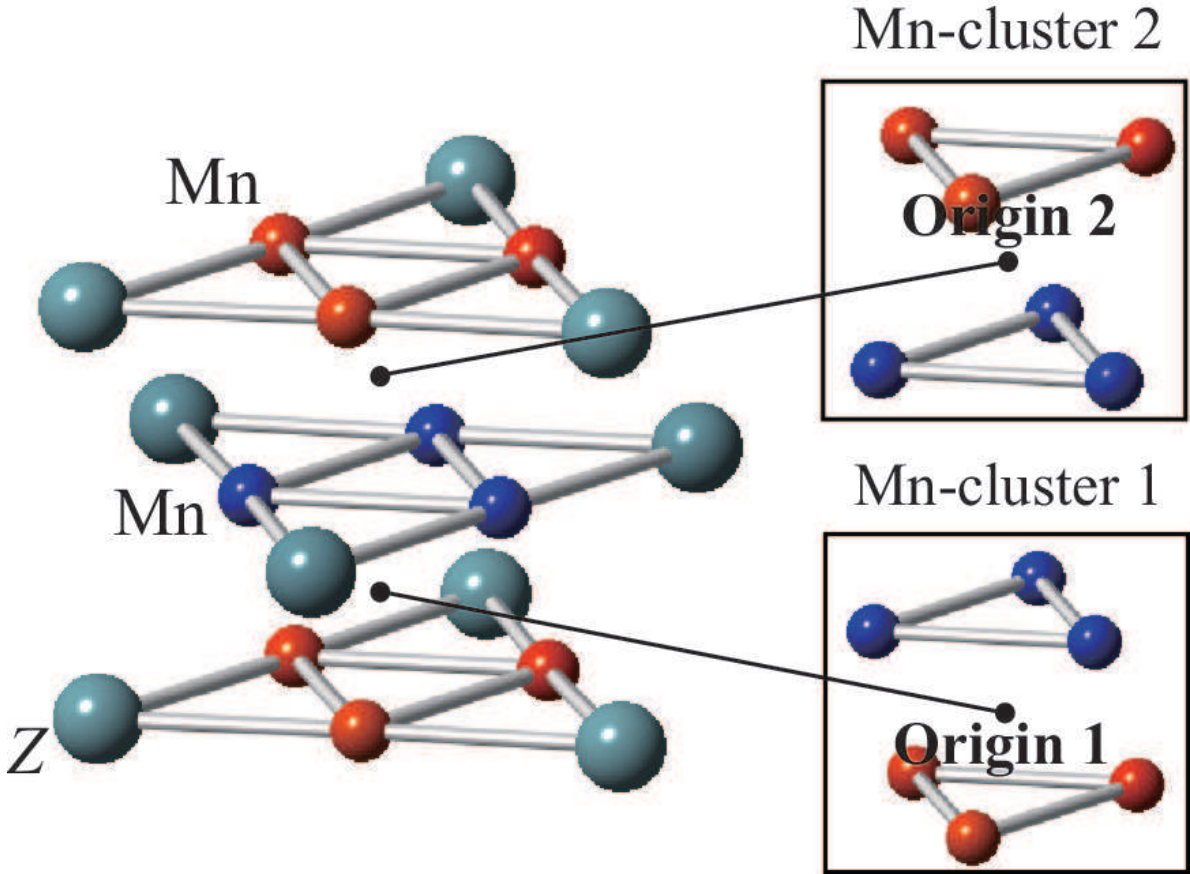


Fig. 18. (Color online) Crystal structure of the Mn_3Z compounds and the inequivalent atomic clusters on which the cluster multipole moments are defined for the $\mathbf{q} = \mathbf{0}$ magnetic order (from Ref.¹⁸¹).

the symmorphic space group $P\bar{3}m1$ such as $P6_3/mmc = P\bar{3}m1 + \{C_{2z}|\tau\}P\bar{3}m1$. Following the procedure discussed in Sec. 6.1, Mn atomic clusters in the Mn_3Z crystal are classified into two types, which consist of the atoms related to each other by the point group symmetry D_{3d} ($\bar{3}m1$), with the representative origins shown in Fig. 18. The cluster multipole moments are calculated on each cluster using Eq. (24), leading to the finite cluster octupole moments T_x^y and T_{xyz} as the lowest rank cluster multipole moment, and the macroscopic contribution is obtained by summing up the cluster multipole moments of these clusters following Eq. (25). Figure 19 shows an image of the procedure to determine the macroscopic order parameter of the cluster octupole moment for the noncollinear antiferromagnetic structure of Mn_3Z . The procedure of summing up the cluster multipole moments of the two types of atomic clusters corresponds to neglect the translation degree of freedom which relates the different clusters (see Fig. 19), and the resultant cluster multipole moments reflect the macroscopic symmetry breaking, i.e. the breaking of the paramagnetic D_{6h} point group symmetry, due to the presence of the magnetic configuration in the crystal.

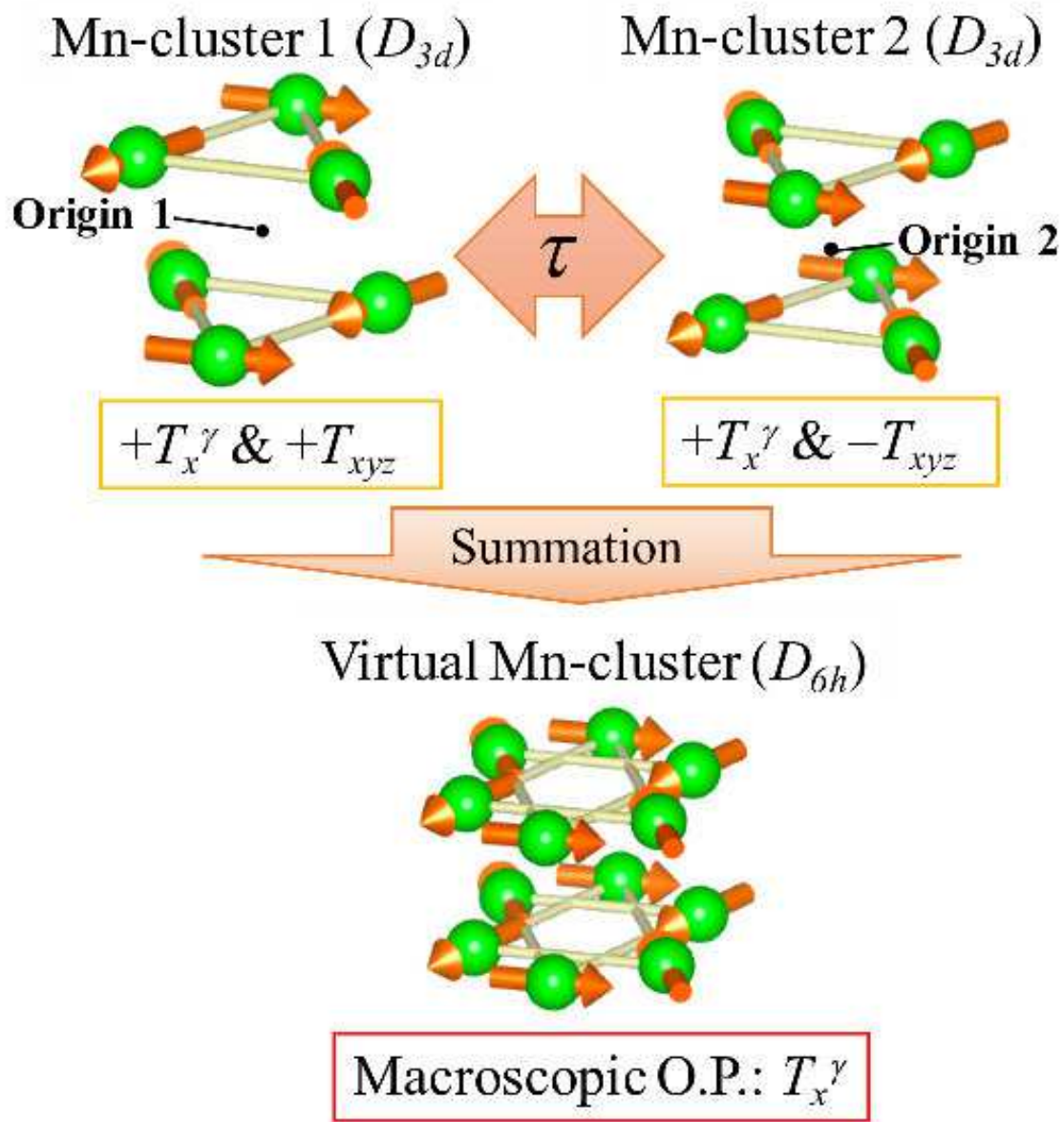


Fig. 19. (Color online) Schematics of the procedure to obtain the contribution of cluster multipole moments to the macroscopic order parameter (O.P.) in Mn_3Z .

The noncollinear antiferromagnetic structure of hexagonal Mn_3Sn has thus been found to be characterized by the rank-3 cluster octupole moment which notably, belongs to the same irreducible representation as the rank-1 cluster dipole moment that is obtained for the ordinary collinear ferromagnetic alignment of the magnetic moments.¹⁸¹⁾ Hence, these collinear ferromagnetic and noncollinear antiferromagnetic orders in fact break the same magnetic symmetry and belong completely to the same magnetic space group. This is the reason, from the view point of symmetry, why the noncollinear antiferromagnetic order of Mn_3Z can induce

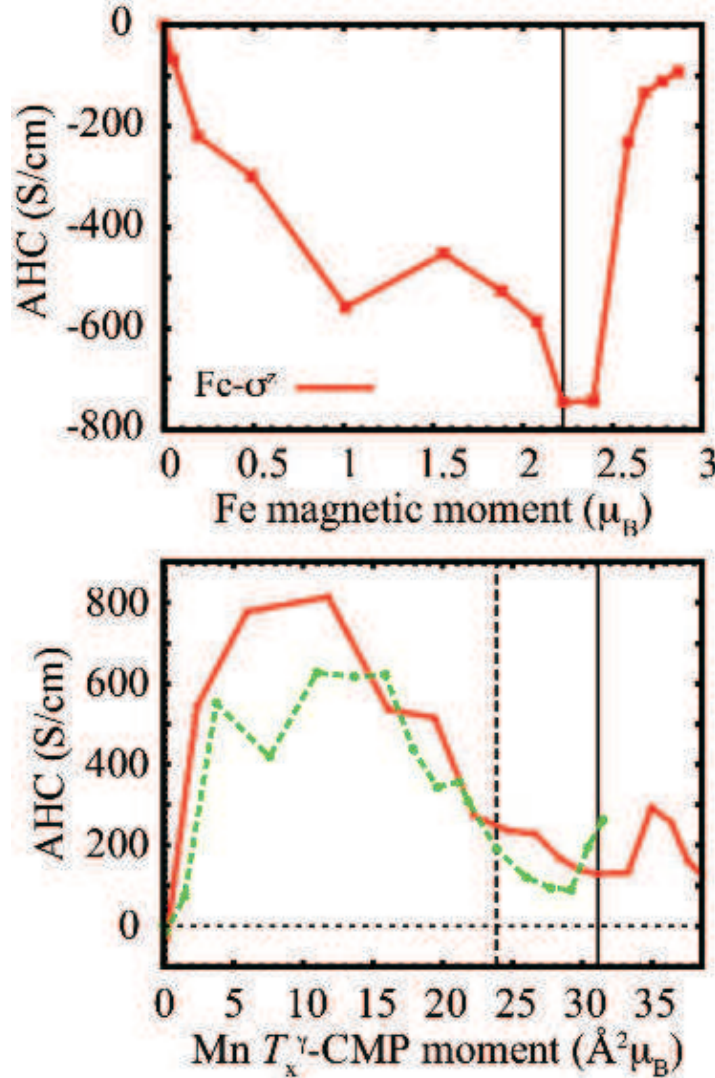


Fig. 20. (Color online) Calculated dependence of the anomalous Hall conductivity (AHC) on the dipole magnetic moment of BCC Fe (top panel) and on the cluster magnetic octupole moment of noncollinear antiferromagnetic Mn₃Z (Z=Sn, Ge) (bottom panel). (from Ref.¹⁸¹⁾) The moments obtained by the first-principles calculations are shown by the solid lines for BCC Fe and Mn₃Sn and by the dashed line for Mn₃Ge.

an AHC with the vanishingly small dipole magnetizations. On the other hand, the parasitic dipole magnetization can always appear for the AFM configurations that induce the AHC, as observed experimentally for Mn₃Z,^{397–401)} since the appearing symmetry conditions both for the dipole magnetization and for the AHC are totally the same when the S-O coupling is considered.¹⁸¹⁾ Importantly, the magnetic symmetry breaking is dominantly caused by the antiferromagnetic configuration that is classified by the cluster octupole moments, and the small dipolar magnetization is not required to induce the large AHC observed in Mn₃Z.

The meaningfulness of the cluster multipole expansion can be exemplified through direct

ab initio calculations of the AHC in relation to the multipole moments. The AHC can be calculated from a \mathbf{k} -space integration of the Berry curvature for the energy bands below the Fermi energy:

$$\sigma_{\alpha\beta} = -\frac{e^2}{\hbar} \int \frac{d\mathbf{k}}{(2\pi)^3} \sum_n f(\varepsilon_n(\mathbf{k}) - \mu) \Omega_{n,\alpha\beta}(\mathbf{k}), \quad (26)$$

where $\sigma_{\alpha\beta}$ is the off-diagonal anti-symmetric conductivity, n is the band index, f the Fermi function, μ the chemical potential, and $\alpha, \beta = x, y, z$ with $\alpha \neq \beta$. The Berry curvature for the AHC is defined as

$$\Omega_{n,\alpha\beta}(\mathbf{k}) = -2\text{Im} \sum_{m \neq n} \frac{v_{\alpha,mn}(\mathbf{k}) v_{\beta,mn}(\mathbf{k})}{[\varepsilon_m(\mathbf{k}) - \varepsilon_n(\mathbf{k})]^2}, \quad (27)$$

from the Kubo linear-response formula,^{402–404} where $v_{\alpha,mn}$ are the velocity matrix elements and $\varepsilon_n(\mathbf{k})$ the band energies. These can conveniently be obtained from a downfolding of *ab initio* calculated bands to a tight binding model that, discussed in Sec. 4.1, is useful to investigate the topological property of the electronic structure, such as Berry curvature and monopole charge, since the obtained tight binding model has a continuous phase factor of the eigenfunctions in \mathbf{k} -space.

Figure 20 shows the *ab initio* calculated dependence of the AHC on the size of the dipole magnetic moment in BCC Fe and the size of the cluster octupole moment of AFM Mn₃Z.¹⁸¹ The figure clearly establishes that the AHC depends on the cluster octupole moment of AFM Mn₃Z similar to the dependence of the AHC on the magnetic dipole moment of ferromagnetic Fe.

7. Concluding remarks

The multipole framework, which has already been employed for a long time in various branches of physics, has recently proven to be a very fruitful concept, too, in condensed matter physics. In the last three decades it has already become established that unconventional phases can be brought about by long-range ordering of multipole moments that have a higher rank than the conventional magnetic dipoles. A striking such example is the magnetic multipolar ordered phase of NpO₂, the origin of which could only be uncovered after more than three decades of intensive investigations.⁹⁾ Although the number of materials exhibiting long-range multipolar ordered phases is presently relatively small, these materials are precisely the ones that permit mankind to study the baffling interplay of several exotic order parameters and unveil as yet unknown aspects of fundamental interactions.

From the perspective of the electronic structure theory of solids it is gratifying that mod-

ern *ab initio* calculation techniques are now accurate enough and capable to predict from first-principles multipolar ordered states in solid state materials.^{122, 128)} These first-principles calculations are a powerful tool to provide deeper insight in the formation of multipole order in real materials. While CEF theory can often already explain the single-ion properties, the hybridizations between orbitals of neighboring atoms that occur in materials are not accounted for. However, these are important as precisely these lead to the formation of long-range order of multipoles in crystals. In the same way as long-range dipole magnetic order requires Heisenberg-Dirac exchange or Anderson super-exchange interactions to become stabilized at elevated temperatures, so do higher-order multipoles require a multipole-multipole exchange interaction for their stabilization.¹²⁸⁾ These exchange interactions can now be calculated using state-of-the-art electronic structure methods. It is however evident that there is still much uncharted territory in the *ab initio* theory of multipole order. For comparison, about two decades ago it became feasible to compute *ab initio* the Heisenberg exchange constants of elemental ferromagnets as Fe, Co, and Ni, and by mapping onto an effective Heisenberg dipole-moment Hamiltonian, compute the Curie ordering temperatures. Also the temperature dependence of the dipole order parameter could be explained (see e.g. Ref.^{405, 406)}). This comparison exemplifies that there is still much unexplored physics; in particular, the step to compute multipolar ordering temperatures and the temperature-dependence of the order parameter is yet to be made.

A second conclusion derived from the recent research on magnetic multipoles is that there is a huge potential for novel, exotic phenomena. One such example is superconductivity mediated by multipole fluctuations. The possibility of superconductivity driven by spin fluctuations has been discussed much in relation to heavy-Fermion superconductors and high-transition temperature cuprates.^{407, 408)} Even though it is difficult to demonstrate superconductivity caused by spin fluctuations, a new horizon opening up would be the possibility of superconductivity mediated by multipole fluctuations. In this respect, the origin of the unconventional superconductivity in URu_2Si_2 that emerges only out of the HO phase is not understood yet. And as discussed in this survey, magnetic multipole fluctuations could play a role for the superconductivity in the archetypal heavy-Fermion superconductor CeCu_2Si_2 .¹⁷⁴⁾

A third, more general conclusion that can be drawn from recent developments in cluster multipole theory, is that the multipole description has important bearings for the understanding of macroscopic phenomena in magnetic crystals. The new emerging understanding is that the multipole moments pertaining to the magnetic structure characterize magneto-electric phenomena. Thus, the cluster multipole theory offer fresh insight in how unexpected macro-

scopic properties can become realized.¹⁸¹⁾ These recent developments illustrate the power of the cluster multipole expansion of the magnetic structures in crystal by combining symmetry arguments. This then in turn opens up for as yet unexplored ways of predicting materials with unusual properties, based purely on the analysis of their crystal and magnetic point group symmetries. Even more, beyond the possibility of performing such analyses, there are prospects to search for such materials by employing numerical search routines in the future. There exist already extensive data bases of crystal structures that need now to be combined with the allowed magnetic configurations to provide multipole classifications. In combination with machine learning this might initiate new pathways for the discovery, and even design, of novel materials with intricate properties in the coming years.

Acknowledgment

We thank N. Magnani, T. Takimoto, Y. Matsuda, T. Shibauchi, T. Koretsune, M. Ochi, R. Arita for the collaborative works and R. Caciuffo, G. H. Lander, J. A. Mydosh, H. Kusunose, S. Nakatsuji, and H. Harima for fruitful discussions. This work has been supported by the JSPS KAKENHI (Grant Numbers JP15K17713, JP15H05883 (J-Physics), and JP16H04021, JP16H01081, JP15H05745, JP15H02014, JP24540369), the Swedish Research Council (VR), the K. and A. Wallenberg Foundation (Grant No. 2015.0060), and the Swedish National Infrastructure for Computing (SNIC).

Appendix: Symmetry of multipolar ordered states

Symmetry analysis is a crucial step to understand the electronic states in complex order phases. Indeed, the experimental identification of an ordered state is often equivalent to detect the physical object or scattering from it accompanied by a conspicuous symmetry breaking. Furthermore, setting an appropriate constraint on the magnetic symmetry is crucial to obtain a multipolar ordered state of interest as a convergent solution in selfconsistent electronic structure calculations. As discussed in Sec. 3.1, an LDA+*U* calculation for a multipolar ordered state requires the introduction of an appropriate symmetry breaking that permits the presence of the multipolar order.

The symmetry operations which preserve the multipolar order are determined from the transformation properties of the local multipole moments, classified according to the irreducible representations of the point group, and its configuration on the atoms which electron and spin density induce the multipole moments in the crystal. The symmetry property of

the multipolar order can be characterized by the magnetic space group (MSG, or Shubnikov group) as well as that of ordinary magnetic order. Once we identify the MSG of the multipolar order, we can further obtain information on local site symmetry of each atomic site in crystal, leading to conclusions about possible atomic distortion or secondary order parameters induced with the primary multipole order.¹⁷²⁾ Since the magnetic multipole moment whose rank is higher than one is often difficult to directly detect experimentally, information on the secondary order induced with the primary magnetic multipole order is often crucial to identify the ordered states.

Although there are exhaustive numbers of MSGs, these are all classified according to the following four types:⁴⁰⁹⁾

$$\mathcal{M} = \mathcal{G} \quad \text{Type I,} \quad (28)$$

$$\mathcal{M} = \mathcal{G} + \theta\mathcal{G} \quad \text{Type II,} \quad (29)$$

$$\mathcal{M} = \mathcal{H} + \theta(\mathcal{G} - \mathcal{H}) \quad \text{Type III,} \quad (30)$$

$$\mathcal{M} = \mathcal{G} + \theta\{E \mid \tau\}\mathcal{G} \quad \text{Type IV.} \quad (31)$$

Here \mathcal{M} is the MSG, θ is the time-reversal operation, \mathcal{G} is the ordinary space group, which do not have the symmetry operations including the time-reversal operation, \mathcal{H} is a subgroup of the ordinary space group \mathcal{G} whose number of symmetry operations is half of that of \mathcal{G} and $\mathcal{G} - \mathcal{H}$ contains no pure translations, $\{R \mid \tau\}$ is a successive transformation of a point group operation R , which is the identity operator E in Eq. (31), and a translation τ . The terms related to the time-reversal operation in Eqs. (29), (30), and (31) are called the anti-unitary part of the MSG. The type II MSG is called grey space groups, and the nonmagnetic orders, including pure electric multipole orders, belongs to the grey groups since these orders preserve the pure time-reversal symmetry. General magnetic multipolar ordered states that break pure time-reversal symmetry, belong either to type I, III, or IV MSG. As discussed below, the difference of the MSG's types of magnetic multipolar ordered states leads to qualitatively different consequences for the secondarily induced electric order parameters.

The type I MSG is called Fedorov group. In magnetic ordered states which belong to the Fedorov group $\mathcal{M} (= \mathcal{G})$, the symmetry of the charge distribution is characterized by the space group \mathcal{G} and is not distinguished from that of the magnetic order. The $3\mathbf{q}$ antiferroic multipolar ordered phases of UO_2 and NpO_2 belong to the MSGs $P\bar{a}3$ and $Pn\bar{3}m$, respectively,²⁸⁷⁾ which both belong to the Fedorov group in Eq. (28). The transverse $3\mathbf{q}$ magnetic T_{1g}^- dipole order of UO_2 and the longitudinal $3\mathbf{q}$ magnetic T_{2g}^- multipole order of NpO_2 induce

a $3\mathbf{q}$ ordering of the electric T_{2g}^+ quadrupole moments (Q_{yz} , Q_{zx} , Q_{xy}) as the secondary order. Concerning the local symmetry, the $Pa\bar{3}$ MSG of UO_2 leaves the oxygen atoms equivalent but allows for displacements of the oxygen sublattice since the Wyckoff position has one parameter, corresponding to the 8c site in $Pa\bar{3}$ space group. On the other hand, the $Pn\bar{3}m$ MSG of NpO_2 does not allow oxygen displacements but splits the oxygen atoms into two inequivalent atomic sites, corresponding to 2a and 6d sites of $Pn\bar{3}m$ space group.²⁸⁷⁾ This crucial difference between UO_2 and NpO_2 is confirmed by NMR experiments.^{410,411)}

The type III and IV MSGs are called black and white space groups, respectively. The magnetic ordered states which belong to these MSGs clearly distinguish the symmetry of the charge distribution from that of the magnetic order through the time-reversal related symmetry operations of the anti-unitary part in Eqs. (30) and (31), i.e. the symmetry of charge distribution belongs to \mathcal{G} and by $\mathcal{G} + \{E \mid \tau\}\mathcal{G}$ in the magnetic order of type III and type IV MSG, respectively, since the charge density is time-reversal even. Remarkably, in the magnetic multipolar ordered states of type IV MSG, the charge distribution is invariant under the pure translation operation τ , and the translation symmetry is broken only by the magnetic degree of freedom. The general consequence of the MSGs, discussed above, leads to a crucial difference between the low temperature magnetic multipolar phase of NpO_2 and the possible magnetic multipolar ordered states of URu_2Si_2 as the main candidates of the HO state.

The space group analysis of the HO phase in URu_2Si_2 identified possible $\mathbf{q} = (0, 0, 1)$ antiferroic multipolar orders that preserve the symmetry which is difficult to detect experimentally.^{157,166,172)} In particular, the antiferroic orders of the magnetic multipole moments which belong to one-dimensional IREPs (A_{1g}^- , A_{2g}^- , B_{1g}^- , B_{2g}^-) of the D_{4h} point group never break the crystal symmetry of the charge distribution, which is a consequence of the fact that the magnetic multipolar states belong to type IV MSG.^{166,172)} Furthermore, since the magnetic dipole moments belongs to the A_{2g}^- IREP, the A_{1g}^- , B_{1g}^- , and B_{2g}^- multipole moments contain no rank-1 magnetic dipole moment, and AF- A_{1g}^- and AF- B_{1g}^- orders especially do not induce the magnetic dipole moment at any atomic site in URu_2Si_2 from the symmetries.¹⁷²⁾ Meanwhile, the E_g^- multipole moments contain the in-plane rank-1 magnetic dipole moments, and AF- E_g^- multipolar order can induce a charge deformation corresponding to the *ferroic* electric E_g^+ multipolar order and the magnetic dipole moments at all of the atomic site in URu_2Si_2 .¹⁷²⁾ The symmetry breaking of the charge distribution can be related to the experimentally observed nematic feature in the HO phase,^{343–347)} although the existence of the nematic feature is still controversial.^{348,349)} On the other hand, the induced magnetic moments have not been experimentally confirmed as an intrinsic effect.^{342,378–380)}

The charge distribution of AF-*magnetic* multipolar ordered states in URu₂Si₂ are thus clearly distinguished from the magnetic distribution in terms of symmetry, and the *magnetic* AF- Γ^- multipolar ordered states always preserve the symmetry of the charge distribution higher than that of the corresponding electric AF- Γ^+ multipolar ordered states. From this perspective, the occurrence of the AF-*magnetic* multipolar ordered states is more effective to conceal the ordered states by preserving the charge symmetries higher than the ones of the electric multipolar ordered state. This crucial difference in the symmetry property of the magnetic multipolar order could be related to the difficulty of experimental detection of the symmetry breaking of the HO phase in URu₂Si₂.

References

- 1) R. E. Raab and O. L. De Lange, *Multipole Theory in Electromagnetism: Classical, quantum, and symmetry aspects, with applications* (Oxford University Press, Oxford, 2004).
- 2) P. A. M. Dirac, Proc. Roy. Soc. (London) A **133**, 60 (1931).
- 3) J. D. Jackson, *Classical Electrodynamics*, 3rd edition (J. Wiley & Sons, New York, 1998).
- 4) R. J. Blin-Stoyle, Rev. Mod. Phys. **28**, 75 (1956).
- 5) J. M. Blatt and V. F. Weisskopf, *Theoretical Nuclear Physics* (J. Wiley & Sons, New York, 1952).
- 6) H. Kusunose, J. Phys. Soc. Jpn. **77**, 064701 (2008).
- 7) Y. Kuramoto, Prog. Theor. Phys. Suppl. **176**, 77 (2008).
- 8) Y. Kuramoto, H. Kusunose, and A. Kiss, J. Phys. Soc. Jpn. **78**, 072001 (2009).
- 9) P. Santini, S. Carretta, G. Amoretti, R. Caciuffo, N. Magnani, and G. H. Lander, Rev. Mod. Phys. **81**, 807 (2009).
- 10) W. A. C. Erkelens, L. P. Regnault, P. Burlet, J. Rossat-Mignod, S. Kunii, and T. Kasuya, J. Magn. Magn. Mater. **63** & **64**, 61 (1987).
- 11) R. Shiina, H. Shiba, and P. Thalmeier, J. Phys. Soc. Jpn. **66**, 1741 (1997).
- 12) H. Nakao, K.-i. Magishi, Y. Wakabayashi, Y. Murakami, K. Koyama, K. Hirota, Y. Endoh, and S. Kunii, J. Phys. Soc. Jpn **70**, 1857 (2001).
- 13) O. Zaharko, P. Fischer, A. Schenck, S. Kunii, P.-J. Brown, F. Tasset, and T. Hansen, Phys. Rev. B **68**, 214401 (2003).
- 14) Y. Tanaka, K. Katsumata, S. Shimomura, and Y. Ōnuki, J. Phys. Soc. Jpn. **74**, 2201 (2005).
- 15) T. Matsumura, T. Yonemura, K. Kunimori, M. Sera, and F. Iga, Phys. Rev. Lett. **103**, 017203 (2009).
- 16) A. Akbari and P. Thalmeier, Phys. Rev. Lett. **108**, 146403 (2012).
- 17) T. Matsumura, T. Yonemura, K. Kunimori, M. Sera, F. Iga, T. Nagao, and J.-i. Igarashi, Phys. Rev. B **85**, 174417 (2012).
- 18) G. Friemel, Y. Li, A. V. Dukhnenko, N. Y. Shitsevalova, N. E. Sluchanko, A. Ivanov, V. B. Filipov, B. Keimer, and D. S. Inosov, Nat. Commun. **3**, 830 (2012).

- 19) T. Matsumura, H. Nakao, and Y. Murakami, *J. Phys. Soc. Jpn.* **82**, 021007 (2013).
- 20) Hoyoung Jang, G. Friemel, J. Ollivier, A. V. Dukhnenko, N. Yu. Shitsevalova, V. B. Filipov, B. Keimer, and D. S. Inosov, *Nat. Mater.* **13**, 682 (2014).
- 21) A. S. Cameron, G. Friemel, and D. S. Inosov, *Rep. Prog. Phys.* **79**, 066502 (2016).
- 22) J. Kitagawa, N. Takeda, and M. Ishikawa, *Phys. Rev. B* **53**, 5101 (1996).
- 23) Y. Nemoto, T. Yamaguchi, T. Horino, M. Akatsu, T. Yanagisawa, T. Goto, O. Suzuki, A. Dönni, and T. Komatsubara, *Phys. Rev. B* **68**, 184109 (2003).
- 24) T. Goto, T. Watanabe, S. Tsuduku, H. Kobayashi, Y. Nemoto, T. Yanagisawa, M. Akatsu, G. Ano, O. Suzuki, N. Takeda, A. Dönni, H. Kitazawa, *J. Phys. Soc. Jpn.* **78**, 024716 (2009).
- 25) L. Steinke, K. Mitsumoto, C. F. Miclea, F. Weickert, A. Dönni, M. Akatsu, Y. Nemoto, T. Goto, H. Kitazawa, P. Thalmeier, and M. Brando, *Phys. Rev. Lett.* **111**, 077202 (2013).
- 26) P. Y. Portnichenko, S. Paschen, A. Prokofiev, M. Vojta, A. S. Cameron, J.-M. Mignot, A. Ivanov, and D. S. Inosov, *Phys. Rev. B* **94**, 245132 (2016).
- 27) G. Ano, M. Akatsu, K. Araki, K. Matsuo, Y. Tachikawa, K. Mitsumoto, T. Yamaguchi, Y. Nemoto, T. Goto, N. Takeda, A. Dönni, and H. Kitazawa, *J. Phys. Soc. Jpn.* **81**, 034710 (2012).
- 28) P. P. Deen, A. M. Strydom, S. Paschen, D. T. Adroja, W. Kockelmann, and S. Rols, *Phys. Rev. B* **81**, 064427 (2010).
- 29) T. Goto, T. Horino, Y. Nemoto, T. Yamaguchi, A. Dönni, O. Suzuki, and T. Komatsubara, *Physica B* **312-313**, 492 (2002).
- 30) Y. Nemoto, T. Yamaguchi, T. Goto, O. Suzuki, T. Horino, A. Dönni, and T. Komatsubara, *J. Phys. Soc. Jpn.* **71**, 121 (2002).
- 31) J. Kitagawa, N. Takeda, M. Ishikawa, M. Nakayama, N. Kimura, and T. Komatsubara, *J. Phys. Soc. Jpn.* **69**, 883 (2000).
- 32) J. Kitagawa, N. Takeda, M. Ishikawa, T. Yoshida, A. Ishiguro, N. Kimura, and T. Komatsubara, *Phys. Rev. B* **57**, 7450 (1998).
- 33) E. Bucher, K. Andres, A. C. Gossard, and J. P. Maita, Proc. 13th Int. Conf. Low Temperature Physics, Vol. 2 (Plenum Publishing, New York, 1974) p. 322.
- 34) T. Tayama, T. Sakakibara, K. Kitami, M. Yokoyama, K. Tenya, H. Amitsuka, D. Aoki, Y. Ōnuki, and Z. Kletowski, *J. Phys. Soc. Jpn.* **70**, 248 (2001).

- 35) T. Onimaru, T. Sakakibara, N. Aso, H. Yoshizawa, H. S. Suzuki, and T. Takeu, *Phys. Rev. Lett.* **94**, 197201 (2005).
- 36) T. Onimaru, T. Sakakibara, N. Aso, H. Yoshizawa, H. S. Suzuki, and T. Takeuchi, *J. Phys. Soc. Jpn.* **75**, 186 (2006).
- 37) T. U. Ito, W. Higemoto, K. Ohishi, R. H. Heffner, N. Nishida, Y. Aoki, T. Onimaru, and H. S. Suzuki, *J. Magn. Magn. Mater.* **310**, 743 (2007).
- 38) O. Sakai, H. S. Suzuki, and H. Kitazawa, *J. Phys. Soc. Jpn.* **77**, 124714 (2008).
- 39) H. Onishi and T. Hotta *J. Phys. Soc. Jpn.* **77**, 199 (2008).
- 40) T. Ito, W. Higemoto, K. Ohishi, N. Nishida, R. Heffner, Y. Aoki, A. Amato, T. Onimaru, and H. Suzuki, *Phys. Rev. Lett.* **102**, 096403 (2009).
- 41) T. Kawae, M. Koga, Y. Sato, S. Makiyama, Y. Inagaki, N. Tateiwa, T. Fujiwara, H. S. Suzuki, and T. Kitai, *J. Phys. Soc. Jpn.* **82**, 073701 (2013).
- 42) K. Kubo and T. Hotta, *Phys. Rev. B* **95**, 054425 (2017).
- 43) H. Tanida, H. S. Suzuki, S. Takagi, H. Onodera, and K. Tanigaki, *J. Phys. Soc. Jpn.* **75**, 073705 (2006).
- 44) T. Morie, T. Sakakibara, H. S. Suzuki, H. Tanida, and S. Takagi, *J. Phys. Soc. Jpn.* **78**, 033705 (2009).
- 45) K. Araki, Y. Nemoto, M. Akatsu, S. Jumonji, T. Goto, H. S. Suzuki, H. Tanida, and S. Takagi *Phys. Rev. B* **84**, 045110 (2011).
- 46) K. Araki, T. Goto, K. Mitsumoto, Y. Nemoto, M. Akatsu, H. S. Suzuki, H. Tanida, S. Takagi, S. Yasin, S. Zherlitsyn, and J. Wosnitza *J. Phys. Soc. Jpn.* **81**, 023710 (2012).
- 47) K. Iwasa, Y. Watanabe, K. Kuwahara, M. Kohgi, H. Sugawara, T. D. Matsuda, Y. Aoki, and H. Sato, *Physica B* **312-312**, 834 (2002)
- 48) L. Hao, K. Iwasa, M. Nakajima, D. Kawana, K. Kuwahara, M. Kohgi, H. Sugawara, T. D. Matsuda, Y. Aoki, and H. Sato, *Acta Phys. Pol. B* **34**, 1113 (2003).
- 49) Y. Aoki, H. Sugawara, H. Harima, and H. Sato, *J. Phys. Soc. Jpn.* **74**, 209 (2005).
- 50) K. Iwasa, L. Hao, M. Kohgi, K. Kuwahara, J.-M. Mignot, H. Sugawara, Y. Aoki, T. D. Matsuda, and H. Sato, *J. Phys. Soc. Jpn.* **81**, 094711 (2012).
- 51) T. Tayama, Y. Isobe, T. Sakakibara, H. Sugawara, and H. Sato, *J. Phys. Soc. Jpn.* **78**, 044708 (2009).

- 52) H. Sugawara, E. Kuramochi, T. Namiki, T. D. Matsuda, Y. Aoki, and H. Sato, *J. Phys. Soc. Jpn.* **77**, 085001 (2008).
- 53) I. Ishii, T. Fujita, I. Mori, H. Sugawara, M. Yoshizawa, and T. Suzuki, *J. Phys. Soc. Jpn.* **77**, 303 (2008).
- 54) J. Kikuchi, M. Takigawa, H. Sugawara, and H. Sato, *J. Phys. Soc. Jpn.* **76**, 043705 (2007).
- 55) O. Sakai, J. Kikuchi, R. Shiina, H. Sato, H. Sugawara, M. Takigawa, H. Shiba, *J. Phys. Soc. Jpn.* **76**, 024710 (2007).
- 56) H. Sato, T. Sakakibara, T. Tayama, T. Onimaru, H. Sugawara, and H. Sato, *J. Phys. Soc. Jpn.* **76**, 064701 (2007).
- 57) L. Hao, K. Iwasa, K. Kuwahara, M. Kohgi, H. Sugawara, Y. Aoki, H. Sato, T. D. Matsuda, J.-M. Mignot, A. Gukasov, and M. Nishi, *Physica B* **359-361**, 871 (2005).
- 58) H. Sugawara, T. D. Matsuda, K. Abe, Y. Aoki, H. Sato, S. Nojiri, Y. Inada, R. Settai, and Y. Ōnuki, *Phys. Rev. B* **66**, 134411 (2002).
- 59) H. Sato, H. Sugawara, Y. Aoki, and H. Harima, in *Handbook of Magnetic Materials*, K. H. J. Buschow, Ed., Vol. **18**, pp. 1–110 (Elsevier, Amsterdam, The Netherlands, 2009).
- 60) T. Hotta, *J. Phys. Soc. Jpn.* **74**, 2425 (2005).
- 61) T. Hotta, *Phys. Research Int.* 762798 (2012).
- 62) H. Harima, *J. Phys. Soc. Jpn.* **77** Suppl. A, 114 (2008).
- 63) T. Goho and H. Harima, *J. Phys.: Conf. Ser.* **592**, 012100 (2015).
- 64) H. Okamura, N. Ohta, A. Takigawa, I. Matsutori, K. Shoji, K. Miyata, M. Matsunami, T. Nanba, H. Sugawara, C. Sekine, I. Shirotani, H. Sato, T. Moriwaki, Y. Ikemoto, Z. Liu, and G. L. Carr, *Phys. Rev. B* **85**, 205116 (2012).
- 65) R. Shiina, *J. Phys.: Conf. Ser.* **273**, 012141 (2011).
- 66) R. Shiina and H. Shiba, *J. Phys. Soc. Jpn.* **79**, 044704 (2010).
- 67) T. Takimoto, *J. Phys. Soc. Jpn.* **75**, 259 (2006).
- 68) K. Iwasa, L. Hao, K. Kuwahara, M. Kohgi, S. R. Saha, H. Sugawara, Y. Aoki, H. Sato, T. Tayama, and T. Sakakibara, *Phys. Rev. B* **72**, 024414 (2005).
- 69) T. Takimoto, *J. Phys. Soc. Jpn.* **75**, 034714 (2006).
- 70) T. Sakakibara, K. Yano, H. Sato, T. Tayama, J. Custers, H. Sugawara, Y. Aoki, and H. Sato, *J. Phys. Soc. Jpn.* **77**, 180 (2008).

- 71) M. Kohgi, K. Iwasa, M. Nakajima, N. Metoki, S. Araki, N. Bernhoeft, J.-M. Mignot, A. Gukasov, H. Sato, Y. Aoki, and H. Sugawara, *J. Phys. Soc. Jpn.* **72**, 1002 (2003).
- 72) Y. Aoki, T. Namiki, S. Ohsaki, S. R. Saha, H. Sugawara, and H. Sato, *J. Phys. Soc. Jpn.* **71**, 2098 (2002).
- 73) T. Tayama, T. Sakakibara, H. Sugawara, Y. Aoki, and H. Sato, *J. Phys. Soc. Jpn.* **72**, 1516 (2003).
- 74) R. Shiina and Y. Aoki, *J. Phys. Soc. Jpn.* **73**, 541 (2004).
- 75) M. Yogi, T. Nagai, Y. Imamura, H. Mukuda, Y. Kitaoka, D. Kikuchi, H. Sugawara, Y. Aoki, H. Sato, and H. Harima, *J. Phys. Soc. Jpn.* **75**, 124702 (2006).
- 76) K. Iwasa, K. Saito, Y. Murakami, and H. Sugawara, *Phys. Rev. B* **79**, 235113 (2009).
- 77) A. Kiss and Y. Kuramoto, *J. Phys. Soc. Jpn.* **75**, 103704 (2006).
- 78) S. Masaki, T. Mito, N. Oki, S. Wada, and N. Takeda, *J. Phys. Soc. Jpn.* **75**, 053708 (2006).
- 79) T. Matsumura, S. Michimura, T. Inami, K. Fushiya, T. D. Matsuda, R. Higashinaka, Y. Aoki, and H. Sugawara, *Phys. Rev. B* **94**, 184425 (2016).
- 80) Y. Aoki, S. Sanada, D. Kikuchi, H. Sugawara, and H. Sato, *J. Phys. Soc. Jpn.* **76**, 113703 (2007).
- 81) R. Shiina, *J. Phys. Soc. Jpn.* **82**, 083713 (2013).
- 82) T. Matsumura, S. Michimura, T. Inami, Y. Hayashi, K. Fushiya, T. D. Matsuda, R. Higashinaka, Y. Aoki, and H. Sugawara, *Phys. Rev. B* **89**, 161116 (2014).
- 83) T. Onimaru, K. T. Matsumoto, Y. F. Inoue, K. Umeo, T. Sakakibara, Y. Karaki, M. Kubota, and T. Takabatake, *Phys. Rev. Lett.* **106**, 177001 (2011)
- 84) T. Onimaru, K. Izawa, K. T. Matsumoto, T. Yoshida, Y. Machida, T. Ikeura, K. Wakiya, K. Umeo, S. Kittaka, K. Araki, T. Sakakibara, and T. Takabatake, *Phys. Rev. B* **94**, 075134 (2016).
- 85) T. Onimaru and H. Kusunose, *J. Phys. Soc. Jpn.* **85**, 082002 (2016).
- 86) K. Iwasa, K. T. Matsumoto, T. Onimaru, T. Takabatake, J.-M. Mignot, and A. Gukasov, *Phys. Rev. B* **95**, 155106 (2017).
- 87) T. Taniguchi, M. Yoshida, H. Takeda, M. Takigawa, M. Tsujimoto, A. Sakai, Y. Matsumoto, and S. Nakatsuji, *J. Phys. Soc. Jpn.* **85**, 113703 (2016).

- 88) Y. Shimura, M. Tsujimoto, B. Zeng, L. Balicas, A. Sakai, and S. Nakatsuji, Phys. Rev. B **91**, 241102 (2015).
- 89) K. T. Matsumoto, T. Onimaru, K. Wakiya, K. Umeo, and T. Takabatake, J. Phys. Soc. Jpn. **84**, 063703 (2015).
- 90) T. Kubo, H. Kotegawa, H. Tou, R. Higashinaka, A. Nakama, Y. Aoki, and H. Sato, J. Phys. Soc. Jpn. **84**, 074701 (2015).
- 91) A. Tsuruta and K. Miyake, J. Phys. Soc. Jpn. **84**, 114714 (2015).
- 92) M. Tsujimoto, Y. Matsumoto, T. Tomita, A. Sakai, and S. Nakatsuji, Phys. Rev. Lett. **113**, 267001 (2014).
- 93) I. Ishii, H. Muneshige, S. Kamikawa, T. K. Fujita, T. Onimaru, N. Nagasawa, T. Takabatake, T. Suzuki, G. Ano, M. Akatsu, Y. Nemoto, and T. Goto Phys. Rev. B **87**, 205106 (2013).
- 94) K. Matsubayashi, T. Tanaka, A. Sakai, S. Nakatsuji, Y. Kubo, and Y. Uwatoko, Phys. Rev. Lett. **109**, 187004 (2012).
- 95) T. Onimaru, N. Nagasawa, K. T. Matsumoto, K. Wakiya, K. Umeo, S. Kittaka, T. Sakakibara, Y. Matsushita, and T. Takabatake, Phys. Rev. B **86**, 184426 (2012).
- 96) A. Sakai, K. Kuga, and S. Nakatsuji, J. Phys. Soc. Jpn. **81**, 083702 (2012).
- 97) I. Ishii, H. Muneshige, Y. Suetomi, T. K. Fujita, T. Onimaru, K. T. Matsumoto, T. Takabatake, K. Araki, M. Akatsu, Y. Nemoto, T. Goto, and T. Suzuki, J. Phys. Soc. Jpn. **80**, 093601 (2011).
- 98) H. Yamauchi, H. Onodera, K. Ohoyama, T. Onimaru, M. Kosaka, M. Ohashi, and Y. Yamaguchi, J. Phys. Soc. Jpn. **68**, 2057 (1999).
- 99) Y. Tanaka, T. Inami, T. Nakamura, H. Yamauchi, H. Onodera, K. Ohoyama, and Y. Yamaguchi, J. Phys.: Condens. Matter **11**, L505 (1999).
- 100) K. Hirota, N. Oumi, T. Matsumura, H. Nakao, Y. Wakabayashi, Y. Murakami, and Y. Endoh, Phys. Rev. Lett. **84**, 2706 (2000).
- 101) S. W. Lovesey, E. Balcar, K. S. Knight, and J. Fernández Rodríguez, Phys. Rep. **411**, 233 (2005).
- 102) Y. Tanaka, T. Inami, S. Lovesey, K. Knight, F. Yakhou, D. Mannix, J. Kokubun, M. Kanazawa, K. Ishida, S. Nanao, T. Nakamura, H. Yamauchi, H. Onodera, K. Ohoyama, and Y. Yamaguchi, Phys. Rev. B **69**, 024417 (2004).

- 103) U. Staub, A. Mulders, O. Zaharko, S. Janssen, T. Nakamura, and S. Lovesey, *Phys. Rev. Lett.* **94**, 036408 (2005).
- 104) A. M. Mulders, U. Staub, V. Scagnoli, S. W. Lovesey, E. Balcar, T. Nakamura, A. Kikkawa, G. van der Laan, J. M. Tonnerre, *J. Phys.: Condens. Matter* **18**, 11195 (2006).
- 105) T. Matsumura, D. Okuyama, N. Oumi, K. Hirota, H. Nakao, Y. Murakami, and Y. Wakabayashi, *J. Phys. Soc. Jpn.* **74**, 1500 (2005).
- 106) T. Matsumura, N. Oumi, K. Hirota, H. Nakao, Y. Murakami, Y. Wakabayashi, T. Arima, S. Ishihara and Y. Endoh, *Phys. Rev. B* **65**, 94420 (2002).
- 107) J. Fernández Rodríguez, A. Mirone, and U. Staub, *J. Phys.: Condens. Matter* **22**, 016001 (2010).
- 108) A. J. Princep, A. M. Mulders, U. Staub, V. Scagnoli, T. Nakamura, A. Kikkawa, S. W. Lovesey, and E. Balcar., *J. Phys.: Condens. Matter* **23**, 266002 (2011).
- 109) T. Yanagisawa, T. Moriwaki, Y. Nemoto, T. Goto, R. Watanuki, and K. Suzuki *J. Phys. Soc. Jpn.* **74**, 1666 (2005).
- 110) T. Yanagisawa, T. Goto, Y. Nemoto, R. Watanuki, K. Suzuki, O. Suzuki, and G. Kido, *Phys. Rev. B* **71**, 104416 (2005).
- 111) P. Manuel, D. T. Adroja, R.I . Bewley, and B. D. Rainford, *J. Magn. Magn. Mater.* **310**, 757 (2007).
- 112) H. Yamauchi, T. Osakabe, E. Matsuoka, and H. Onodera, *J. Phys. Soc. Jpn.* **81**, 034715 (2012).
- 113) E. Matsuoka, J. Kitagawa, K. Ohoyama, H. Yoshizawa, and M. Ishikawa, *J. Phys: Condens. Matter* **13**, 11009 (2001).
- 114) E. Matsuoka, Z. Hiroi, and M. Ishikawa, *J. Phys. Chem. Solids* **63**, 1219 (2002).
- 115) L. Keller, V. Pomjakushin, K. Conder, and A. Schenck, *Phys. Rev. B* **70**, 060407(R) (2004).
- 116) E. Matsuoka, T. Tayama, T. Sakakibara, Z. Hiroi, N. Shirakawa, N. Takeda, and M. Ishikawa, *J. Phys. Soc. Jpn.* **76**, 084717 (2007).
- 117) E. Matsuoka, D. Usui, Y. Sasaki, H. Nakao, H. Shida, K. Ohoyama, and H. Onodera, *J. Phys. Soc. Jpn.* **77**, 114706 (2008).
- 118) S. Michimura, T. Inami, E. Matsuoka, M. Watahiki, K. Tanigaki, and H. Onodera, *J. Phys. Soc. Jpn.* **81**, 044711 (2012).

- 119) K. Abe, J. Kitagawa, N. Takeda, and M. Ishikawa, Phys. Rev. Lett. **83**, 5366 (1999).
- 120) S. Carretta, P. Santini, R. Caciuffo, and G. Amoretti, Phys. Rev. Lett. **105**, 167201 (2010).
- 121) R. Caciuffo, P. Santini, S. Carretta, G. Amoretti, A. Hiess, N. Magnani, L.-P. Regnault, and G. H. Lander, Phys. Rev. B **84**, 104409 (2011).
- 122) M.-T. Suzuki, N. Magnani, and P. M. Oppeneer, Phys. Rev. B **88**, 195146 (2013).
- 123) S. B. Wilkins, R. Caciuffo, C. Detlefs, J. Rebizant, E. Colineau, F. Wastin, and G. H. Lander, Phys. Rev. B **73**, 060406(R) (2006).
- 124) P. Burlet, J. Rossat-Mignod, S. Quezel, O. Vogt, J. C. Spirlet, and J. Rebizant, J. Less-Common Metals **121**, 121 (1986).
- 125) S. Di Matteo, N. Magnani, F. Wastin, J. Rebizant, and R. Caciuffo, J. Alloys Compnd. **444-445**, 278 (2007).
- 126) J. A. Paixão, C. Detlefs, M. J. Longfield, R. Caciuffo, P. Santini, N. Bernhoeft, J. Rebizant, and G. H. Lander, Phys. Rev. Lett. **89**, 187202 (2002).
- 127) Y. Tokunaga, Y. Homma, S. Kambe, D. Aoki, H. Sakai, E. Yamamoto, A. Nakamura, Y. Shiokawa, R. E. Walstedt, and H. Yasuoka, Phys. Rev. Lett. **94**, 137209 (2005).
- 128) M.-T. Suzuki, N. Magnani, and P. M. Oppeneer, Phys. Rev. B **82**, 241103(R) (2010).
- 129) P. Erdös, G. Solt, Z. Żolnierk, A. Blaise, and J. M. Fournier, Physica B **102**, 164 (1980).
- 130) R. Caciuffo, G. H. Lander, J. M. Fournier, and W. F. Kuhs, Solid State Commun. **64**, 149 (1987).
- 131) W. Kopmann, F. J. Litterst, H.-H. Klauß, M. Hillberg, W. Wagener, G. M. Kalvius, E. Schreier, F. J. Burghart, J. Rebizant, and G. H. Lander, J. Alloys Compnd. **271-273**, 463 (1998).
- 132) P. Santini and G. Amoretti, Phys. Rev. Lett. **85**, 2188 (2000).
- 133) R. Caciuffo, J. A. Paixão, C. Detlefs, M. J. Longfield, P. Santini, N. Bernhoeft, J. Rebizant, and G. H. Lander, J. Phys.: Condens. Matter **15**, S2287 (2003).
- 134) Y. Tokunaga, D. Aoki, Y. Homma, S. Kambe, H. Sakai, S. Ikeda, T. Fujimoto, R. E. Walstedt, H. Yasuoka, E. Yamamoto, A. Nakamura, and Y. Shiokawa, Phys. Rev. Lett. **97**, 257601 (2006).
- 135) O. Sakai, R. Shiina, and H. Shiba, J. Phys. Soc. Jpn. **74**, 457 (2005).

- 136) P. Santini, S. Carretta, N. Magnani, G. Amoretti, and R. Caciuffo, *Phys. Rev. Lett.* **97**, 207203 (2006).
- 137) K. Kubo and T. Hotta, *Phys. Rev. B* **72**, 144401 (2005).
- 138) T. Hotta, *Phys. Rev. B* **80**, 024408 (2009).
- 139) R. E. Walstedt, Y. Tokunaga, S. Kambe, *Compt. Rend. Physiq.* **15**, 563 (2014).
- 140) Y. Tokunaga, T. Nishi, M. Nakada, A. Itoh, H. Sakai, S. Kambe, Y. Homma, F. Honda, D. Aoki, and R. E. Walstedt, *Phys. Rev. B* **89**, 214416 (2014).
- 141) N. Lingg, D. Maurer, V. Müller, and K. A. McEwen, *Phys. Rev. B* **60**, R8430 (1999).
- 142) K. A. McEwen, U. Steigenberger, K. N. Clausen, J. Kulda, J.-G. Park, and M. B. Walker, *J. Magn. Magn. Mater.* **177-181**, 37 (1998).
- 143) Y. Tokiwa, K. Sugiyama, T. Takeuchi, M. Nakashima, R. Settai, Y. Inada, Y. Haga, E. Yamamoto, K. Kindo, H. Harima, and Y. Ōnuki, *J. Phys. Soc. Jpn.* **70**, 1731 (2001).
- 144) D. McMorrow, K. McEwen, U. Steigenberger, H. Rönnow, and F. Yakhou, *Phys. Rev. Lett.* **87**, 057201 (2001).
- 145) A. Schenck, F. N. Gygax, and K. A. McEwen, *J. Phys.: Condens. Matter* **14**, 4595 (2002).
- 146) W. Sikora, F. Bialas, L. Pytlik, and J. Malinowski, *J. Phys.: Conf. Ser.* **30**, 237 (2006).
- 147) H. Walker, K. McEwen, D. McMorrow, S. Wilkins, F. Wastin, E. Colineau, and D. Fort, *Phys. Rev. Lett.* **97**, 137203 (2006).
- 148) T. Fujimoto, Y. Haga, H. Sakai, Y. Tokunaga, S. Kambe, and Y. Ōnuki, *J. Magn. Magn. Marer.* **310**, 746 (2007).
- 149) H. C. Walker, K. A. McEwen, M. D. Le, L. Paolasini, and D. Fort, *J. Phys.: Condens. Matter* **20**, 395221 (2008).
- 150) J. Fernández Rodríguez, S. W. Lovesey, and J. A. Blanco, *J. Phys.: Condens. Matter* **22**, 022202 (2010).
- 151) H. C. Walker, M. D. Le, K. A. McEwen, M. Bleckmann, S. Süllow, C. Mazzoli, S. B. Wilkins, and D. Fort, *Phys. Rev. B* **84**, 235142 (2011).
- 152) A. Kiss and P. Fazekas, *Phys. Rev. B* **71**, 054415 (2005).
- 153) K. Hanzawa and N. Watanabe, *J. Phys.: Condens. Matter* **17**, L419 (2005).
- 154) K. Hanzawa, *J. Phys.: Condens. Matter* **19**, 072202 (2007).

- 155) F. Cricchio, F. Bultmark, O. Gränäs, and L. Nordström, *Phys. Rev. Lett.* **103**, 107202 (2009).
- 156) K. Haule and G. Kotliar, *Nature Phys.* **5**, 796 (2009).
- 157) H. Harima, K. Miyake, and J. Flouquet, *J. Phys. Soc. Jpn.* **79**, 033705 (2010).
- 158) P. Thalmeier and T. Takimoto, *Phys. Rev. B* **83**, 165110 (2011).
- 159) H. Kusunose and H. Harima, *J. Phys. Soc. Jpn.* **80**, 084702 (2010).
- 160) H. Ikeda, M.-T. Suzuki, R. Arita, T. Takimoto, T. Shibauchi, and Y. Matsuda, *Nat. Phys.* **8**, 528 (2012).
- 161) J. A. Mydosh and P. M. Oppeneer, *Rev. Mod. Phys.* **83**, 1301 (2011).
- 162) H.-H. Kung, R. E. Baumbach, E. D. Bauer, V. K. Thorsmolle, W.-L. Zhang, K. Haule, J. A. Mydosh, and G. Blumberg, *Science* **347**, 1339 (2015).
- 163) H.-H. Kung, S. Ran, N. Kanchanavatee, V. Krapivin, A. Lee, J. A. Mydosh, K. Haule, M. B. Maple, and G. Blumberg, *Phys. Rev. Lett.* **117**, 227601 (2016).
- 164) P. Santini and G. Amoretti, *Phys. Rev. Lett.* **73**, 1027 (1994).
- 165) H. C. Walker, R. Caciuffo, D. Aoki, F. Bourdarot, G. H. Lander, and J. Flouquet, *Phys. Rev. B* **83**, 193102 (2011).
- 166) D. D. Khalyavin, S. W. Lovesey, A. N. Dobrynin, E. Ressouche, R. Ballou, and J. Flouquet, *J. Phys.: Condens. Matter* **26**, 046003 (2014).
- 167) E. Ressouche, R. Ballou, F. Bourdarot, D. Aoki, V. Simonet, M. T. Fernandez-Diaz, A. Stunault, and J. Flouquet, *Phys. Rev. Lett.* **109**, 067202 (2012).
- 168) P. Chandra, P. Coleman, and R. Flint, *Phil. Mag. B* **94**, 3803 (2014).
- 169) A. Kiss and P. Fazekas, *Phys. Rev. B* **68**, 174425 (2003).
- 170) R. O. Jones, and O. Gunnarsson, *Rev. Mod. Phys.* **61**, 689 (1989).
- 171) F. Bultmark, F. Cricchio, O. Gränäs, and L. Nordström, *Phys. Rev. B* **80**, 035121 (2009).
- 172) M.-T. Suzuki and H. Ikeda, *Phys. Rev. B* **90**, 184407 (2014).
- 173) A. A. Mostofi, J. R. Yates, Y.-S. Lee, I. Souza, D. Vanderbilt, and N. Marzari, *Comput. Phys. Commun.* **178**, 685 (2008).
- 174) H. Ikeda, M.-T. Suzuki, and R. Arita, *Phys. Rev. Lett.* **114**, 147003 (2015).
- 175) C. Ederer and N. A. Spaldin, *Phys. Rev. B* **76**, 214404 (2007).
- 176) N. A. Spaldin, M. Fiebig, and M. Mostovoy, *J. Phys.: Condens. Matter* **20**, 434203 (2008).

- 177) N. A. Spaldin, M. Fechner, E. Bousquet, A. Balatsky, and L. Nordström, Phys. Rev. B **88**, 094429 (2013).
- 178) S. Hayami, H. Kusunose, and Y. Motome, Phys. Rev. B **90**, 024432 (2014).
- 179) S. Hayami, H. Kusunose, and Y. Motome, J. Phys.: Condens. Matter **28**, 395601 (2016).
- 180) S. Sumita, T. Nomoto, and Y. Yanase, Phys. Rev. Lett. **119**, 027001 (2017).
- 181) M.-T. Suzuki, T. Koretsune, M. Ochi, and R. Arita, Phys. Rev. B **95**, 094406 (2017).
- 182) D. A. Varshalovich, A. N. Moskalev, V. K. Khersonskii, *Quantum Theory of Angular Momentum* (World Scientific Publishing, Singapore, 1988).
- 183) C. Castelnovo, R. Moessner, and S. L. Sondhi, Nature **451**, 42 (2008).
- 184) D. I. Khomskii, Nat. Commun. **3**, 904 (2012).
- 185) V. I. Anisimov, F. Aryasetiawan, and A. I. Liechtenstein, J. Phys.: Condens. Matter **9**, 767 (1997).
- 186) G. Kotliar, S. Y. Savrasov, K. Haule, V. S. Oudovenko, O. Parcollet, and C. A. Marianetti, Rev. Mod. Phys. **78**, 865 (2006).
- 187) A. B. Shick and W. E. Pickett, Phys. Rev. Lett. **86**, 300 (2001).
- 188) A. B. Shick, W. E. Pickett, and A. I. Liechtenstein, J. Elec. Spec. and Rel. Phen. **114**, 753 (2001).
- 189) H. Harima, J. Magn. Magn. Mater. **226-230**, 83 (2001).
- 190) H. Harima and K. Takegahara, Physica B **312-313**, 843 (2002).
- 191) D. B. Ghosh, S. K. De, P. M. Oppeneer, and M. S. S. Brooks, Phys. Rev. B **72**, 115123 (2005).
- 192) A. O. Shorikov, A. V. Lukoyanov, M. A. Korotin, and V. I. Anisimov, Phys. Rev. B **72**, 024458 (2005).
- 193) A. B. Shick, V. Drchal, and L. Havela, Europhys. Lett. **69**, 588 (2005).
- 194) A. B. Shick, V. Janiš, and P. M. Oppeneer, Phys. Rev. Lett. **94**, 016401 (2005).
- 195) A. B. Shick, L. Havela, J. Kolorenč, V. Drchal, T. Gouder, and P. M. Oppeneer, Phys. Rev. B **73**, 104415 (2006).
- 196) M.-T. Suzuki and H. Harima, J. Phys. Soc. Jpn. **79**, 024705 (2010).
- 197) P. Söderlind, G. Kotliar, K. Haule, P. M. Oppeneer, and D. Guillaumont, Mater. Res. Soc.-Bull. **35**, 883 (2010).

- 198) V. I. Anisimov, J. Zaanen, and O. K. Andersen, Phys. Rev. B **44**, 943 (1991).
- 199) M. T. Czyżyk and G. A. Sawatzky, Phys. Rev. B **49**, 14211 (1994).
- 200) A. B. Shick, A. I. Liechtenstein, and W. E. Pickett, Phys. Rev. B **60**, 10763 (1999).
- 201) V. I. Anisimov, I. V. Solovyev, M. A. Korotin, M. T. Czyżyk, and G. A. Sawatzky, Phys. Rev. B **48**, 16929 (1993).
- 202) J. Slater, Phys. Rev. **34**, 1293 (1929).
- 203) E. Condon and G. Shortley, Phys. Rev. **37**, 1025 (1931).
- 204) J. Gaunt, Philos. Trans. Roy. Soc. Ser. A **228**, 195 (1929).
- 205) G. Racah, Phys. Rev. **62**, 438 (1942).
- 206) B. R. Judd, Proc. Roy. Soc. (London) A **228**, 120 (1955).
- 207) M. Weinert, J. Math. Phys. **22**, 2433 (1981).
- 208) M.-T. Suzuki and P. M. Oppeneer, Phys. Rev. B **80**, 161103(R) (2009).
- 209) G. Jomard, B. Amadon, F. Bottin, and M. Torrent, Phys. Rev. B **78**, 075125 (2008).
- 210) P. Larson and W. R. L. Lambrecht, A. Chantis, and M. van Schilfgaarde, Phys. Rev. B **75**, 045114 (2007).
- 211) B. Dorado, B. Amadon, M. Freyss, and M. Bertolus, Phys. Rev. B **79**, 235125 (2009).
- 212) B. Dorado, P. Garcia, G. Carlot, C. Davoisne, M. Fraczkiewicz, B. Pasquet, M. Freyss, C. Valot, G. Baldinozzi, D. Siméone, and M. Bertolus, Phys. Rev. B **83**, 035126 (2011).
- 213) D. W. Osborne and E. F. Westrum, J. Chem. Phys. **21**, 1884 (1953).
- 214) J. W. Ross and D. J. Lam, J. Appl. Phys. **38**, 1451 (1967).
- 215) D. E. Cox and B. C. Frazer, J. Phys. Chem. Solids **28**, 1649 (1967).
- 216) B. D. Dunlap, G. M. Kalvius, D. Lam, and M. B. Brodsky, J. Phys. Chem. Solids **29**, 1365 (1968).
- 217) J. M. Friedt, F. J. Litterst, and J. Rebizant, Phys. Rev. B **32**, 257 (1985).
- 218) P. Santini and G. Amoretti, J. Phys. Soc. Jpn. Suppl. **71**, 11 (2002).
- 219) D. Mannix, G. H. Lander, J. Rebizant, R. Caciuffo, N. Bernhoeft, E. Lidström, and C. Vettier, Phys. Rev. B **60**, 15187 (1999).
- 220) S. W. Lovesey, E. Balcar, C. Detlefs, G. van der Laan, D. S. Sivia, and U. Staub, J. Phys.: Condens. Matter **15**, 4511 (2003).

- 221) S. W. Lovesey, C. Detlefs, and A. Rodríguez-Fernández, *J. Phys.: Condens. Matter* **24**, 256009 (2012).
- 222) R. E. Walstedt, S. Kambe, Y. Tokunaga, and H. Sakai, *J. Phys. Soc. Jpn.* **76**, 072001 (2007).
- 223) O. Sakai, R. Shiina, and H. Shiba, *J. Phys. Soc. Jpn.* **72**, 1534 (2003).
- 224) N. Magnani, S. Carretta, R. Caciuffo, P. Santini, G. Amoretti, A. Hiess, J. Rebizant, and G. H. Lander, *Phys. Rev. B* **78**, 104425 (2008).
- 225) P. Santini, R. Lémanski, and P. Erdös, *Adv. Phys.* **48**, 537 (1999).
- 226) C. E. Mcneilly, *J. Nucl. Mater.* **11**, 53 (1964).
- 227) J. Schoenes, *Phys. Rep.* **63**, 301 (1980).
- 228) T. M. McCleskey, E. Bauer, Q. Jia, A. K. Burrell, B. L. Scott, S. D. Conradson, A. Mueller, L. Roy, X. Wen, G. E. Scuseria, and R. L. Martin, *J. Appl. Phys.* **113**, 013515 (2013).
- 229) K. Kubo and T. Hotta, *Phys. Rev. B* **71**, 140404(R) (2005).
- 230) S. Kern, C.-K. Loong, and G. H. Lander, *Phys. Rev. B* **32**, 3051 (1985).
- 231) G. Amoretti, A. Blaise, R. Caciuffo, J. M. Fournier, M. T. Hutchings, R. Osborn, and A. D. Taylor, *Phys. Rev. B* **40** 1856 (1989).
- 232) J. M. Fournier, A. Blaise, G. Amoretti, R. Caciuffo, J. Larroque, M. T. Hutchings, R. Osborn, and A. D. Taylor, *Phys. Rev. B* **43**, 1142 (1991).
- 233) G. Amoretti, A. Blaise, R. Caciuffo, D. Di Cola, J. M. Fournier, M. T. Hutchings, G. H. Lander, R. Osborn, A. Severing, and A. D. Taylor, *J. Phys.: Condens. Matter* **4**, 3459 (1992).
- 234) S. Kern, C.-K. Loong, G. L. Goodman, B. Cort, and G. H. Lander, *J. Phys.: Condens. Matter* **2** 1933 (1990).
- 235) S. Kern, R. A. Robinson, H. Nakotte, G. H. Lander, B. Cort, P. Watson, and F. A. Vigil, *Phys. Rev. B* **59**, 104 (1999).
- 236) B. C. Frazer, G. Shirane, D. E. Cox, and C. E. Olsen, *Phys. Rev.* **140**, A1448 (1965).
- 237) J. Faber, G. H. Lander, and B. R. Cooper, *Phys. Rev. Lett.* **35**, 1770 (1975).
- 238) J. Faber, Jr. and G. H. Lander, *Phys. Rev. B* **14**, 1151 (1976).
- 239) B. T. M. Willis and R. I. Taylor, *Phys. Lett.* **17**, 188 (1965).

- 240) K. Ikushima, S. Tsutsui, Y. Haga, H. Yasuoka, R. E. Walstedt, N. M. Masaki, A. Nakamura, S. Nasu, and Y. Ōnuki, *Phys. Rev. B* **63**, 104404 (2001).
- 241) S. B. Wilkins, J. A. Paixão, R. Caciuffo, P. Javorsky, F. Wastin, J. Rebizant, C. Detlefs, N. Bernhoeft, P. Santini, and G. H. Lander, *Phys. Rev. B* **70**, 214402 (2004).
- 242) G. Raphael and R. Lallement, *Solid State Commun.* **6**, 383 (1968).
- 243) H. Yasuoka, G. Koutroulakis, H. Chudo, S. Richmond, D. K. Veirs, A. I. Smith, E. D. Bauer, J. D. Thompson, G. D. Jarvinen, and D. L. Clark, *Science* **336**, 901 (2012).
- 244) D. G. Karraker, *J. Chem. Phys.* **63**, 3174 (1975).
- 245) A. Bœuf, J. M. Fournier, J. F. Gueugnon, L. Manes, J. Rebizant, and F. Rustichelli, *J. Phys. (France)* **40**, L335 (1979).
- 246) G. M. Kalvius, S. L. Ruby, B. D. Dunlap, G. K. Shenoy, D. Cohen, and M. B. Brodsky, *Phys. Lett.* **29B**, 489 (1969).
- 247) M. M. Abraham, L. A. Boatner, C. B. Finch, and R. W. Reynolds, *Phys. Rev. B* **3**, 2864 (1971).
- 248) W. Kolbe, N. M. Edelstein, C. B. Finch, and M. M. Abraham, *J. Chem. Phys.* **60**, 607 (1974).
- 249) U. Benedict and C. Dufour, *Physica B* **102**, 303 (1980).
- 250) N. M. Edelstein and G. H. Lander, in *The Chemistry of the Actinide and Transactinide Elements* (Springer, Dordrecht, The Netherlands, 2006), edited by L. R. Morss, N. M. Edelstein, and J. Fuger, Vol. **4**, pp. 2225–2306.
- 251) Y. Tokunaga, T. Nishi, S. Kambe, M. Nakada, A. Itoh, Y. Homma, H. Sakai, and H. Chudo, *J. Phys. Soc. Jpn.* **79**, 053705 (2010).
- 252) Y. Tokunaga, T. Nishi, S. Kambe, M. Nakada, Y. Homma, H. Sakai, and H. Chudo, *J. Phys. Soc. Jpn.* **80**, SA110 (2011).
- 253) L. R. Morss, J. W. Richardson, Jr., C. W. Williams, G. H. Lander, A. C. Lawson, N. M. Edelstein, and G. V. Shalimoff, *J. Less-Common Metals* **156**, 273 (1989).
- 254) K. O. Kvashnina, S. M. Butorin, D. K. Shuh, J.-H. Guo, L. Werme, and J. Nordgren, *Phys. Rev. B* **75**, 115107 (2007).
- 255) F. Niikura and T. Hotta, *Phys. Rev. B* **83**, 172402 (2011).
- 256) H. U. Rahman and W. A. Runciman, *J. Phys. Chem. Solids* **27**, 1833 (1966).
- 257) F. Zhou and V. Ozoliņš, *Phys. Rev. B* **83**, 085106 (2011).

- 258) N. Magnani, P. Santini, G. Amoretti, and R. Caciuffo, *Phys. Rev. B* **71**, 054405 (2005).
- 259) P. Giannozzi and P. Erdös, *J. Magn. Magn. Mater.* **67**, 75 (1987).
- 260) V. S. Mironov, L. F. Chibotaru, and A. Ceulemans, *Adv. Quantum Chem.* **44**, 599 (2003).
- 261) S. J. Allen, *Phys. Rev.* **166**, 530 (1968).
- 262) S. J. Allen, *Phys. Rev.* **167**, 492 (1968).
- 263) K. Kubo and T. Hotta, *Phys. Rev. B* **72**, 132411 (2005).
- 264) M. S. S. Brooks and P. J. Kelly, *Solid State Commun.* **45**, 689 (1983).
- 265) K. N. Kudin, G. E. Scuseria, and R. L. Martin, *Phys. Rev. Lett.* **89**, 266402 (2002).
- 266) R. Laskowski, G. K. H. Madsen, P. Blaha, and K. Schwarz, *Phys. Rev. B* **69**, 140408(R) (2004).
- 267) I. D. Prodan and G. E. Scuseria, R. L. Martin, *Phys. Rev. B* **73**, 045104 (2006).
- 268) I. D. Prodan, G. E. Scuseria, and R. L. Martin, *Phys. Rev. B* **76**, 033101 (2007).
- 269) S.-W. Yu, J. G. Tobin, J. C. Crowhurst, S. Sharma, J. K. Dewhurst, P. Olalde-Velasco, W. L. Yang, and W. J. Siekhaus, *Phys. Rev. B* **83**, 165102 (2011).
- 270) X. Wen, R. L. Martin, L. E. Roy, G. E. Scuseria, S. P. Rudin, E. R. Batista, T. M. McCleskey, B. L. Scott, E. Bauer, J. J. Joyce, and T. Durakiewicz, *J. Chem. Phys.* **137**, 154707 (2012).
- 271) M. Colarieti-Tosti, O. Eriksson, L. Nordström, J. Wills, and M. S. S. Brooks, *Phys. Rev. B* **65**, 195102 (2002).
- 272) Q. Yin, A. Kutzepov, K. Haule, G. Kotliar, S. Y. Savrasov, and W. E. Pickett, *Phys. Rev. B* **84**, 195111 (2011).
- 273) P. Maldonado, L. Paolasini, P. M. Oppeneer, T. R. Forrest, A. Prodi, N. Magnani, A. Bosak, G. H. Lander, and R. Caciuffo, *Phys. Rev. B* **93**, 144301 (2016).
- 274) J. W. L. Pang, A. Chernatynskiy, B. C. Larson, W. J. L. Buyers, D. L. Abernathy, K. J. McClellan, and S. R. Phillpot, *Phys. Rev. B* **89**, 115132 (2014).
- 275) T. Petit, B. Morel, C. Lemaigman, A. Pasturel, and B. Bigot, *Philos. Mag. B* **73**, 893 (1996).
- 276) T. Maehira and T. Hotta, *J. Magn. Magn. Mater.* **310**, 754 (2007).
- 277) Y. Hasegawa, T. Maehira, and T. Hotta, *J. Mod. Phys.* **4**, 1574 (2013).

- 278) A. Modin, Y. Yun, M.-T. Suzuki, J. Vegelius, L. Werme, J. Nordgren, P. M. Oppeneer, and S. M. Butorin, *Phys. Rev. B* **83**, 075113 (2011).
- 279) L. Petit, A. Svane, Z. Szotek, and W. M. Temmerman, *Science* **301**, 498 (2003).
- 280) B. Sun, P. Zhang, and X.-G. Zhao, *J. Chem. Phys.* **128**, 084705 (2008).
- 281) H. Nakamura, M. Machida, and M. Kato, *Prog. Nucl. Sci. Technol.* **2**, 16 (2011).
- 282) H. Wang and K. Konashi, *J. Alloys Compnd.* **533**, 53 (2012).
- 283) Q. Yin and S. Y. Savrasov, *Phys. Rev. Lett.* **100**, 225504 (2008).
- 284) S. L. Dudarev, D. Nguyen Manh, and A. P. Sutton, *Philos. Mag. B* **75**, 613 (1997).
- 285) S. L. Dudarev, G. A. Botton, S. Y. Savrasov, Z. Szotek, W. M. Temmerman, and A. P. Sutton, *Phys. Status Solidi* **166**, 429 (1998).
- 286) A. I. Liechtenstein, V. I. Anisimov, and J. Zaanen, *Phys. Rev. B* **52**, R5467 (1995).
- 287) A. V. Nikolaev and K. H. Michel, *Phys. Rev. B*, **68**, 054112 (2003).
- 288) H. Ikeda, M.-T. Suzuki, R. Arita, and T. Takimoto, *Comp. Rend. Physiq.* **15**, 587 (2014).
- 289) J. Kuneš, R. Arita, P. Wissgott, A. Toschi, H. Ikeda, and K. Held, *Comput. Phys. Commun.* **181**, 1888 (2010).
- 290) H. Ikeda, R. Arita, and J. Kuneš, *Phys. Rev. B* **81**, 054502 (2010).
- 291) F. Steglich, J. Aarts, C. Bredl, W. Lieke, D. Meschede, W. Franz, and H. Schäfer, *Phys. Rev. Lett.* **43**, 1892 (1979).
- 292) C. D. Bredl, H. Spille, U. Rauchschwalbe, W. Lieke, F. Steglich, G. Cordier, W. Assmus, M. Herrmann, and J. Aarts, *J. Magn. Magn. Mater.* **31-34**, 373 (1983).
- 293) J. Arndt, O. Stockert, K. Schmalzl, E. Faulhaber, H. S. Jeevan, C. Geibel, W. Schmidt, M. Loewenhaupt, and F. Steglich, *Phys. Rev. Lett.* **106**, 246401 (2011).
- 294) Y. Kitaoka, Koh-ichi Ueda, K. Fujiwara, H. Arimoto, H. Iida, and K. Asayama, *J. Phys. Soc. Jpn.* **55**, 723 (1986).
- 295) K. Ishida, Y. Kawasaki, K. Tabuchi, K. Kashima, Y. Kitaoka, K. Asayama, C. Geibel, and F. Steglich, *Phys. Rev. Lett.* **82**, 5353 (1999).
- 296) K. Fujiwara, Y. Hata, K. Kobayashi, K. Miyoshi, J. Takeuchi, Y. Shimaoka, H. Kotegawa, T. C. Kobayashi, C. Geibel, and F. Steglich, *J. Phys. Soc. Jpn.* **77**, 123711 (2008).
- 297) O. Stockert, J. Arndt, E. Faulhaber, C. Geibel, H. S. Jeevan, S. Kirchner, M. Loewenhaupt, K. Schmalzl, W. Schmidt, Q. Si, and F. Steglich, *Nat. Phys.* **7**, 119 (2011).

- 298) C. Pfleiderer, Rev. Mod. Phys. **81**, 1551 (2009).
- 299) S. Kittaka, Y. Aoki, Y. Shimura, T. Sakakibara, S. Seiro, C. Geibel, F. Steglich, H. Ikeda, and K. Machida, Phys. Rev. Lett. **112**, 067002 (2014).
- 300) T. Yamashita, T. Takenaka, Y. Tokiwa, J. A. Wilcox, Y. Mizukami, D. Terazawa, Y. Kasahara, S. Kittaka, T. Sakakibara, M. Konczykowski, S. Seiro, H. S. Jeevan, C. Geibel, C. Putzke, T. Onishi, H. Ikeda, A. Carrington, T. Shibauchi, and Y. Matsuda, Sci. Adv. **3**, e1601667 (2017).
- 301) H. Harima and A. Yanase, J. Phys. Soc. Jpn. **60**, 21 (1991).
- 302) G. Zwicknagl and U. Pulst, Physica B **186-188**, 895 (1993).
- 303) T. Takenaka, Y. Mizukami, J. A. Wilcox, M. Konczykowski, S. Seiro, C. Geibel, Y. Tokiwa, Y. Kasahara, C. Putzke, Y. Matsuda, A. Carrington, and T. Shibauchi, Phys. Rev. Lett. **119**, 077001 (2017).
- 304) T. T. M. Palstra, A. A. Menovsky, J. van den Berg, A. J. Dirkmaat, P. H. Kes, G. J. Nieuwenhuys, and J. A. Mydosh, Phys. Rev. Lett. **55**, 2727 (1985).
- 305) M. B. Maple, J. W. Chen, Y. Dalichaouch, T. Kohara, C. Rossel, M. S. Torikachvili, M. W. McElfresh, and J. D. Thompson, Phys. Rev. Lett. **56**, 185 (1986).
- 306) W. Schlabitz, J. Baumann, B. Pollit, U. Rauchschwalbe, H. M. Mayer, U. Ahlheim, and C. D. Bredl, Z. Phys. B **62**, 171 (1986).
- 307) K. Behnia, R. Bel, Y. Kasahara, Y. Nakajima, H. Jin, H. Aubin, K. Izawa, Y. Matsuda, J. Flouquet, Y. Haga, Y. Ōnuki, and P. Lejay, Phys. Rev. Lett. **94**, 156405 (2005).
- 308) Y. Kasahara, T. Iwasawa, H. Shishido, T. Shibauchi, K. Behnia, Y. Haga, T. D. Matsuda, Y. Ōnuki, M. Sigrist, and Y. Matsuda, Phys. Rev. Lett. **99**, 116402 (2007).
- 309) R. Escudero and F. Morales, Phys. Rev. B **49**, 15271 (1994).
- 310) J. G. Rodrigo, F. Guinea, S. Vieira, and F. G. Aliev, Phys. Rev. B **55**, 14318 (1997).
- 311) P. Aynajian, E. H. da Silva Neto, C. V. Parker, Y. Huang, A. Pasupathy, J. Mydosh, and A. Yazdani, PNAS **107**, 10383 (2010).
- 312) A. R. Schmidt, M. H. Hamidian, P. Wahl, F. Meier, A. V. Balatsky, J. D. Garrett, T. J. Williams, G. M Luke, and J. C. Davis, Nature **465**, 570 (2010).
- 313) C. Broholm, J. K. Kjems, W. J. L. Buyers, P. Matthews, T. T. M. Palstra, A. A. Menovsky, and J. A. Mydosh, Phys. Rev. Lett. **58**, 1467 (1987).

- 314) E. D. Isaacs, D. B. McWhan, R. N. Kleiman, D. J. Bishop, G. E. Ice, P. Zschack, B. D. Gaulin, T. E. Mason, J. D. Garrett, and W. J. L. Buyers, *Phys. Rev. Lett.* **65**, 3185 (1990).
- 315) T. E. Mason, B. D. Gaulin, J. D. Garrett, Z Tun, W. J. L. Buyers, and E. D. Isaacs, *Phys. Rev. Lett.* **65**, 3189 (1990).
- 316) W. J. L. Buyers, *Physica B* **223–224**, 9 (1996).
- 317) J. A. Mydosh and P. M. Oppeneer, *Phil. Mag. B* **94**, 3642 (2014).
- 318) P. M. Oppeneer, J. Rusz, S. Elgazzar, M.-T. Suzuki, T. Durakiewicz, and J. A. Mydosh, *Phys. Rev. B* **82**, 205103 (2010).
- 319) S.-i. Fujimori, Y. Takeda, T. Okane, Y. Saitoh, A. Fujimori, H. Yamagami, Y. Haga, E. Yamamoto, and Y. Ōnuki, *J. Phys. Soc. Jpn.* **85**, 062001 (2016).
- 320) H. Amitsuka, K. Tenya, M. Yokoyama, A. Schenck, D. Andreica, F. N. Gygax, A. Amato, Y. Miyako, Y. K. Huang, and J. A. Mydosh, *Physica B* **326**, 418 (2003).
- 321) A. Amato, M. J. Graf, A. De Visser, H. Amitsuka, D. Andreica, and A. Schenck, *J. Phys.: Condens. Matter* **16**, S4403 (2004).
- 322) H. Amitsuka, K. Matsuda, I. Kawasaki, K. Tenya, M. Yokoyama, C. Sekine, N. Tateiwa, T. C. Kobayashi, S. Kawarazaki, and H. Yoshizawa, *J. Magn. Magn. Mater.* **310**, 214 (2007).
- 323) S. Takagi, S. Ishihara, S. Saitoh, H. I. Sasaki, H. Tanida, M. Yokoyama, and H. Amitsuka, *J. Phys. Soc. Jpn.* **76**, 033708 (2007).
- 324) H. Amitsuka, M. Sato, N. Metoki, M. Yokoyama, K. Kuwahara, T. Sakakibara, H. Morimoto, S. Kawarazaki, Y. Miyako, and J. A. Mydosh, *Phys. Rev. Lett.* **83**, 5114 (1999).
- 325) K. Matsuda, Y. Kohori, T. Kohara, K. Kuwahara, and H. Amitsuka, *Phys. Rev. Lett.* **87**, 087203 (2001).
- 326) G. Motoyama, T. Nishioka, and N. K. Sato, *Phys. Rev. Lett.* **90**, 166402 (2003).
- 327) G. Motoyama, N. Yokoyama, A. Sumiyama, and Y. Oda, *J. Phys. Soc. Jpn.* **77**, 123710 (2008).
- 328) E. Hassinger, G. Knebel, K. Izawa, P. Lejay, B. Salce, and J. Flouquet, *Phys. Rev. B* **77**, 115117 (2008).
- 329) N. P. Butch, J. R. Jeffries, S. Chi, J. B. Leão, J. W. Lynn, and M. B. Maple, *Phys. Rev. B* **82**, 060408 (2010).

- 330) H. Ohkuni, Y. Tokiwa, K. Sakurai, R. Settai, T. Haga, E. Yamamoto, Y. Ōnuki, H. Yamagami, S. Takahashi, and T. Yanagisawa, *Phil. Mag. B* **79**, 1045 (1999).
- 331) N. Nakashima, H. Ohkuni, Y. Inada, R. Settai, Y. Haga, E. Yamamoto, and Y. Ōnuki, *J. Phys.: Condens. Matter* **15**, S2011 (2003).
- 332) Y. J. Jo, L. Balicas, C. Capan, K. Behnia, P. Lejay, J. Flouquet, J. A. Mydosh, and P. Schlottmann, *Phys. Rev. Lett.* **98**, 166404 (2007).
- 333) E. Hassinger, G. Knebel, T. D. Matsuda, D. Aoki, V. Taufour, and J. Flouquet, *Phys. Rev. Lett.* **105**, 216409 (2010).
- 334) K. Yano, T. Sakakibara, T. Tayama, M. Yokoyama, H. Amitsuka, Y. Homma, P. Miranović, M. Ichioka, Y. Tsutsumi, and K. Machida, *Phys. Rev. Lett.* **100**, 017004 (2008).
- 335) F. Bourdarot, E. Hassinger, S. Raymond, D. Aoki, V. Taufour, L.-P. Regnault, and J. Flouquet, *J. Phys. Soc. Jpn.* **79**, 064719 (2010).
- 336) A. Villaume, F. Bourdarot, E. Hassinger, S. Raymond, V. Taufour, D. Aoki, and J. Flouquet, *Phys. Rev. B* **78**, 012504 (2008).
- 337) J.-Q. Meng, P. M. Oppeneer, J. A. Mydosh, P. S. Riseborough, K. Gofryk, J. J. Joyce, E. D. Bauer, Y. Li and T. Durakiewicz, *Phys. Rev. Lett.* **111**, 127002 (2013).
- 338) R. Yoshida, M. Fukui, Y. Haga, E. Yamamoto, Y. Onuki, M. Okawa, W. Malaeb, S. Shin, Y. Muraoka and T. Yokoya, *Phys. Rev. B* **85**, 241102(R) (2012).
- 339) J. Buhot, M.-A. Méasson, Y. Gallais, M. Cazayous, A. Sacuto, G. Lapertot, and D. Aoki, *Phys. Rev. Lett.* **113**, 266405 (2014).
- 340) E. R. Schemm, R. E. Baumbach, P. H. Tobash, F. Ronning, E. D. Bauer, and A. Kapitulnik, *Phys. Rev. B* **91**, 140506(R) (2015).
- 341) M. B. Walker, W. J. L. Buyers, Z. Tun, W. Que, A. A. Menovsky, and J. D. Garrett, *Phys. Rev. Lett.* **71**, 2630 (1993).
- 342) S. Takagi, S. Ishihara, M. Yokoyama, and H. Amitsuka, *J. Phys. Soc. Jpn.* **81**, 114710 (2012).
- 343) S. C. Riggs, M. C. Shapiro, A. V. Maharaj, S. Raghu, E. D. Bauer, R. E. Baumbach, P. Giraldo-Gallo, M. Wartenbe, and I. R. Fisher, *Nat. Commun.* **6**, 7425 (2015).
- 344) R. Okazaki, T. Shibauchi, H. J. Shi, Y. Haga, T. D. Matsuda, E. Yamamoto, Y. Onuki, H. Ikeda, Y. Matsuda, *Science* **331**, 439 (2011).

- 345) S. Tonegawa, K. Hashimoto, K. Ikada, Y.-H. Lin, H. Shishido, Y. Haga, T. D. Matsuda, E. Yamamoto, Y. Onuki, H. Ikeda, Y. Matsuda, and T. Shibauchi, *Phys. Rev. Lett.* **109**, 036401 (2012).
- 346) S. Tonegawa, S. Kasahara, T. Fukuda, K. Sugimoto, N. Yasuda, Y. Tsuruhara, D. Watanabe, Y. Mizukami, Y. Haga, T.D. Matsuda, E. Yamamoto, Y. Onuki, H. Ikeda, Y. Matsuda, and T. Shibauchi, *Nat. Commun.* **5**, 4188 (2014).
- 347) S. Kambe, Y. Tokunaga, H. Sakai, T. D. Matsuda, Y. Haga, Z. Fisk, and R. E. Walstedt, *Phys. Rev. Lett.* **110**, 246406 (2013).
- 348) S. Saitoh, S. Takagi, M. Yokoyama, and H. Amitsuka, *J. Phys. Soc. Jpn.* **74**, 2209 (2005).
- 349) T. Mito, M. Hattori, G. Motoyama, Y. Sakai, T. Koyama, K. Ueda, T. Kohara, M. Yokoyama, and H. Amitsuka, *J. Phys. Soc. Jpn.* **82**, 123704 (2013).
- 350) G. J. Nieuwenhuys, *Phys. Rev. B* **35**, 5260 (1987).
- 351) F. J. Ohkawa and H. Shimizu, *J. Phys.: Condens. Matter* **11**, L519 (1999).
- 352) K. Miyake and J. Flouquet, *J. Phys. Soc. Jpn.* **79**, 035001 (2010).
- 353) K. Haule and G. Kotliar, *Europhys. Lett.* **89**, 57006 (2010).
- 354) J. G. Rau and Hae-Young Kee, *Phys. Rev. B* **85**, 245112 (2012).
- 355) P. Fazekas, A. Kiss, and K. Radnóczki, *Prog. Theor. Phys. Suppl.* **160**, 114 (2005).
- 356) T. Das, *Sci. Rep.* **2**, 596 (2012).
- 357) P. S. Riseborough, B. Coqblin, and S. G. Magalhaes, *Phys. Rev. B* **85**, 165116 (2012).
- 358) P. Chandra, P. Coleman, J. A. Mydosh, and V. Tripathi, *Nature* **417**, 831 (2002).
- 359) H. Ikeda and Y. Ohashi, *Phys. Rev. Lett.* **81**, 3723 (1998).
- 360) B. Lüthi, B. Wolf, P. Thalmeier, M. Günther, W. Sixl, and G. Bruls, *Phys. Lett. A* **175**, 237 (1993).
- 361) S. Elgazzar, J. Rusz, M. Amft, P. M. Oppeneer, and J. A. Mydosh, *Nat. Mater.* **8**, 337 (2009).
- 362) C.-H. Hsu and S. Chakravarty, *Phys. Rev. B* **87**, 085114 (2013).
- 363) P. Kotetes, A. Aperis, and G. Varelogiannis, *Phil. Mag. B* **94**, 3789 (2014).
- 364) Y. Dubi and A.V. Balatsky, *Phys. Rev. Lett.* **106**, 086401 (2011).
- 365) S. Fujimoto, *Phys. Rev. Lett.* **106**, 196407 (2011).

- 366) C. Pépin, M. R. Norman, S. Burdin, and A. Ferraz, Phys. Rev. Lett. **106**, 106601 (2011).
- 367) V. P. Mineev and M. E. Zhitomirsky, Phys. Rev. B **72**, 014432 (2005).
- 368) C. M. Varma and L. Zhu, Phys. Rev. Lett. **96**, 036405 (2006).
- 369) T. Nagao and J.-i. Igashira, Phys. Rev. B **74**, 765 (2005).
- 370) Y. L. Wang, G. Fabbris, D. Meyers, N. H. Sung, R. E. Baumbach, E. D. Bauer, P. J. Ryan, J.-W. Kim, X. Liu, M. P. M. Dean, G. Kotliar, and X. Dai, Phys. Rev. B **96**, 085146 (2017).
- 371) P. M. Oppeneer, S. Elgazzar, J. Rusz, Q. Feng, T. Durakiewicz, and J. A. Mydosh, Phys. Rev. B **84**, 241102(R) (2011).
- 372) H. Yamagami and N. Hamada, Physica B **284**, 1295 (2000).
- 373) M. Werwiński, J. Rusz, J. A. Mydosh, and P. M. Oppeneer, Phys. Rev. B **90**, 064430 (2014).
- 374) C. H. Booth, S. A. Medling, J. G. Tobin, R. E. Baumbach, E. D. Bauer, D. Sokaras, D. Nordlund, and T.-C. Weng, Phys. Rev. B **94**, 045121 (2016).
- 375) J. R. Jeffries, K. T. Moore, N. P. Butch, and M. B. Maple, Phys. Rev. B **82**, 033103 (2010).
- 376) C. R. Wiebe, J. A. Janik, G. J. Macdougall, G. M. Luke, J. D. Garrett, H. D. Zhou, Y.-J. Jo, L. Balicas, Y. Qiu, J. R. D. Copley, Z. Yamani, W. J. L. Buyers, Nat. Phys. **3**, 1 (2007).
- 377) I. Kawasaki, I. Watanabe, A. Hillier, and D. Aoki, J. Phys. Soc. Jpn. **83**, 094720 (2014).
- 378) P. Das, R. Baumbach, K. Huang, M. Maple, Y. Zhao, J. S. Helton, J. Lynn, E. Bauer, and M. Janoschek, New J. Phys. **15**, 05303 (2013).
- 379) N. Metoki, H. Sakai, E. Yamamoto, N. Tateiwa, T. Matsuda, and Y. Haga, J. Phys. Soc. Jpn. **82**, 055004 (2013).
- 380) K. A. Ross, I. Harriger, Z. Yamani, W. J. L. Buyers, J. D. Garrett, A. A. Menovsky, J. A. Mydosh and C. L. Broholm, Phys. Rev. B **89**, 155122 (2014).
- 381) M. Sundermann, M. W. Haverkort, S. Agrestini, A. Al-Zein, M. M. Sala, Y. Huang, M. Golden, A. de Visser, P. Thalmeier, L. H. Tjeng, and A. Severing, PNAS **113**, 13989 (2016).
- 382) K. Kuwahara, H. Amitsuka, T. Sakakibara, O. Suzuki, S. Nakamura, T. Goto, M. Mihalik, A. A. Menovsky, A. de Visser, and J. J. M Franse, J. Phys. Soc. Jpn. **66**, 3251 (1997).

- 383) T. Yanagisawa, S. Mombetsu, H. Hidaka, H. Amitsuka, M. Akatsu, S. Yasin, S. Zherlitsyn, J. Wosnitza, K. Huang, M. Janoschek, and M. B. Maple, Phys. Rev. B **88**, 195150 (2013).
- 384) R. Shindou and N. Nagaosa, Phys. Rev. Lett. **87**, 116801 (2001).
- 385) H. Watanabe and Y. Yanase, Phys. Rev. B **96**, 064432 (2017).
- 386) N. Nagaosa, J. Sinova, S. Onoda, A. H. MacDonald, and N. P. Ong, Rev. Mod. Phys. **82**, 1539 (2010).
- 387) S. Yoshii, S. Iikubo, T. Kageyama, K. Oda, Y. Kondo, K. Murata, and M. Sato, J. Phys. Soc. Jpn. **69**, 3777 (2000).
- 388) Y. Taguchi, Y. Oohara, H. Yoshizawa, N. Nagaosa, and Y. Tokura, Science **291**, 2573 (2003).
- 389) Y. Yasui, T. Kageyama, T. Moyoshi, M. Soda, M. Sato, and K. Kakurai, J. Phys. Soc. Jpn. **75**, 084711 (2006)
- 390) T. Tomizawa and H. Kontani, Phys. Rev. B **80**, 100401 (2009).
- 391) T. Tomizawa and H. Kontani, Phys. Rev. B **82**, 104412 (2010).
- 392) Y. Taguchi, T. Sasaki, S. Awaji, Y. Iwasa, T. Tayama, T. Sakakibara, S. Iguchi, T. Ito, and Y. Tokura, Phys. Rev. Lett. **90**, 257202 (2003).
- 393) Y. Taguchi, Y. Oohara, H. Yoshizawa, N. Nagaosa, T. Sasaki, S. Awaji, Y. Iwasa, T. Tayama, T. Sakakibara, S. Iguchi, K. Ohgushi, T. Ito, and Y. Tokura, J. Phys.: Condens. Matter **16**, S599 (2004).
- 394) H. Chen, Q. Niu, and A. H. MacDonald, Phys. Rev. Lett. **112**, 017205 (2014).
- 395) J. Kübler and C. Felser, Europhys. Lett. **108**, 67001 (2014).
- 396) S. Nakatsuji, N. Kiyohara, and T. Higo, Nature **527**, 212 (2015).
- 397) N. Kiyohara, T. Tomita, and S. Nakatsuji, Phys. Rev. Appl. **5**, 064009 (2016).
- 398) A. K. Nayak, J. E. Fischer, Y. Sun, B. Yan, J. Karel, A. C. Komarek, C. Shekhar, N. Kumar, W. Schnelle, J. Kübler, C. Felser, and S. S. P. Parkin, Sci. Adv. **2**, e1501870 (2016).
- 399) S. Tomiyoshi and Y. Yamaguchi, J. Phys. Soc. Jpn. **51**, 2478 (1982).
- 400) P. J. Brown, V. Nunez, F. Tasset, J. B. Forsyth, and P. Radhakrishna, J. Phys.: Condens. Matter **2**, 9409 (1990).
- 401) N. Yamada, H. Sakai, H. Mori, T. Ohoyama, Physica B+C **149**, 311 (1988).

- 402) D. J. Thouless, M. Kohmoto, M. P. Nightingale, and M. den Nijs, Phys. Rev. Lett. **49**, 405 (1982).
- 403) Z. Fang, N. Nagaosa, K. S. Takahashi, A. Asamitsu, R. Mathieu, T. Ogasawara, H. Yamada, M. Kawasaki, Y. Tokura, K. Terakura, Science **302**, 92 (2003).
- 404) X. Wang, J. R. Yates, I. Souza, and D. Vanderbilt, Phys. Rev. B **74**, 195118 (2006).
- 405) M. Uhl and J. Kübler, Phys. Rev. Lett. **77**, 334 (1996).
- 406) S. V. Halilov, A. Y. Perlov, P. M. Oppeneer, and H. Eschrig, Europhys. Lett. **39**, 91 (1997).
- 407) N. K. Sato, N. Aso, K. Miyake, R. Shiina, P. Thalmeier, G. Varelogiannis, C. Geibel, F. Steglich, P. Fulde, and T. Komatsubara, Nature **410**, 340 (2001).
- 408) T. Moriya and K. Ueda, Adv. Phys. **49**, 555 (2000); Rep. Prog. Phys. **66**, 1299 (2003).
- 409) C. J. Bradley and A. P. Cracknell, *The Mathematical Theory of Symmetry in Solids* (Oxford University Press, Oxford, 1972).
- 410) Y. Tokunaga, Y. Homma, S. Kambe, D. Aoki, H. Sakai, E. Yamamoto, A. Nakamura, Y. Shiokawa, R. E. Walstedt, and H. Yasuoka, Physica B **359-361**, 1096 (2005).
- 411) Y. Tokunaga, Y. Homma, S. Kambe, D. Aoki, K. Ikushima, H. Sakai, S. Ikeda, E. Yamamoto, A. Nakamura, Y. Shiokawa, T. Fujimoto, R. E. Walstedt, and H. Yasuoka, J. Phys. Soc. Jpn. **75** Suppl., 33 (2006).